

**SHEAR BEHAVIOUR OF RC BEAMS STRENGTHENED BY  
ULTRA- HIGH PERFORMANCE CONCRETE**

BY  
**ASHRAF AWADH BAHARQ**

A Thesis Presented to the  
DEANSHIP OF GRADUATE STUDIES

**KING FAHD UNIVERSITY OF PETROLEUM & MINERALS**

DHAHRAN, SAUDI ARABIA

In Partial Fulfillment of the  
Requirements for the Degree of

**MASTER OF SCIENCE**

In  
**CIVIL ENGINEERING**

**MAY 2017**

KING FAHD UNIVERSITY OF PETROLEUM & MINERALS

DHAHRAN- 31261, SAUDI ARABIA

**DEANSHIP OF GRADUATE STUDIES**

This thesis, written by **ASHRAF AWADH BAHARAQ** under the direction of his thesis advisor and approved by his thesis committee, has been presented and accepted by the Dean of Graduate Studies, in partial fulfillment of the requirements for the degree of **MASTER OF SCIENCE IN CIVIL ENGINEERING**.



Dr. Salah U. Al-Dulaijan  
Department Chairman

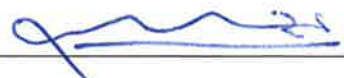


Prof. Salam A. Zummo  
Dean of Graduate Studies



8/8/2017

Date



Dr. Mohammad A. Al-Osta  
(Advisor)



Dr. Mesfer M. Al-Zahrani  
(Member)



Dr. Salah U. Al-Dulaijan  
(Member)

© ASHRAF AWADH BAHRAQ

2017

بِسْمِ اللَّهِ الرَّحْمَنِ الرَّحِيمِ

*Dedicated to*

*My beloved parents, wife, son  
and brothers and sisters*

## ACKNOWLEDGMENTS

First of all, I thank ALLAH who gave me the opportunity, health, strength, and patience to complete this research work.

Then, I would like to express my gratitude thanks to KING FAHD UNIVERSITY OF PETROLEUM & MINERALS for gave me the opportunity to study this degree program. I am greatly proud to be one of the KFUPM graduating students. In addition, I would like to thank the Civil Engineering Department, Faculty and Staff, for their supporting and always helping.

My special thanks to my advisor **Dr. Mohammad A. Al-Osta** for his greatly effort, help, guidance, presence, and encouragement. Dr. Al-Osta was being with me during the whole time of my thesis work and he provided me with the vision for becoming an excellent researcher in the future. In addition, I would like to express my sincere thanks to my committee members **Dr. Mesfer M. Al-Zahrani** (*Dean, College of Engineering Sciences*) and **Dr. Salah U. Al-Dulaijan** (*Chairman of Civil and Environmental Engineering Department*) for their valuable comments and feedback. Here, I wish to show my thanks to **Dr. Mohammed Baluch** and **Dr. Mohammed Maslehuddin** who provided me the necessary tools for success in both my personal and academic life.

I would like to show gratitude thanks to all technicians at KFUPM laboratories, namely: *Eng. Syed Imran (Concrete Lab) & Eng. Omer Hussein (Structural Lab), and Eng. Syed Najamuddin (Heavy Structures Testing Lab)* for their cooperation and help during all processes of my experimental work. Thanks also to *Prainsa Factory* for giving me the chance to use their factory facilities to cast the concrete beams.

My sincere thank goes to the Hadramout-Yemeni Community at KFUPM for their supporting and friendly help during my master studying program.

Finally, my most basic thanks to my father and mother for their prayer and supporting during my whole life. Also, I would like to express my great thanks to my wife and my son (*Mohammad Ashraf*) who are standing behind me by the encouragement and prayer. I thank all my brothers (*Mr. Zain, Eng. Abdullah and Mr. Mohmmad*) and my sisters for their motivation and tremendous supporting. To all my family here in Saudi Arabia and in Hadramout, May Allah bless you all.

# TABLE OF CONTENTS

ACKNOWLEDGMENTS .....	V
TABLE OF CONTENTS.....	VII
LIST OF TABLES.....	XI
LIST OF FIGURES.....	XII
LIST OF ABBREVIATIONS.....	XV
ABSTRACT.....	XVII
ملخص الرسالة .....	XIX
 CHAPTER 1 INTRODUCTION .....	 1
1.1 General .....	1
1.2 Significance of this Research .....	3
1.3 Research Objectives .....	4
1.4 Thesis Structure .....	5
 CHAPTER 2 LITERATURE REVIEW.....	 6
2.1 Outline .....	6
2.2 Ultra-High Performance Concrete – A state of the Art .....	7
2.2.1 Mix Design.....	7
2.2.2 Mechanical Properties.....	8
2.2.3 Durability Characteristics .....	9
2.3 Strengthening Techniques of RC Beams – A Review Study .....	10
2.3.1 Flexural Strengthening .....	11

2.3.2	Shear Strengthening .....	14
<b>CHAPTER 3 EXPERIMENTAL PROGRAM .....</b>		<b>23</b>
3.1	General .....	23
3.2	Casting the RC Beams.....	25
3.2.1	Design of RC Beams .....	26
3.2.2	Preparation of Molds and Steel Cages .....	26
3.2.3	Installing the Steel Strain Gauges .....	27
3.2.4	Casting the Normal Concrete .....	27
3.2.5	Mechanical Properties of Normal Concrete .....	28
3.2.6	Uniaxial Direct Tensile Test of Reinforcement Steel .....	31
3.3	Casting The UHPC.....	32
3.3.1	UHPC Mix Design .....	33
3.3.2	UHPC Mixing Methodology .....	35
3.4	UHPC Strengthening Techniques .....	38
3.4.1	Applying UHPC using Sandblasting Technique .....	39
3.4.2	Applying UHPC using Epoxy Adhesive Technique .....	40
3.5	Test of UHPC Material Properties.....	42
3.5.1	Uniaxial Compression Test .....	42
3.5.2	Elasticity Test .....	43
3.5.3	Uniaxial Direct Tensile Test .....	45
3.5.4	Flexural Tensile Strength Test.....	47
3.6	Evaluation of Bond Strength .....	49
3.6.1	Splitting Tensile Strength Test .....	50
3.6.2	Slant Shear Strength Test .....	51
3.6.3	Results and Discussion of Bonding Tests.....	53



3.7	Experimental Tests of Beams .....	54
3.7.1	Outline .....	54
3.7.2	Test Beams with $a/d=1.0$ .....	57
3.7.3	Test Beams with $a/d=1.5$ .....	62
3.7.4	Test Beams with $a/d=2.0$ .....	66
3.8	Summary of Experimental Test Program .....	68
CHAPTER 4 FINITE ELEMENT MODEL .....		73
4.1	Introduction .....	73
4.2	Finite Element Model .....	74
4.2.1	General .....	74
4.2.2	Concrete Damage Plasticity Model (CDP) .....	74
4.3	Parameters of Materials for FEM .....	77
4.4	Finite Element Model of Beams .....	79
4.4.1	Outline .....	79
4.4.2	Modeling Considerations .....	80
4.4.3	FE Results of Beams with $a/d=1.0$ .....	82
4.4.4	FE Results of Beams with $a/d=1.5$ .....	82
4.4.5	FE Results of Beams with $a/d=2.0$ .....	83
4.5	Outcome of Experimental Test Program .....	83
4.6	Comparative Study of Experimental and FE Results .....	83
4.6.1	Beams with $a/d=1.0$ .....	83
4.6.2	Beams with $a/d=1.5$ .....	85
4.6.3	Beams with $a/d=2.0$ .....	87
4.7	Summary of FE Results .....	89

<b>CHAPTER 5 MECHANISTIC MODEL .....</b>	<b>91</b>
5.1 General .....	91
5.2 Analytical Models: A State-of-the-Art Review .....	91
5.3 Proposed Analytical Model .....	93
5.3.1 Regression of Experimental Data .....	96
5.4 Validation of the Proposed Analytical Model .....	98
<b>CHAPTER 6 CONCLUSIONS AND RECOMMENDATIONS.....</b>	<b>100</b>
6.1 General .....	100
6.2 Application of the Research Study .....	101
6.3 Conclusions .....	101
6.4 Recommendations for Future Research .....	104
<b>REFERENCES.....</b>	<b>106</b>
<b>VITAE.....</b>	<b>114</b>

## LIST OF TABLES

Table 2.1 Mix-design of UHPC [9] .....	7
Table 3.1 Beams ID and description.....	24
Table 3.2 Specimen details for the properties of materials.....	25
Table 3.3 Mechanical properties of normal concrete (at 28-days) .....	30
Table 3.4 Mechanical properties of Steel Reinforcement.....	32
Table 3.5 Results of compression test on UHPC cube specimens.....	43
Table 3.6 Mechanical properties of UHPC (at 28-days).....	49
Table 3.7 Summary of bond testing results .....	54
Table 3.8 Results of Experimental tested beams .....	71
Table 4.1 Input parameters for Abaqus modeling .....	77
Table 4.2 Comparison of Failure Loads between Experimental Tests and FE Results....	89
Table 5.1 Input Data and Output Result of Proposed Analytical Model (for Sandblasted Cast-in Beams) .....	97
Table 5.2 Input Data and Output Result of Proposed Analytical Model (for Epoxy-Bonding Beams).....	97
Table 5.3 Comparison of Failure Loads between Experimental, FE and Analytical Model .....	97
Table 5.4 Validation of Model using Experimental Results of Ruano et al (2014) [26]..	99

## LIST OF FIGURES

Figure 2.1 Tensile behaviour of UHPC [15].....	9
Figure 2.2 Shrinkage strain of UHPC [19] .....	10
Figure 2.3 Force-deflection response of control and strengthened beams [20].....	12
Figure 2.4 Crack pattern of experimental FE results [20] .....	12
Figure 2.5 (a): FE modeling, (b) Jacketing configurations [19] .....	13
Figure 2.6 Load-displacement behaviour of strengthened beams [22].....	14
Figure 2.7 Strengthening arrangement [23].....	16
Figure 2.8 Load-deflection curves [24] .....	16
Figure 2.9 Beam details [25].....	17
Figure 2.10 Failure of UHPC -NSC beams [25].....	17
Figure 2.11 Test set-up of composite beam and force-deflection response of tested beams [29].....	19
Figure 2.12 Wrapping the RC beams with fibers of FRCM [31] .....	20
Figure 2.13 External bonding of steel plates with different arrangements [2] .....	21
Figure 2.14 Using Aluminum Alloys (AA) to strengthen the RC beams in shear [33]...	22
Figure 3.1 Flowchart of all works involved in the experimental program .....	24
Figure 3.2 (a) RC beams details, (b) strengthening configuration.....	26
Figure 3.3 (a) Reinforcement steel cage, (b) Installation of strain gauge on the stirrup ..	27
Figure 3.4 (a) Casting the normal concrete beams, (b) Curing tank.....	28
Figure 3.5 Stress-strain behaviour of normal concrete .....	31
Figure 3.6 Uniaxial direct tensile test of steel rebar: (a) Test setup, (b) specimen failure, (c) stress-strain response.....	32
Figure 3.7 UHPC ingredients.....	34
Figure 3.8 UHPC mixing methodology .....	35
Figure 3.9 (a) Molds for 2SJ and 3SJ, (b) casing UHPC inside the beam mold.....	36
Figure 3.10 (a) Casting the UHPC strips, (b) UHPC layers after demolding .....	36
Figure 3.11 Temporary curing the UHPC for 24-hours.....	37
Figure 3.12 Strengthened beams after demolding .....	37
Figure 3.13 UHPC specimens for evaluation the mechanical properties .....	38
Figure 3.14 Applying sandblasting technique on the surfaces of RC beams.....	39
Figure 3.15 Procedure for epoxy technique .....	41
Figure 3.16 Epoxy technique: (a) Surface preparation of UHPC strips and substrate, (b) applying epoxy bonding .....	41
Figure 3.17 Applying the retrofitted strips to the beam substrate: (a) 2SJ, (b) 3SJ.....	42
Figure 3.18 Test Setup for determination the Modulus of Elasticity.....	44
Figure 3.19 Compressive stress-strain behaviour of UHPC .....	45
Figure 3.20 Setup for uniaxial direct tensile test on the UHPC dogbone specimen.....	46
Figure 3.21 failure of dogbone HUPC-specimen: (left) Dogbone with SFRP, (right) dogbone with notch.....	47

Figure 3.22 Tensile stress-strain behaviour of UHPC .....	47
Figure 3.23 Flexural test of UHPC prisms .....	48
Figure 3.24 Load-deflection curve of UHPC prism under flexural test .....	49
Figure 3.25 Splitting Tensile Test, (left) the tests setup, (b) the failure mode .....	51
Figure 3.26 The failure modes of splitting tensile test.....	51
Figure 3.27 Slant shear test: (a) Cutting the specimens, (b) composite cylinder of NC/UHPC .....	52
Figure 3.28 Failure modes of specimens under slant shear test.....	52
Figure 3.29 Schematic representation of beam testing setup.....	56
Figure 3.30 Beam test setup.....	57
Figure 3.31 Crack patterns of control beam (CT-1.0) with $a/d=1.0$ .....	58
Figure 3.32 Load-deflection curve of control beam (CT-1.0) .....	59
Figure 3.33 Failure mode of strengthened beam (SB-2SJ-1.0) .....	59
Figure 3.34 Failure mode of strengthened beam (EP-2SJ-1.0).....	60
Figure 3.35 Crack pattern of retrofitted beam (SB-3SJ-1.0) .....	61
Figure 3.36 Failure mode of strengthened beam (EP-3SJ-1.0).....	61
Figure 3.37 Load-deflection curves of all beams with $a/d=1.0$ .....	62
Figure 3.38 Failure mode of control beam (CT-1.5) with $a/d=1.5$ .....	63
Figure 3.39 Failure modes of retrofitted beams (SB-2SJ-1.5) and (EP-2SJ-1.5) .....	64
Figure 3.40 Failure modes of retrofitted beams (SB-3SJ-1.5) and (EP-3SJ-1.5) .....	65
Figure 3.41 Load-deflection curves of all beams with $a/d=1.5$ .....	66
Figure 3.42 Failure mode of control beam (CT-2.0) with $a/d=2.0$ .....	67
Figure 3.43 Failure modes of retrofitted beams (SB-2SJ-2.0) and (SB-3SJ-2.0).....	67
Figure 3.44 Load-deflection curves of all beams with $a/d=2.0$ .....	68
Figure 3.45 Comparative results of all tested beams .....	71
Figure 3.46 Effect of $a/d$ ratio and strengthening jacketing in the failure load .....	72
Figure 4.1 Damage variables: (a) in tension, (b) in compression [54] .....	75
Figure 4.2 Nonlinear behaviour of materials: (a) concrete in compression (b) concrete in tension (d) UHPC in compression (d) UHPC in tension .....	78
Figure 4.3 Modeling the retrofitted beams: (a) steel cage, (b) NC, (c) UHPC strips, (d) retrofitted beam .....	80
Figure 4.4 (a) beam constraints, (b) meshing of beam .....	81
Figure 4.5 Control beam (CT-1.0): (a) failure mode of experimental and FE, (b) Load-deflection response .....	84
Figure 4.6 Retrofitted I beam (SB-2SJ-1.0): (a) failure mode, (b) Load-deflection response.....	85
Figure 4.7 Retrofitted beam (SB-2SJ-1.0): (a) interfacial surface of NC – shear failure, (b) flexural failure at retrofitted beam .....	85
Figure 4.8 Control beam (CT-1.5): (a) failure mode, (b) Load-deflection response .....	86

Figure 4.9 Retrofitted beam (SB-2SJ-1.5): (a) failure mode, (b) Lad-deflection response.....	87
Figure 4.10 Retrofitted beam (SB-3SJ-1.5): (a) failure mode, (b) Lad-deflection response.....	87
Figure 4.11 Control beam (CT-2.0): (a) failure mode, (b) Lad-deflection response .....	88
Figure 4.12 Retrofitted beam (SB-2SJ-2.0): (a) failure mode, (b) Lad-deflection response.....	88
Figure 4.13 Retrofitted beam (SB-3SJ-2.0): (a) failure mode, (b) Lad-deflection response.....	88
Figure 5.1 Symbols used in the proposed analytical model .....	95
Figure 5.2 Effect of a/d ration on the shear failure of beams [63].....	96
Figure 5.3 Beam details and strengthening configurations of work done by Runao et al (2014) [26] .....	99
Figure 6.1 Application of UHPC strengthening technique .....	101

## LIST OF ABBREVIATIONS

<b>2SJ</b>	:	Two-sided Jacketing
<b>3SJ</b>	:	Three-sided Jacketing
<b>a/d</b>	:	Shear span-to-depth ratio
<b>ACI</b>	:	American Concrete Institute
<b>ASTM</b>	:	American Society for Testing and Materials
<b>CDP</b>	:	Concrete Damage Plasticity
<b>CFRP</b>	:	Carbon Fibre Reinforced Polymer
<b>EP</b>	:	Epoxy
<b>EXP</b>	:	Experimental
<b>FEM</b>	:	Finite Element Model
<b>FRP</b>	:	Fibre Reinforced Polymer
<b>LVDT</b>	:	Linear Variable Differential Transformer
<b>MS</b>	:	Micro-Silica
<b>NC</b>	:	Normal Concrete
<b>RC</b>	:	Reinforced Concrete
<b>SB</b>	:	Sandblast
<b>SG</b>	:	Strain Gauge

<b>SFRC</b>	:	Steel Fibre Reinforced Concrete
<b>SP</b>	:	Super-Plasticizer
<b>UHPC</b>	:	Ultra-High Performance Concrete
<b>UTM</b>	:	Universal Testing Machine



## **ABSTRACT**

Full Name : [Ashraf Awadh Abdullah Bahraq]

Thesis Title : [Shear Behaviour of RC Beams Strengthened by Ultra- High Performance Concrete (UHPC)]

Major Field : [Civil Engineering]

Date of Degree : [May 2017]

Recent advances in concrete materials make it possible to repair or strengthen the existing concrete structures to extend their service life and ultimate load. One of these modern concretes is Ultra-High Performance Concrete (UHPC), which is strong and durable concrete.

In this research, an experimental investigation of using UHPC for shear strengthening of conventional reinforced concrete (RC) beams was conducted. Thirteen RC beams that are deficient in shear were cast and strengthened with UHPC layers in different configurations. Two different strengthening techniques were used, either by casting the UHPC inside the beam mold using sandblasting preparation, or by bonding the precast UHPC strips using epoxy adhesive. The experimental tests of beams were carried out by varying the shear span-to-depth ratio ( $a/d = 1.0; 1.5; 2.0$ ). The results of experimental tested beams revealed that the using of UHPC strengthening technique enhanced the shear capacity and shifted the failure mode from brittle to ductile.

A numerical non-linear finite element model (FEM) using Abaqus package was developed to predict the behavior and failure load of retrofitted beams. In addition, a comparison study was presented between the experimental test results and the developed FE model. The

results, namely: load-deflection response, ultimate load and failure modes, showed a high accuracy of the proposed numerical model.

Finally, an analytical model was developed by setting an expression to predict the shear failure load and demonstrate the contribution of UHPC to the shear capacity of RC beams. In addition, the proposed model was validated using one of the previous researches. The results showed that the proposed model predicts the shear strength in good accuracy.

## ملخص الرسالة

الاسم الكامل: اشرف عوض عبدالله بحرق

عنوان الرسالة: تقوية الجسور الخرسانية باستخدام الخرسانة فائقة الأداء – دراسة سلوك قوى القص

التخصص: هندسة مدنية

تاريخ الدرجة العلمية: مايو 2017

التطور في مواد البناء الخرسانية جعل من إصلاح وتقوية المنشآت الخرسانية القائمة أمراً ممكناً هذه الأيام. واحدة من تلك الخرسانات الحديثة هي الخرسانة فائقة الأداء (UHPC) والتي تمتاز بأنها قوية وديمومتها عالية. في هذا البحث، سلوك قوى القص في الجسور الخرسانية المقوية باستخدام تلك الخرسانة تمت دراستها معملياً. أربعة عشر جسراً خرسانياً ضعيف في مقاومة القص تم صبها بالخرسانة العادية ومن ثم تمت التقوية بالخرسانة الفائقة الأداء (UHPC) بعدة طبقات مختلفة. في هذا البحث تم استخدام طريقتين في التقوية: إما بعملية صب الخرسانة فائقة الأداء مباشرة على الجسور العادية، أو باستخدام تقنية الإيبوكسي حيث تمت صب قوالب الخرسانة الفائقة مسبقاً ومن ثم تمت عملية لصق هذه القوالب على اسطح الجسر الخرساني المراد تقويته. جميع الجسور المقوية والعادية تم إختبارها عملياً (في معامل قسم الهندسة المدنية بجامعة الملك فهد للبترول والمعادن) حيث تم دراسة تأثير تغير النسبة بين مسافة القص (المسافة من نقطة الحمل إلى الدعامه) إلى عمق الجسر، كل النتائج العملية أظهرت أن تقنية التقوية هذه ناجحة وقد عملت على زيادة مقاومة قوى القص، كما إنها قد حولت فشل الجسور من إنهيار مفاجئ وهش الى إنهيار مرن. أيضاً في هذه الدراسة البحثية، تم عمل نمذجة للجسور باستخدام البرامج الهندسية من أجل دراسة توقع الفشل وأيضاً سلوك تلك الجسور أثناء زيادة الأحمال. مقارنة نتائج التحليل الهندسي مع نتائج الإختبارات العملية أظهرت توافقاً كبيراً في منحنيات الحمل والانحناء كما أن توقع الإنهيار كان في توافق تام مع نتائج المعمل. أخيراً، تم إيجاد معادلة تقريبية لحساب حمل الفشل وتوقع الحمل الذي تشارك به الخرسانة الجديدة (خرسانة فائقة الأداء). أيضاً تمت التحقق من المعادلة باستخدام أحد الأبحاث السابقة في هذا المجال، حيث أظهرت النتائج تقارباً كبيراً في النتائج مما جعل المعادلة التقريبية من الأهمية بمكان.

# **CHAPTER 1**

## **INTRODUCTION**

### **1.1 General**

The concrete becomes one of the most important materials around the world [1]. The concrete structures exhibit a good structural performance and to somewhat durability aspects. Over the time, many developments have been adopted to enhance the properties of concrete. Nevertheless, the reinforced concrete (RC) structures are suffering from several deterioration problems. Therefore, the task of strengthening of these RC structures has been raised.

Concrete structures need to be repaired or strengthened when they have some deficiencies in their structural performance and/or durability properties. Such deficiencies could be due to: errors in design calculations or construction practices; unexpected increasing in loads; change in service conditions; deteriorations resulting from corrosion of steel rebars or other chemical attacks. Therefore, the performance criteria of repair materials must meet the code requirements and standards. Longer life, low cost, lighter structure, efficiency, safety, compatibility with substrate, structural behavior, bond strength, stiffness, durability are the most important properties of any repaired or strengthened material.

As structural performance is concerned, both flexural and shear strengths should meet the design requirements. In fact, RC members should be designed to develop their full flexural

strength [2]. However, in some cases shear failure occurs, which characterized to be sudden and catastrophic. Accordingly, some researches have been devoted for strengthening the RC structures which deficient in shear. Heretofore, the traditional strengthening and repairing techniques have some drawbacks and limitations. Therefore, the novel strengthening technique by using Ultra-High Performance Concrete (UHPC), which is a hybrid of the cementitious materials and high-tensile strength steel fibers, have been established.

UHPC strengthening system is an alternative approach to rehabilitate or restore the deteriorated concrete members or to retrofit or strengthen the sound concrete members. It has exceptional advantages over traditional methods such as steel plate-bonding [2], FRP strengthening [3], [4], section enlargement, etc. These strengthening systems required a substrate preparation and sound surface. For example, Fiber Reinforced Polymer (FRP) [3] possess desired properties such as ultra-high strength, corrosion resistance, ease to apply and minimal size change, however, FRP system has some shortcomings, which mainly related to bonding and fire-resistance problems. On the other hand, UHPC as strengthening material of existing structures could be applied on either sound or deteriorated concrete surfaces. Therefore, for repair or rehabilitate concrete structures UHPC is a good option which mostly provided structural and durability requirements with substrate concrete [5].

UHPC was reported to have outstanding properties such as ultra-high strength, good flowability, excellent ductility, high serviceability, high strength-to-weight ratio, aesthetically appearance through self-levelling property, and overall superior durability properties such as low permeability. Moreover, UHPC is easily to apply on the existing old

reinforced structures and this making it suitable for rehabilitation and strengthening of RC structures.

UHPC is characterized as strain hardening cementitious-based materials [6]. The composition of UHPC is sand; cement; silica-fume; water; super-plasticizer and steel fibers of tensile strength over 3000 MPa [7], which introduce very high strength of matrix. This mix proportion with ultra-fine particles guarantees the homogeneity and low-permeability of UHPC.

In summary, in this thesis work, UHPC is utilized as strengthening material to retrofit the shear-deficient RC beams. A total of thirteen RC beams were prepared, cast and cured. Then, ten beams were retrofitted in different configurations and arrangements. The experimental test program was carried out to study the behaviour of such retrofitting technique. Both numerical and analytical models were developed. All experimental, numerical and analytical results were processed and interpreted.

## **1.2 Significance of this Research**

RC structural elements have deteriorated over the time and leading to reduce its load carrying capacity and service life. Efficient low-cost and easily applied repair materials are required for strengthening of such structures to increase their service life. CFRP laminates one of the methods that can be used for retrofitting of RC beams. However, using CFRP for strengthening of RC structures has proved to be very expensive, and it has some shortcomings, therefore, a new strengthening system should be implemented in construction industry such as using UHPC. The use of UHPC strengthening technique is more economical and possesses desired properties. The ease of application of UHPC and

availability of local raw materials in the Arab Gulf countries will significantly reduce the cost of producing UHPC.

Some researches have been conducted on using UHPC for retrofitting of conventional RC beams. However, most of those works studied the flexural behavior of retrofitted beams, and very limited works were found regarding the shear behaviour. Since shear failure is brittle and catastrophic, therefore, it is critically significant to examine the shear behaviour of such strengthened beams and a better understand of shear crack patterns.

### **1.3 Research Objectives**

The main objective of this thesis work is to conduct experimental, numerical and analytical investigations to study the shear behavior of conventional RC beams strengthened by UHPC.

The specific objectives are to:

1. Experimentally investigate the effect of UHPC strengthening on the shear capacity of conventional RC beam.
2. Study the effect of UHPC strengthening on crack propagation pattern and failure modes.
3. Evaluate the mechanical properties of UHPC and the bond assessment between the UHPC and NC.
4. Develop a numerical model using non-linear finite element software Abaqus to predict the behavior of conventional RC beams retrofitted in shear with UHPC.
5. Present a comparative study between the experimental test and FE results.

6. Develop an analytical model to estimate the contribution of UHPC to the overall shear capacity of retrofitted beams.

## **1.4 Thesis Structure**

This thesis is organized and documented into six chapters. *Chapters 1* and *2* present an introduction and a historical review of the previous research works that have been conducted in strengthening of conventional RC beams. *Chapter 3* describes the experimental test program where all research methodology and results are discussed in detail. The results of experimentally tested beams are validated using a numerical model in *Chapter 4*. *Chapter 5* develops an analytical solution to predict the shear strength of strengthened beams. Finally, some conclusions and recommendations are summarized in *Chapter 6*.

\*\*\*\*\*



## **CHAPTER 2**

### **LITERATURE REVIEW**

#### **2.1 Outline**

Ultra-high performance concrete (UHPC) was developed over the last two decades. Through this period, some researches have been conducted on utilizing this new concrete for constructions. Some of these studies were focused in materials development of UHPC, and others conducted exploratory investigations on possibility of utilizing UHPC for composite section. Although, the use of UHPC in real applications is still limited, the research is ongoing to set a design standard and construction guideline. In this chapter, a historical review of some of researches that have been conducted in UHPC is presented.

The constituent of UHPC made it a unique concrete with superior properties. Cementitious materials are mixing with steel fibers in optimum proportions to make a strain-hardening concrete with good ductility. The mechanical properties of UHPC were well studied and documented by many researchers. In addition, the durability aspects were evaluated through different examined tests and environments.

Recently, the novel ideas have been proposed for using UHPC as strengthening or repair materials. The excellent structural behaviour of UHPC made it possible to use for strengthening of structural members which deficient either in flexure or in shear.

## 2.2 Ultra-High Performance Concrete – A state of the Art

### 2.2.1 Mix Design

The mix proportion of UHPC is different from those for normal or high-strength concrete. In UHPC, a high cement and microsilica contents with low water-to-cementitious materials are adopted. Furthermore, the coarse aggregate was eliminated and replaced by fine sand to make a dense matrix. Adding the steel fibers made the concrete unique with high strength, ductility, and crack arresting property [8], [9]. UHPC is characterized as self-compacting concrete with outstanding mechanical properties [10]. There are different types of UHPC which vary in the mix proportions and types of constituents (mainly the metallic fibers and the cementitious materials)[11].

S. Ahmad et al. (2015) [9] developed an optimum mix design of UHPC which was made of local dune sand and other cementitious materials. [Table \(2.1\)](#) shows the mix proportions of UHPC. The Experimental tests were revealed that such mix gives compressive strength around 161 MPa, with flexural strength of 31 MPa.

**Table 2.1 Mix-design of UHPC [9]**

<i><b>Ingredients</b></i>	<i>Cement</i>	<i>Micro-silica</i>	<i>Fine sand</i>	<i>water</i>	<i>Superplasticizer</i>	<i>Steel fibers</i>
<i><b>Proportion (kg/m<sup>3</sup>)</b></i>	900	220	1005	163	40	157

Other mixes were also developed, for example Ductal Concrete [11] was a name given for UHPC with certain mix proportion. Ductal was made of premix: 2355 kg/m<sup>3</sup>; superplasticizer: 44.6 kg/m<sup>3</sup>; steel fibers: 195 kg/m<sup>3</sup>; and w/c ratio = 0.22. The results

showed that the compressive and flexural strengths were in range of 170-230MPa and 25-60MPa, respectively.

## **2.2.2 Mechanical Properties**

### ***1- Compressive Behaviour***

The compressive strength of UHPC is a topmost property, it was reported to be more than 150 MPa at age of 28-days, [8], [9]. The compressive strength of UHPC is a subjective factor which affected by the curing regime and the specimen geometry [8]. Lubbers (2003) [12] indicated that the compressive and flexural strengths of UHPC could be 2 to 3 times and 2 to 6 times higher than those for high performance concrete.

### ***2- Tensile Behaviour***

The tensile strength of UHPC was found to be proportion with steel fibers volume [13]. A range of (2% to 10%) of steel fibers are generally used to obtain the desired properties of concrete [14].

Graybeal and Baby [15] developed a test method for evaluation the tensile behaviour of ultra-high performance concrete (UHPC). [Fig. 2.1](#) shows a four-distinct response of UHPC in tensions , namely: elastic range, multi-cracking, crack straining, and localization [15]. After the cracks initiate (at the end of elastic range), the strain hardening takes place with microcracks, then the non-visible multi-cracks occur. Once the concrete reaches the ultimate resistance, the crack-localization is formed and the strain-softening phase will begin [16].

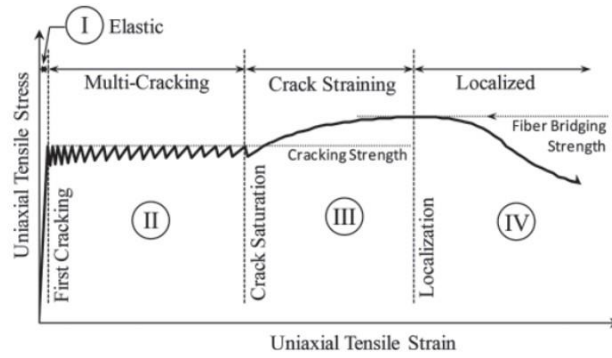


Figure 2.1 Tensile behaviour of UHPC [15]

### 3- *Flexural Behaviour*

The flexural behaviour of UHPC is more effective due to presence of steel fibers. Steel fibers develop the strain hardening of concrete, therefore they enhance the overall ductility response [17]. Lubbers [12] reported that the flexural strength of UHPC was 48 MPa which 2-6 times as compared to high strength concrete.

### 4- *Shear Behaviour*

It was reported by Son et al (1992) [17] that the presence of steel fibers in concrete will increase three times the initial and ultimate shear strength. Both stirrups and steel fibers act as shear reinforcement to arrest the opening of cracks [18].

### 2.2.3 Durability Characteristics

The UHPC has an excellent durability property, such as corrosion and abrasion resistances, chloride permeability, water penetration and low creep and shrinkage strains. Nevertheless, the construction practices of UHPC plays an important role in developing of these properties. The dense microstructure should be produced through proper batching, enough mixing time, right casting method, appropriate compaction and optimum curing.

S. Ahmad et al. (2015) [9] studied the durability characteristics of UHPC through conducting different tests. The UHPC showed negligible values of water penetration as well as chloride permeability. Moreover, the UHPC had resistance against the corrosion and sulfate. They concluded that the UHPC with proposed mix design is suitable for the severe environmental conditions.

The shrinkage and creep characteristics of UHPC were reported by many researches [8] [9]. It was found that UHPC has exhibited a good shrinkage and creep behaviors in both early-age and long-term testing. Lampropoulos et al [19] studied the effect of steel fibers on the shrinkage strains. They found that presence of 3% of steel fibers reduced the shrinkage strains by 30% over the time *Fig. 2.2*.

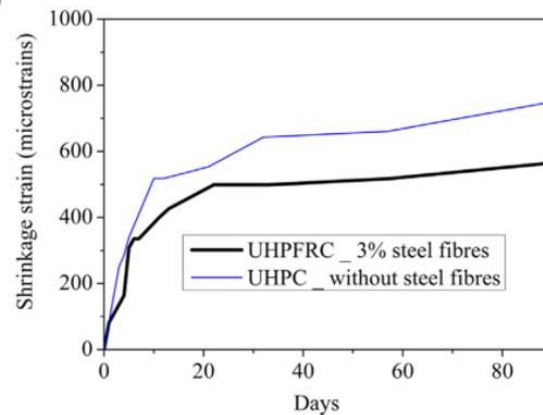


Figure 2.2 Shrinkage strain of UHPC [19]

### 2.3 Strengthening Techniques of RC Beams – A Review Study

Recently, many structures have been strengthened by different retrofitting techniques. Several research works have been conducted in this area, either by experimental testing of strengthened beams and study their structural behaviors (flexural or shear), or by developing a numerical modelling.

The strengthening techniques are widely varied, such as using glass or carbon fiber reinforced polymer (FRP), steel-plate bonding, aluminum plate or using high strength concretes. Moreover, the strengthening could be warping the whole section, U-wrapped or using jacketing arrangement at specific regions. Hereafter the review of some studies that have been done regarding the strengthening and restoring of structural members.

### **2.3.1 Flexural Strengthening**

The flexural behaviour of strengthened conventional RC beams using ultra-high performance concrete (UHPC) was experimentally investigated by Al-Osta et al (2017) [20]. The UHPC were applied to the normal concrete by two different techniques: either by sandblasting the substrate surfaces or by using epoxy adhesive bonding. In addition, three different configurations were done to evaluate the most effective scheme for flexural enhancement. The experimental tests were carried out in the strengthened beams and in the materials to evaluate their properties as well as the bonding assessment. Beside the experimental investigation, the numerical and analytical models were developed. The results showed that the proposed strengthening technique was enhanced the structural performance of retrofitted beams through increasing flexural capacity and overall stiffness. Moreover, the study revealed that the strengthening in three-sided jacketing was the most enhancement in moment capacity, *Fig. 2.3*. In addition, the proposed Finite element model expected the load-deflection response and the crack pattern in good matching with experimental tests, thereafter, FE modelling is a reliable tool for estimating the flexural behaviour of such strengthening technique, *Fig. 2.4*.

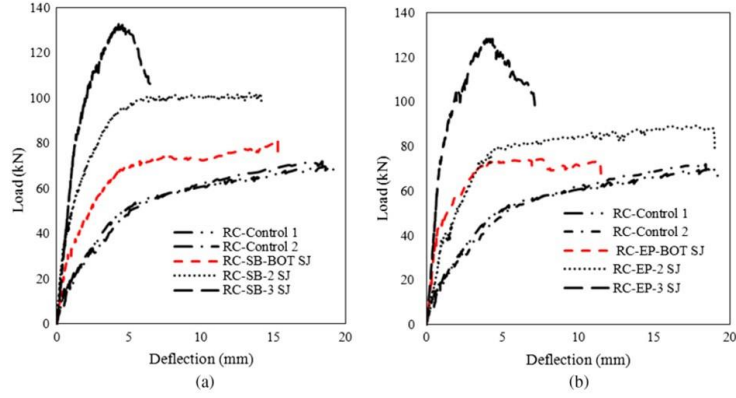


Figure 2.3 Force-deflection response of control and strengthened beams [20]

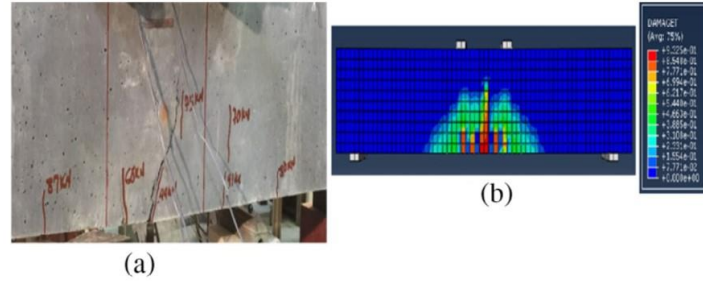


Figure 2.4 Crack pattern of experimental FE results [20]

Masse & Bruhwiler (2014) [16] investigated the structural behavior of using UHPC for retrofitting the beams and slabs. They prepared composite beams and slabs, which included 50mm layer of UHPC, and testing them under different types of loading. The analytical models were also developed to assess the capacity of the composite beams. The results clearly demonstrated that the use of UHPC layer over RC section had an effective enhancement on the load bearing capacity.

The efficiency of using UHPC for strengthening of conventional RC beams was demonstrated by Lampropoulos et al (2016) [19]. The experimental investigation and numerical modeling were conducted. Different types of configuration of UHPC layers were used, in tensile face, compressive face and with three-face jacketing [Fig. 2.5](#). The results

revealed that a significant moment increment when three sides jacketing was used as shown in.

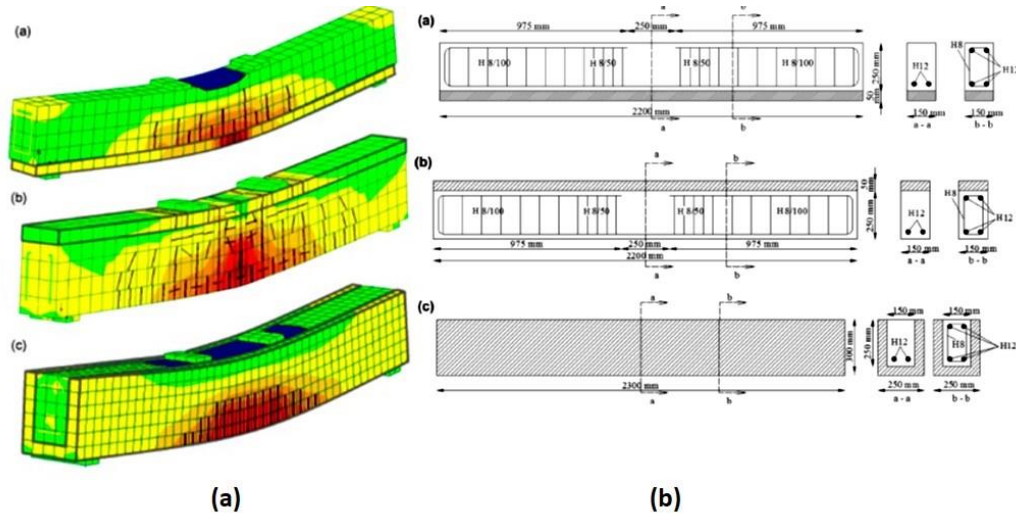


Figure 2.5 (a) FE modeling, (b) Jacketing configurations [19]

Iqbal et al (2016) [6] examined the use of Steel Fiber Reinforced High Strength Lightweight Self Compacting Concrete (SHLSCC) as strengthening technique of RC beams. This study developed an analytical model to predict the flexural capacities of such strengthened beams. They claimed that SHLSCC method is an effective technique to strengthen the flexural members. The experimental results showed that the improvement in strength was dependent on the thickness of strengthening layer (SHLSCC layer) in the tension zone.

The strengthening technique using a 40mm layer of High Performance Fiber Reinforced Concrete - HPFRC was experimentally and numerically studied by Martinola et al (2010) [21]. Full-scale beams (4.55 m long) were prepared, cast and strengthened with HPFRC layers. The finite element model (FEM) was developed using Diana package in order to study the effects of different parameters on the structural behaviour of strengthened beams.



The results of both experimental and FEM investigations showed that the using of HPFRC jacket for strengthening or retrofitting has a significant role in the increasing of the load bearing capacity (increasing in the ultimate load up to 2.15 times). Furthermore, a good enhancement in the durability of the beams was observed due to using of HPFRC jacket, *Fig. 2.6.*

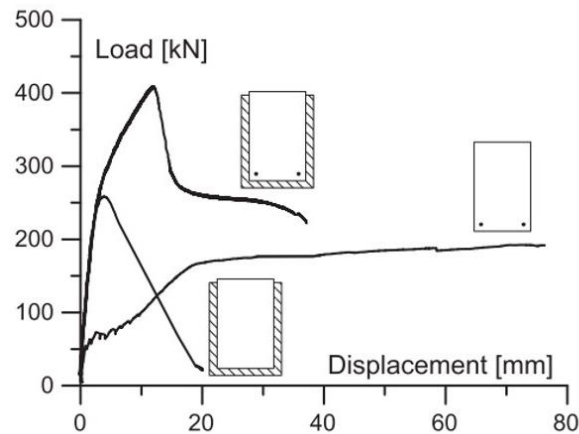


Figure 2.6 Load-displacement behaviour of strengthened beams [22]

### 2.3.2 Shear Strengthening

Although the shear behaviour of normal concrete is not easy to predict because of many factors that are contributing to the total shear strength, the assessment of shear capacity of members is important because of brittle and sudden failure of shear. As such, the shear strengthening of existing RC structures becomes necessary in many cases.

In the literature, different strengthening techniques were used. However, the drawbacks of some of these techniques made it necessary to look for an alternative strengthening system which ensure all repairing requirements. The following are a review of some previous works that have been done in shear strengthening of RC beams.

### ***1- Shear strengthening using High-Strength Concretes***

Several high strength concretes have been developed. Classification of these concretes is mainly based on the compressive strength, such as High Strength Concrete (HSC); Very High Strength Concrete (VHSC); Ultra High Strength Concrete (UHSC); Super High Strength Concrete (SHSC) [11]. Since the last two decades, the using of these high-strength concretes in strengthening of existing deteriorated structures has been widely utilized.

The flexural and shear behaviour of using High-Performance Fiber-Reinforced Concrete (HPFRC) for retrofitting the RC beams was studied by Alaei and Karihaloo (2003) [23]. Both experimental and analytical studies were carried out. The experimental work comprises preparing the conventional RC beams and HPFRCC strips which adhesively bonded to the substrate surfaces using adhesive epoxy. Different configuration with different scheme dimensions were used in order to prove which is the significant for flexural improvement, *Fig. 2.7*. The results of this study proved the feasibility of using HPFRCC for upgrading the flexural and shear capacities of member as well as enhancing the durability properties.

Noshiravani et al (2013) [24] experimentally investigated the composite section of reinforced concrete and ultra-high performance concrete (UHPC). The composite beams have 250mm deep of RC and 50mm thick of UHPC. This study concluded that adding a layer of UHPC at tension face is an effective shear strengthening technique. In addition, it was noticed the improvement in the deformation capacity of the member. *Fig. 2.8* shows beams failing in flexure, load-deflection response and cracking modes.

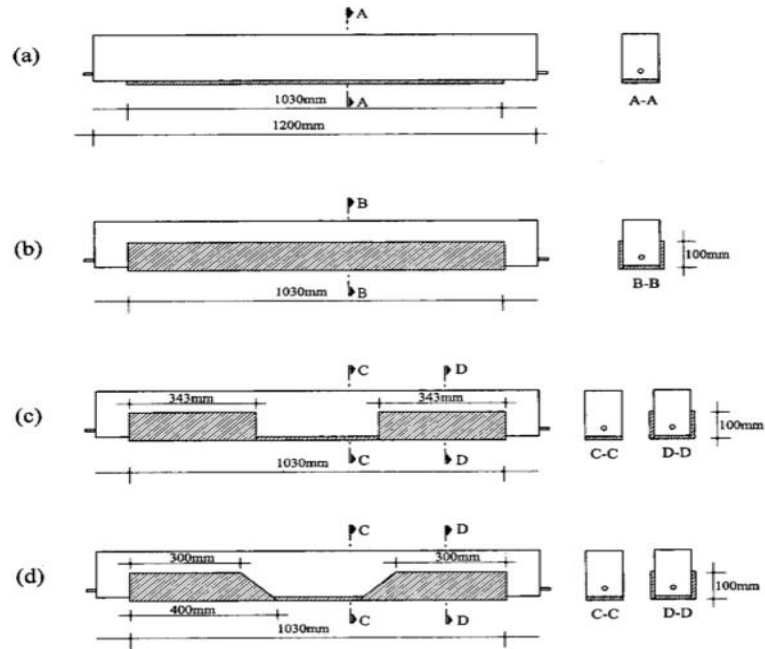


Figure 2.7 Strengthening arrangement [23]

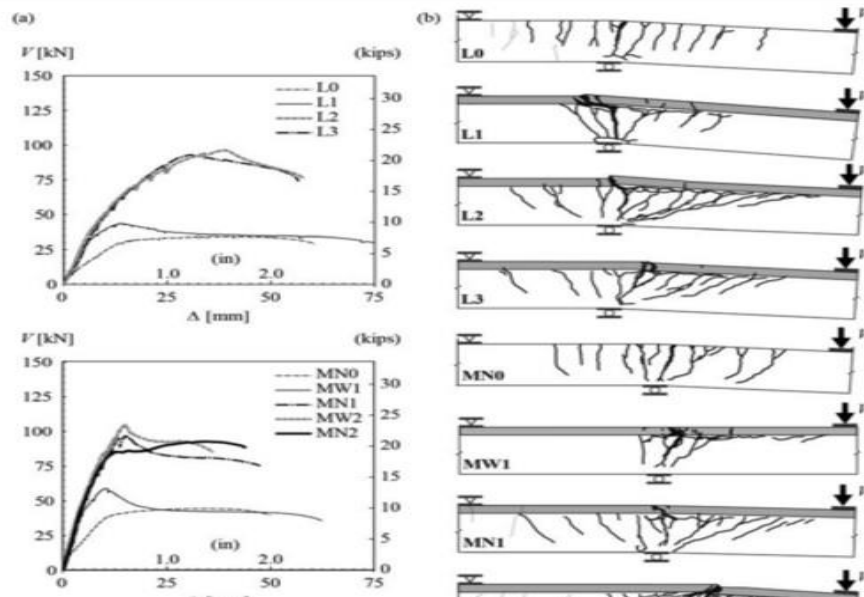


Figure 2.8 Load-deflection curves [24]

The flexural and shear capacities of UHPC – normal strength concrete composite beams without stirrups were evaluated by Hussein and Amleh (2015) [25]. The beam specimen had the UHPC in tension and the normal concrete layer in compression. The results showed

that the performance of such composite technique was improved in both flexural and shear capacities. *Fig. 2.9* and *Fig. 2.10* show the reinforcement pattern and test configuration and cracking mode for UHPC -NSC flexural prisms, respectively.

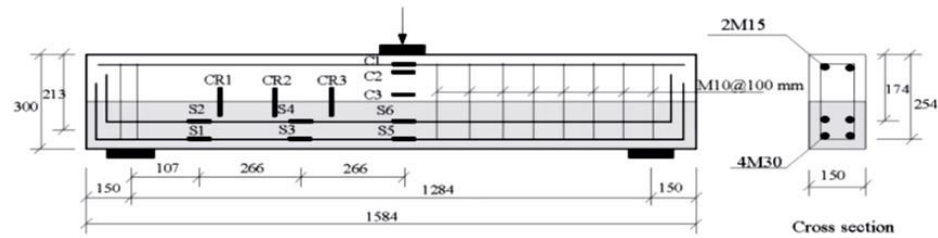


Figure 2.9 Beam details [25]

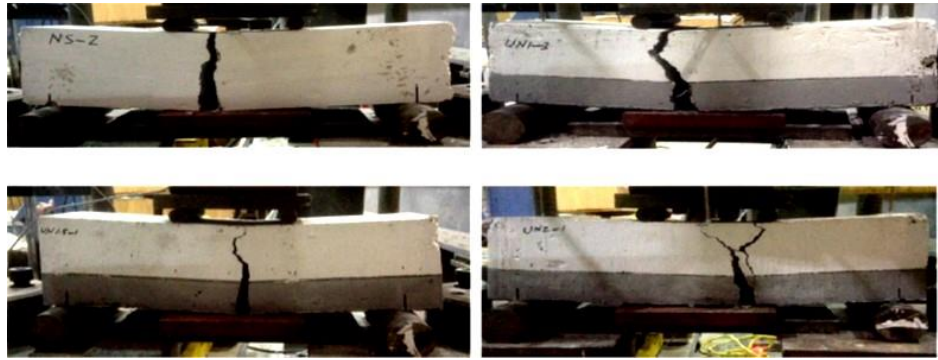


Figure 2.10 Failure of UHPC -NSC beams [25]

Ruano et al (2014) [26] demonstrated the structural performance of using Steel Fiber Reinforced Concrete (SFRC) in shear retrofitting of RC beams. In order to assess the contribution of fiber content, different dosages of fiber were used ( $30\text{kg/m}^3$  and  $60\text{kg/m}^3$ ). The experimental program involved 18 RC beams where 8 of them were damaged and repaired and the rest were initially strengthened. The results proved that the presence of steel fibers prevent debonding and generally enhance overall integrity of the beams. In addition, the effectiveness of the SFRC for shear strengthening is directly related to the use of steel stirrups.

Chalioris et al (2014) [27] investigated the use of thin reinforced self-compacting concrete (SCC) for strengthening of conventional RC beams. The experimental study comprised 20-beams, which designed to present a shear failure. The results showed an increase in the flexural strength with improved in the ductility and favorable failure behavior. The study claimed that the high strength self-compacting concrete (SCC) is a quick option for rehabilitation or strengthening the existing RC beams.

Farhat et al (2007) [28] studied the application and behavior of the high-performance fiber reinforced cementitious composite – HPFRCC (commercially known as CARDIFRC) for retrofitting the damaged beams. The experimental work consists of testing 24 RC beams. Sixteen of them were strengthened with CARDIFRC strips and the remaining left as control. The results of the experimental work showed that if the configuration of retrofitting is used on the tension face as well as to the sides, then the failure load will increase up to 86%. Moreover, the thermal cycling load was carried out on the retrofitted RC beams to evaluate the bond between the parent concrete and the repaired concrete (CARDIFRC). The results of such testing exhibited a very good bond after the thermal loading. Therefore, the authors recommended the use of this retrofitting in the hot climate.

Habel et al (2007) [29] conducted a study on the structural response of 12 – full-scale composite beams made of ultra-high performance fiber reinforced concrete and conventional concrete. The conventional beams were prepared by casting UHPC layer on tension face. Moreover, the steel reinforcement was embedded in UHPC layer to increase the stiffness and resistance. It was observed that, the UHPC significantly improved the structural capacity of the composite member including, reducing the cracks and localized

cracks, increasing stiffness and minimizing the deflections. [Fig. 2.11](#) shows the test set-up of composite beam and force-deflection response of tested beams.

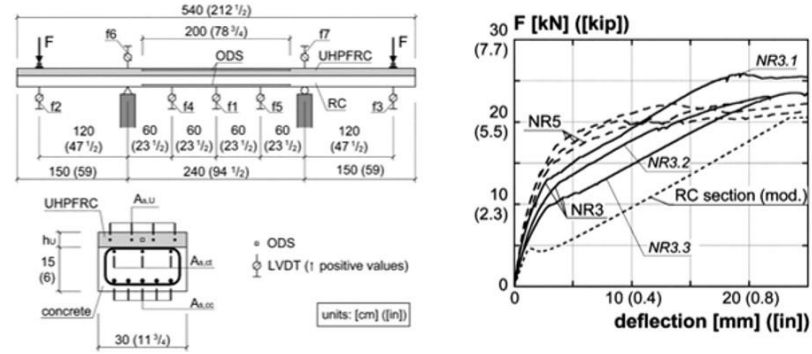


Figure 2.11 Test set-up of composite beam and force-deflection response of tested beams [29]

A 2D nonlinear finite element modeling of RC beams retrofitted in shear with high-performance self-compacting concrete was developed by Ruano et al. (2015) [30]. The numerical results demonstrated that the fiber content enhanced the load bearing capacity of retrofitted RC beams. However, the proposed numerical model did not capture the debonding issue. In addition, the numerical results showed that the type and content of steel fibers were insignificant in overall behaviour of repaired or strengthened beams.

## 2- Shear strengthening using FRP

The using of Fiber Reinforced Polymer (FRP) for strengthening of structures becomes a popular due to its high tensile strength and easy to apply. FRP laminate is externally bonding on the concrete substrate followed by applying a coating [3]. Extensive experimentally studies and application fields have been undertaken using FRP for retrofitting task.

Ombres (2014) [31] studied the shear behavior of RC beams strengthened by Fabric Reinforced Cementitious Matrix (FRCM). The fibers of FRCM system was made of PBO (Polypara-phenylene-benzo bisthiazole) meshes as shown in [Fig. 2.12](#). Different configuration of FRCM strips (U-wrapped continuous and discontinuous). Moreover, an analytical model was formulated to predict the contributions of FRCM in shear strength of strengthened beam. The results showed that FRCM strengthening method increased the shear strength of RC beam when adequate strengthening configuration is adopted.



[Figure 2.12](#) Wrapping the RC beams with fibers of FRCM [31]

ACI developed a design guideline for FRP externally bonding strengthening system. ACI 440.2R-08 pointed all properties of FRP and relating construction practices as well as the maintenance [3].

A finite element model to simulate the shear behaviour of strengthened RC beam with carbon fiber reinforced polymer (CFRP) laminates was developed by Khan et al (2017) [32]. The validation of experimentally tested full-scale T beams was also presented. The results of the numerical modeling pointed that the special care should be taken on the bond between the different components of strengthened beams, i.e. concrete, steel and CFRP strips. The proposed model predicted the shear behaviour in good agreement with the

experimental investigations, and this attributed to the appropriate material models and proper interaction between these materials.

### 3- Shear strengthening using Steel Plates or Aluminum Alloys

Many researchers studied the utilizing of strengthening the shear-deficient reinforced beams with externally bonding steel-plated or aluminum alloys. Altin et al (2005) [2] prepared, cast and retrofitted a total of ten RC beams. The retrofitting of beams was by using the external bonding of steel plates with different configuration. The results showed that an improvement in shear capacity and ductility of strengthened beams. As the arrangement of steel straps was concern, the closed-spacing and large-area of plates in the shear span zones had increased the shear capacity and reduced the inclined cracks, [Fig. 2.13](#).

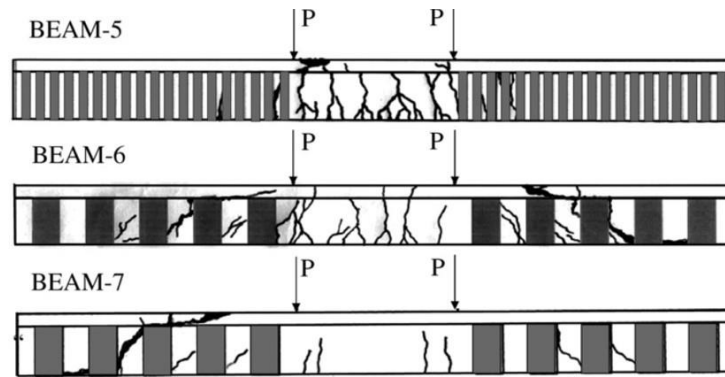


[Figure 2.13](#) External bonding of steel plates with different arrangements [2]

Abdalla et al (2016) [33] applied the high strength Aluminum Alloys (AA) to strengthen the RC beams in shear. AA strips were externally bonded to the beam surfaces in different orientations and configurations (at angles of 90 or 45 degrees). It was observed that the shear capacity of retrofitted beams was increased in range of 24% to 89% depending on



the orientation of AA plates. The plates with angle of 45-degree was the most efficient orientation in increasing the load bearing capacity of retrofitted beams, *Fig. 2.14*.

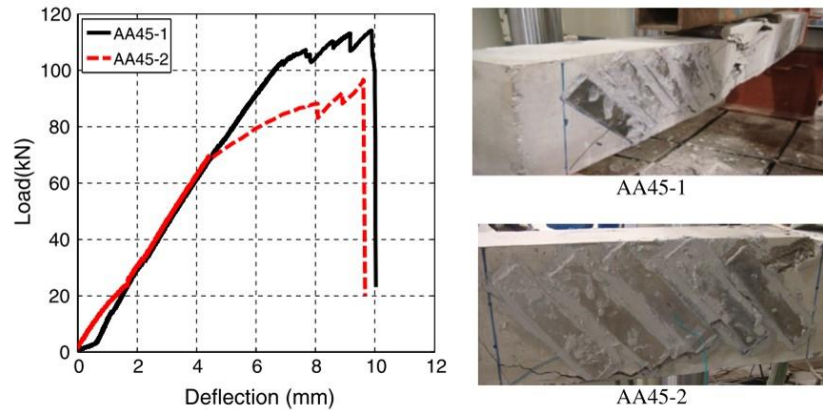


**Figure 2.14 Using Aluminum Alloys (AA) to strengthen the RC beams in shear [33]**

*In Summary*, despite these research works on using UHPC in repairing and strengthening of RC beams, it can be noted that none of these works had considered the individual contribution of longitudinal sides strengthening on the shear. In addition, information regarding a comparison of two techniques for shear strengthening of RC beams using UHPC is lacking in the literature i.e. using sandblasting RC beams surfaces and casting UHPC around the beams inside a mold or by bonding prefabricated UHPC strips to the RC beams using epoxy adhesive. Moreover, the effect of shear span-to-depth ratio on the behaviour of strengthened beams was not investigated. Therefore, the objective of this study is to assess the individual as well as the combined effect of jacketing of the sides of RC beam with UHPC. Additionally, comparison of the two techniques used to apply UHPC strengthening to the beams is also studied.

\*\*\*\*\*

## CHAPTER 3

### EXPERIMENTAL PROGRAM

#### 3.1 General

In this research, a comprehensive experimental work was conducted including mainly four phases as shown in *Fig. 3.1*. Experimental investigations started by casting a total of thirteen conventional reinforced concrete beams which present a shear failure. Then, some of these beams were retrofitted by ultra-high performance concrete (UHPC) jacketing in two different configurations using two different applying techniques (*Table 3.1*). Meanwhile, more than 100 small specimens were prepared and tested in order to evaluate the mechanical properties of all used materials (*Table 3.2*). In addition, the bond testing was carried out to evaluate the bond strength between concrete substrate and UHPC. Finally, the beam tested program was conducted by test the beam specimens by varying the shear span-to-depth ratio ( $a/d$ ). All experimental tests were performed at KFUPM laboratories (Concrete Lab, Structural Lab and Heavy Structures Testing - Reaction Floor Lab). The data of these tests was processed and interpolated into useful results which help in understanding the structural behaviour of retrofitted beam. This chapter elaborates in detail all experimental works and discusses the results.

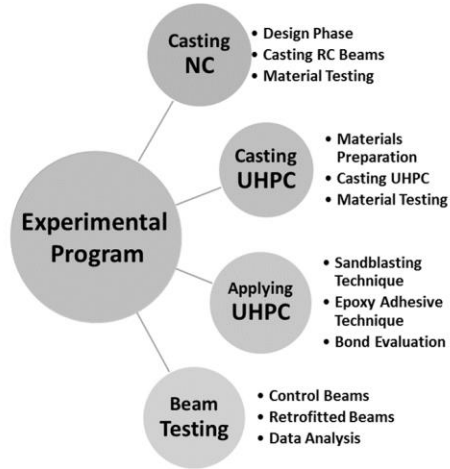


Figure 3.1 Flowchart of all works involved in the experimental program

Table 3.1 Beams ID and description

Group	Beam ID	Beam Designation	Strengthening Technique	Dimensions $b \times h \times L$ (mm)	a/d ratio	Shear Span (mm)
1st	<i>CT-1.0</i>	Control Beam	N/A	140 x 230 x 1120	1.0	200
	<i>SB-2SJ-1.0</i>	Strengthened Beam at 2-sides	Sandblast (SB)	200 x 230 x 1120	1.0	200
	<i>SB-3SJ-1.0</i>	Strengthened Beam at 3- sides	Sandblast (SB)	200 x 260 x 1120	1.0	200
2nd	<i>CT-1.5</i>	Control Beam	N/A	140 x 230 x 1120	1.5	280
	<i>SB-2SJ-1.5</i>	Strengthened Beam at 2- sides	Sandblast (SB)	200 x 230 x 1120	1.5	280
	<i>SB-3SJ-1.5</i>	Strengthened Beam at 3- sides	Sandblast (SB)	200 x 260 x 1120	1.5	280
3rd	<i>CT-2.0</i>	Control Beam	N/A	140 x 230 x 1120	2.0	384
	<i>SB-2SJ-2.0</i>	Strengthened Beam at 2- sides	Sandblast (SB)	200 x 230 x 1120	2.0	384
	<i>SB-3SJ-2.0</i>	Strengthened Beam at 3- sides	Sandblast (SB)	200 x 260 x 1120	2.0	384
4th	<i>EP-2SJ-1.0</i>	Strengthened Beam at 2- sides	Epoxy Adhesive (EP)	200 x 230 x 1120	1.0	200
	<i>EP-3SJ-1.0</i>	Strengthened Beam at 3- sides	Epoxy Adhesive (EP)	200 x 260 x 1120	1.0	200
5th	<i>EP-2SJ-1.5</i>	Strengthened Beam at 2- sides	Epoxy Adhesive (EP)	200 x 230 x 1120	1.5	280
	<i>EP-3SJ-1.5</i>	Strengthened Beam at 3- sides	Epoxy Adhesive (EP)	200 x 260 x 1120	1.5	280

**Table 3.2 Specimen details for the properties of materials**

<b>Material</b>	<b>Test type</b>	<b>Specimen size</b>	<b>No. of samples</b>
<b>Normal Concrete (NC)</b>	Compressive strength	75×150 mm cylinder	6
	Modulus of elasticity	75×150 mm cylinder	6
<b>Ultra-high performance concrete (UHPC)</b>	Compressive strength	50×50×50 mm cube	15
	Stress-strain behaviour and modulus of elasticity	75×150 mm cylinder	20
	Direct tension	490×116×35 dogbone	15
	Flexural strength	40×40×160 prism	15
<b>Composite NC/UHPC</b>	Splitting tensile strength	75×150 mm composite cylinder	6
	Slant shear strength	75×150 mm composite cylinder	6
<b>Steel Reinforcement</b>	Direct tension	Ø8, Ø12, Ø20	6

### **3.2 Casting the RC Beams**

Most of the reinforced concrete structures are suffering from deficiencies either in their structural performance or durability properties, thus they need to be repaired or retrofitted. The strengthening technique of existing structures becomes most important and engineering issue. Recently, the existing reinforced concrete beams have been retrofitted with a new technique called UHPC strengthening. To demonstrate this strengthening technique, conventional reinforced concrete beams need to be designed, prepared, cast, cured and then strengthened. The casting of RC beams was done in the factory using ready-mix concrete for the purpose of casting all beams from the same concrete mixture.

### 3.2.1 Design of RC Beams

The RC beams were designed in compliance with ACI 318-14 [34] and the drawings of reinforcement details were prepared. The design had considered that the beams were deficient in shear by placing the stirrups in wide spacing. Moreover, large steel rebars were provided in the bottom and top of the section (bottom:  $2\phi 20$ ; top:  $2\phi 12$ ), where these longitudinal bars hooked upward at the ends. The shear reinforcement was provided by stirrups of  $\phi 8$  at spacing of  $120\text{mm}$ , where the first stirrups near the supports placed at one-half of that spacing as it is common used in practice. All beams had identical cross-section as  $140\text{mm}$  wide by  $230\text{mm}$  high with overall length of  $1120\text{mm}$ , *Fig. 3.2* shows the details of designed RC beams. The beams are classified as short beam in order to ensure the failure to be in shear.

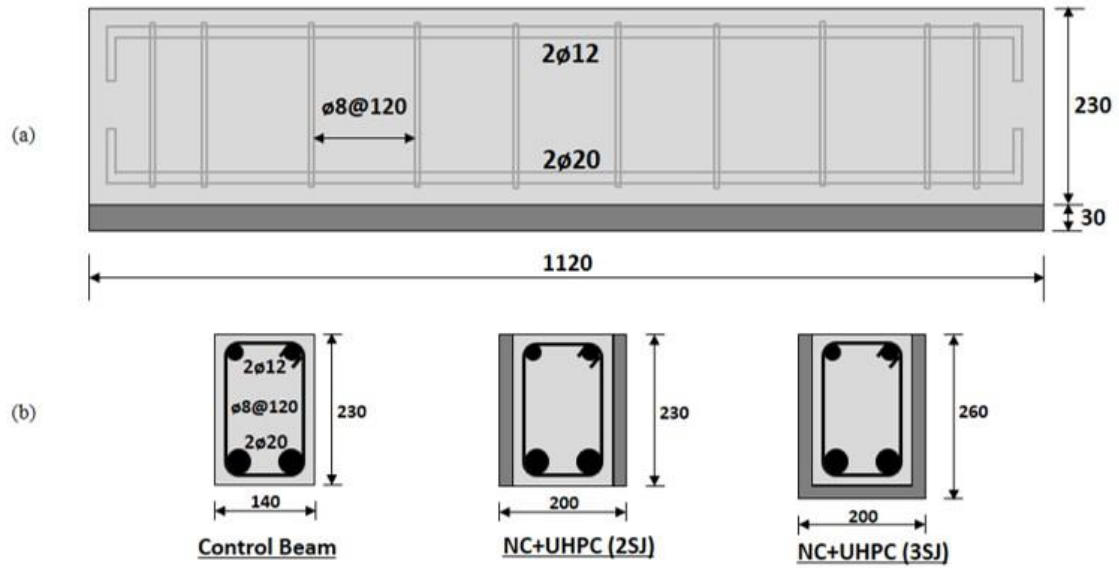


Figure 3.2 (a) RC beams details, (b) strengthening configuration

### 3.2.2 Preparation of Molds and Steel Cages

The formwork was prepared using the steel molds with dimensions of ( $140\text{mm}\times 230\text{mm}\times 1120\text{mm}$ ). Thirteen molds were prepared inside the PRAINSA factory

and lubricated by the oil for easily demolding the beams. In the steel workshop, reinforcing steels were prepared with considered specifications and required dimensions. All longitudinal and transverse steels were fabricated and placed inside the molds as shown in [Fig. 3.3](#). A 20mm cover was adjusted at all sides using plastic spacers.

### 3.2.3 Installing the Steel Strain Gauges

A strain gauge is an electrical device used to record strains over a certain area and these strains are used to calculate the resulting stresses. A strain gauge is used frequently in research work and structural engineering testing. In this work, the surface of steel was cleaned by using sandpapers. Then, strain gauges were installed on both main rebars and stirrups which near the supports, i.e. at the critical shear zones as shown in [Fig. 3.3](#). Mainly, the strain recordings of stirrups are of importance in order to study the effectiveness of the strengthening technique in shear.



Figure 3.3 (a) Reinforcement steel cage, (b) Installation of strain gauge on the stirrup

### 3.2.4 Casting the Normal Concrete

At the stage where all molds, reinforcement steel, and instrumentation were arranged, the constituents of normal concrete were prepared inside the factory. A normal ready-mix concrete was used without any admixtures. The concrete was poured into the molds using

the pumping and vibrator. A slump test was checked for specification compliance and control quality. In addition, the cylinder specimens were taken from the same mixture to evaluate the mechanical properties of concrete as will be explained in the next section.

Next day of casting, all beams were demolded and transferred to the KFUPM laboratories and kept inside a water tank for 28-days curing, [Fig. 3.4](#).

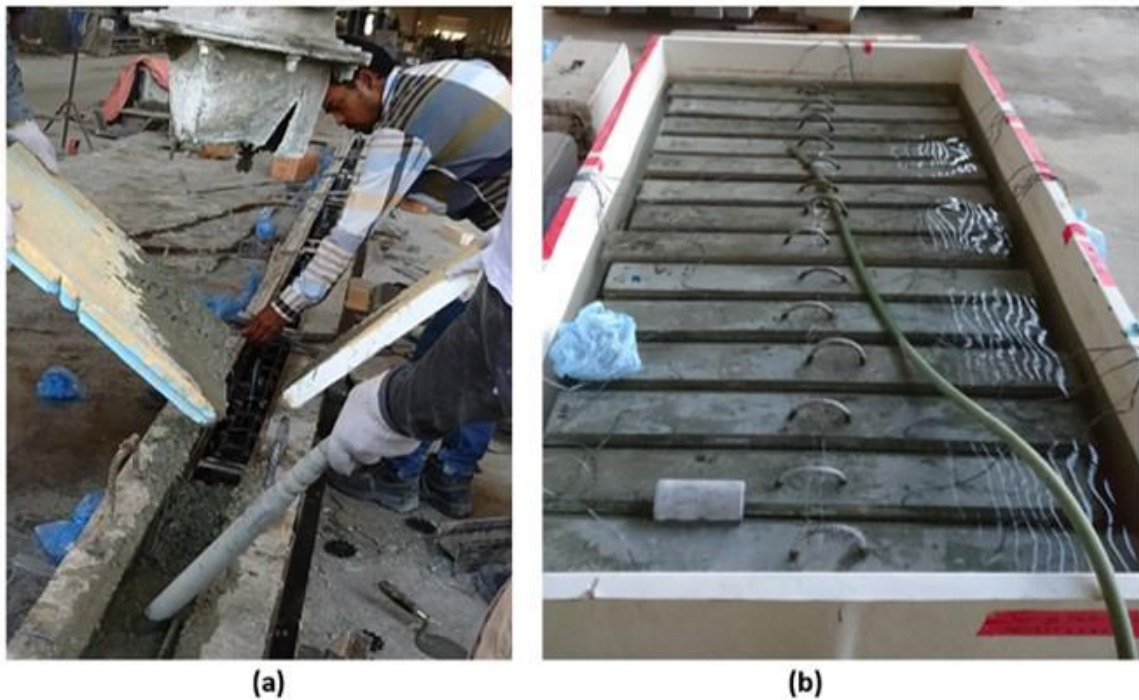


[Figure 3.4 \(a\) Casting the normal concrete beams, \(b\) Curing tank](#)

### **3.2.5 Mechanical Properties of Normal Concrete**

A total of twelve cylindrical specimens (75×150mm) were prepared from the same concrete mix in order to evaluate the mechanical properties of concrete. Mainly, the compressive strength, modulus of elasticity and stress-strain behaviour, are needed for both numerical and analytical modeling.



### ***1- Uniaxial Compression Test:***

The uniaxial compression test is an important test to measure the compressive strength of brittle materials. It is simple and quick test and it gives an indication of quality of concrete. It is recognized by many material standards, ASTM C39 [35] explained this test method. The cylindrical specimen (28-day age) was placed in the digital compression test machine, which has ultimate load capacity of 3000kN, and the load was applied continuously up to the crushing of concrete had occurred. For accurate results and equally load distributed, the upper surface of the specimen was prepared by sulfur-capped.

The average value of compressive strength was obtained as 65MPa with minimum and maximum value of 59MPa and 71MPa respectively and standard of deviation of 4.6 as shown in [Table 3.3](#). The result of compressive strength of this concrete is in the lower side of high strength concrete.

### ***2- Elasticity Test:***

The modulus of elasticity is a fundamental property of concrete. It is used in calculation of deflection and modeling the concrete in finite element method. ASTM C469 [36] gives the procedure for conducting this test. A cylinder specimen of 150×75mm was used and the surface was prepared by sulfur capping. Test setup consists of steel ring and the two compressometer gauges (LVDT's) that were installed to monitor the axial deformation. The concrete specimen was fixed inside this setup and the compression-testing machine applied static load up to 40% of failure load. The stresses versus strains was plotted and from the linear part of the curve, [Fig. 3.5](#), the modulus of elasticity can be calculated using following equation:



$$E = (S_2 - S_1)/(\epsilon_2 - 0.000050)$$

where:

E = modulus of elasticity, MPa,

S<sub>2</sub> = stress at 40 % of ultimate load, MPa

S<sub>1</sub> = stress associated with strain  $\epsilon_1$  of 50 microstrain, MPa, and

$\epsilon_2$  = longitudinal strain corresponding to stress S<sub>2</sub>.

The average value of modulus of elasticity was obtained as 31GPa with minimum and maximum value of 26GPa and 34GPa respectively and standard of deviation of 2.9 as shown in [Table 3.4](#).

**Table 3.3 Mechanical properties of normal concrete (at 28-days)**

<i>Property</i>	<i>Min. value</i>	<i>Max. value</i>	<i>Average value</i>	<i>Standard od deviation</i>
Compressive Strength, MPa	59	71	65	4.6
Modulus of Elasticity, GPa	26	34	31	2.9

### ***3- Stress-Strain behaviour***

The complete stress-strain behaviour of concrete can be obtained in the same procedure as the elasticity test. Instead of stopping the test at 40% of failure load, the load should be continued until failure of specimen. The typical stress-strain curve of concrete in compression is shown in [Fig. 3.5](#).

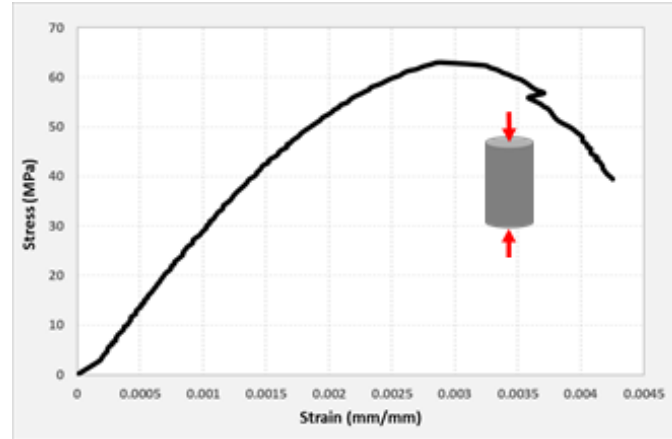


Figure 3.5 Stress-strain behaviour of normal concrete

### 3.2.6 Uniaxial Direct Tensile Test of Reinforcement Steel

The tensile testing of steel reinforcement was carried out in the structural lab at KFUPM. A total of six samples of steel rebars (280mm in length) with different diameters ( $\phi 8$ ,  $\phi 12$ ,  $\phi 20$ ) were prepared for testing. This test method is documented by ASTM A370 [37]. The results of this test, specifically: yielding strength and elastic modulus of steel, will be used in the analytical calculations and later in modelling the steel rebars in finite element simulation.

The testing setup comprises Universal Testing Machine - UTM (*Instron-5589* with capacity of 600kN), extensometer device with gauge-length of 50mm, LVDT and data-logger. The UTM applied the tensile load at rate of 1.5mm/min and the loads were recording every 0.05mm as displacement-controlled. The axial elongations were monitoring by the extensometer, which attached to the steel rebar between the machine's grips, where the LVDT controlled the data recordings in the data-logger.

The load was continuously increased until the complete failure of specimen after the necking was formed. [Table 3.4](#) presents the results of this test which shows that the steel

reinforcement has the following properties: average yield strength equals 610.2MPa with yielding strain of 0.00378mm/mm; the modulus of elasticity equals 204.6 GPa; and the ultimate strength was 710.1MPa. The typical stress-strain curve of the steel reinforcement is shown in *Fig. 3.6*.

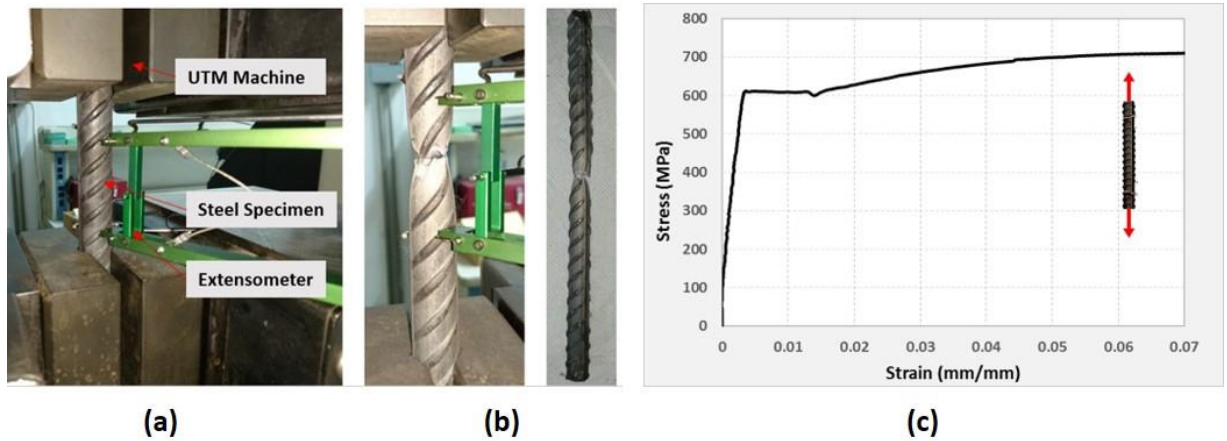


Figure 3.6 Uniaxial direct tensile test of steel rebar: (a) Test setup, (b) specimen failure, (c) stress-strain response

Table 3.4 Mechanical properties of Steel Reinforcement

<i>Property</i>	<i>Average value</i>
Yield Strength, MPa	610
Yield Strain, mm/mm	0.00378
Elastic Modulus, GPa	204.6
Ultimate Strength, MPa	710.1

### 3.3 Casting The UHPC

In this stage, wood molds were prepared with the desired dimensions. Since there are two different strengthening techniques were used, therefore two types of molds were fabricated at KFUPM workshop. The beam-size molds used for directly cast-in the fresh UHPC to the RC beams. Second type, the strips wood molds utilized for epoxy-adhesive

strengthening technique where the UHPC strips cast separately and then applied to the RC beam surfaces using epoxy adhesive bonding.

The batching of UHPC including: cement; sand; microsilica; superplasticizer; steel fibers; and water as shown in [Fig. 3.7](#), was arranged and then concrete was cast and cured.

### **3.3.1 UHPC Mix Design**

UHPC is a new concrete with outstanding properties. In this work, the mix design in [Table 2.1](#), that was developed by Ahmad et al [9], was used. The following is a brief overview for each ingredient of UHPC concrete:

#### ***1- Cement, Sand and Water:***

Ordinary Portland cement (Type-1) was used in this mix of UHPC. The water-to-binder ratio was 0.145 which is very low ratio. The fine dune sand was added to the mixture and the coarse aggregated was eliminated to improve the homogeneity of the mix.

#### ***2- Microsilica***

The microsilica was added to the mix of UHPC which is very fine material. The main role of microsilica is to fill the voids between the cement and the sand particles, therefore this will increase the impermeability of concrete. In this work, the Elkem microsilica was provided from one company in the KSA.

#### ***3- Steel Fibers***

The enormous properties of UHPC is coming from the steel fibers through reducing the brittleness of cementitious materials and increasing the strain-hardening of concrete. The

steel fibers are the essential component of such concrete. Adding the steel fibers to the mix will take up the additional tensile stresses developed in concrete, therefore this will enhance the ductility property of concrete. Two types of steel fibers (with ratio of 1:1) were added: Straight fibers (0.1mm in diameter with length of 12.5mm; and tensile strength is 2500MPa) and Hooked fibers (0.2mm in diameter with length of 25mm; and tensile strength is 2500MPa) for purpose of increasing the interlock between fibers and therefore increase the crack bridging. However, according to published studies [38][19], the distribution and orientation of steel fibers through the concrete have a significant effect in post-cracking response.

#### ***4- Superplasticizer***

A relatively high dosage of liquid superplasticizer (commercially known as Glenium-51) was added to the mix. The superplasticizer will increase the strength and workability of concrete. On the other hand, it will reduce the water demand.

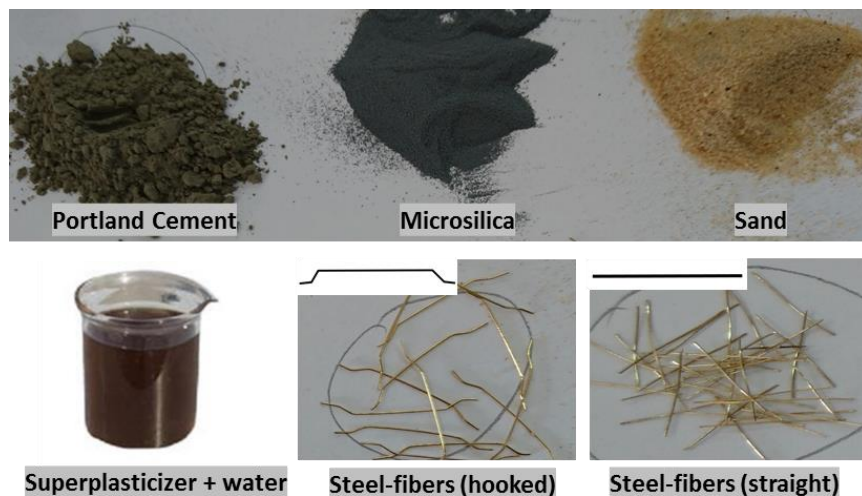


**Figure 3.7 UHPC ingredients**

### 3.3.2 UHPC Mixing Methodology

All UHPC constituents were weighted and prepared, the mixing procedure was done according to the report prepared by *Federal Highway Administration in US (FHWA)* [8]. The special mixer called horizontal planetary mixer was used as shown in [Fig. 3.8](#). The first step was adding the drying materials (cement, sand and microsilica) separately to the mixer and mixed then for 3-minutes. Then the liquids (water and superplasticizer) were mixing separately in a container and adding slowly over the whole mixing-time. Finally, the steel fibers (straight and hooked) were added in slow rate to avoid the accumulation of fibers in one place and to ensure equally distributed of the them through the mix. The total mixing time was around (15-20) minutes. This long time of mixing was required for UHPC because of ultra-fine particles which need to be lubricated and thoroughly mixed together to produce a dense concrete.



Figure 3.8 UHPC mixing methodology



Then the UHPC mixture was poured into the molds, which were placed on vibrating table as shown in *Fig. 3.9* and *Fig. 3.10*, and here the key point is to pour the concrete from one side and let it self-flow through the form [8].

The flowability of UHPC mixture was checked using impact table test according to ASTM C1437 [39]. The flowability was found in average of 190mm which is in acceptable range as reported by S. Ahmad et al [9].

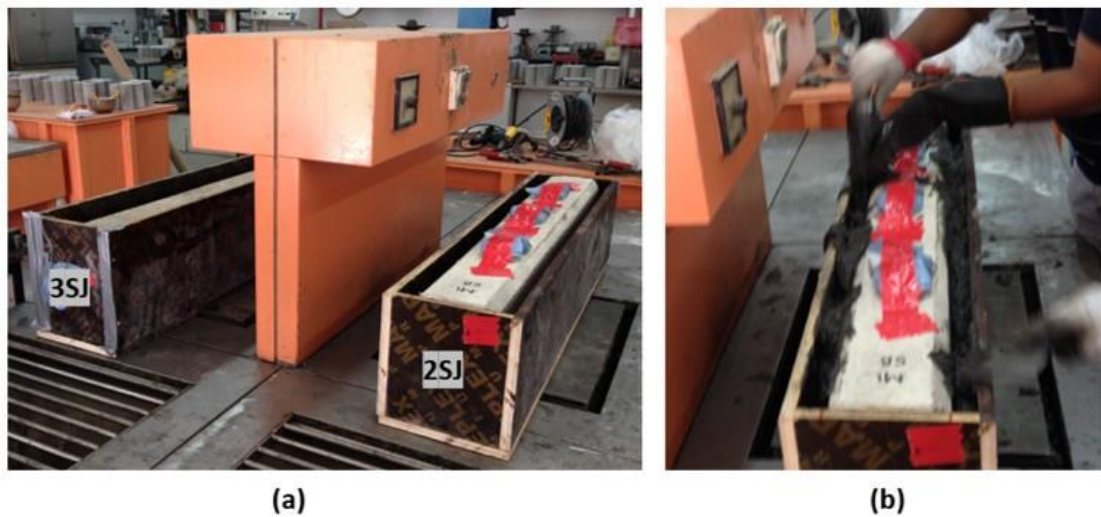


Figure 3.9 (a) Molds for 2SJ and 3SJ, (b) casing UHPC inside the beam mold

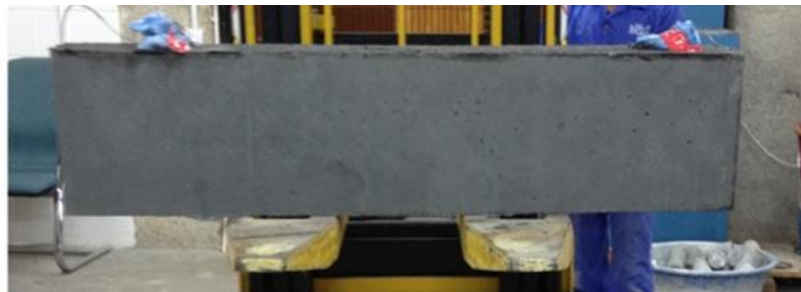


Figure 3.10 (a) Casting the UHPC strips, (b) UHPC layers after demolding

The screeding of concrete was carried out followed by curing procedure. Since UHPC has high cement content, the heat of hydration evaluated rapidly through the first 3 hours after the casting which led to moisture loss and therefore plastic cracks will take place. As such, the UHPC was immediately covered by wet burlap and plastic sheets for first 24 hours as shown in *Fig. 3.11*. After 24 hours of casting, all UHPC specimens were demolding and taken out to the curing tank for 28-days, *Fig. 3.12*.



**Figure 3.11 Temporary curing the UHPC for 24-hours**



**Figure 3.12 Strengthened beams after demolding**

Once the casting of specimens was done, the samples were prepared from the same mix, *Fig. 3.13*. Namely, small cubes, cylinders, prisms and dogbone-shape samples were taken and cured in the same conditions as UHPC specimens. Later, these samples will be used to



evaluate the UHPC mechanical properties as they are explained in this chapter, see section 3.5.



Figure 3.13 UHPC specimens for evaluation the mechanical properties

### 3.4 UHPC Strengthening Techniques

The main objective of this research work is to study the UHPC strengthened against the shear in conventional RC beams, therefore two strengthening techniques were studied. Either cast-in the UHPC inside a mold or bonding the precast UHPC strips to the beam using adhesive epoxy. Both techniques were carried out to prove which is more suitable and practical for shear strengthening. Owing to that different techniques, the beams are divided into two main groups as shown in [Table 3.1](#): first group used the sandblasting surfaces with cast-in UHPC, and second group used epoxy adhesive method.

Moreover, two different configuration schemes ([Fig. 3.2](#)) either (i) three-sided jacketing or (ii) two-sided jacketing over the entire length of the beam, were utilized to show the most efficient strengthening scheme against shear failure. In most cases of real situations, the monotonic casting of slabs with beams makes impossible to cover the beams in all four sides. Therefore, mostly three-sides and two-sides jacketing are accessible for

strengthening. Although, the complete jacketing is most efficient in strengthening, in our case of shear-strengthening it makes no significant difference when the top side of beam is retrofitted.

### **3.4.1 Applying UHPC using Sandblasting Technique**

In this technique, the beam surfaces were prepared by applying sandblasting of 2mm depth to obtain a rough surface, [Fig. 3.14](#). This was done in the PRAINSA factory where the skilled employees and sandblasting machine are available. Six beams were prepared for different strengthening configurations as following:

- Three beams with two-sides and bottom side sandblasting (they designated for three-sides jacketing - 3SJ),
- Three beams with two-sides sandblasting (they designated for two-sides jacketing - 2SJ).

Thereafter, the fresh UHPC was cast over the sandblasted surfaces. For casting the UHPC on three-sided jacketing, the beam was inverted in order to make an accessible to the bottom surface.



**Figure 3.14 Applying sandblasting technique on the surfaces of RC beams**

### 3.4.2 Applying UHPC using Epoxy Adhesive Technique

In this method of strengthening, UHPC strips were cast separately and moist cured for 28-days. The substrate and the surface of UHPC strips were cleaned and prepared using the grinding and sandpapers as shown in [Fig. 3.15](#) and [Fig. 3.16](#). A special adhesive epoxy (commercially known as *Sikadur-32LP 2-Part Structural Epoxy Bonding Agent*) was used and the two parts of epoxy were mixing according to the manufacturer's recommendation. The mechanical properties of the epoxy bonding at seven days of curing (30°C) were reported by the manufacturer [40] as: compressive strength of 38MPa; flexural strength of 28MPa; tensile strength of 18MPa; and the bond strength of 3MPa. So far, the epoxy was applied on the surfaces with approximate thickeners of 1.5mm (2.1 kg/m<sup>2</sup>) and the retrofitted strips were bonded to the beams. The steel clamps were used to fix the retrofitted strips on the substrate and to ensure good and equally adhesion, [Fig. 3.17](#). As the sandblast techniques, different configurators were used (either two-sides jacketing or U-jacketing). Consequently, the retrofitted beams were cured for 7-days at the temperature of 30°C in order to develop the full bond-strength according to the manufacturer's recommendation [40].

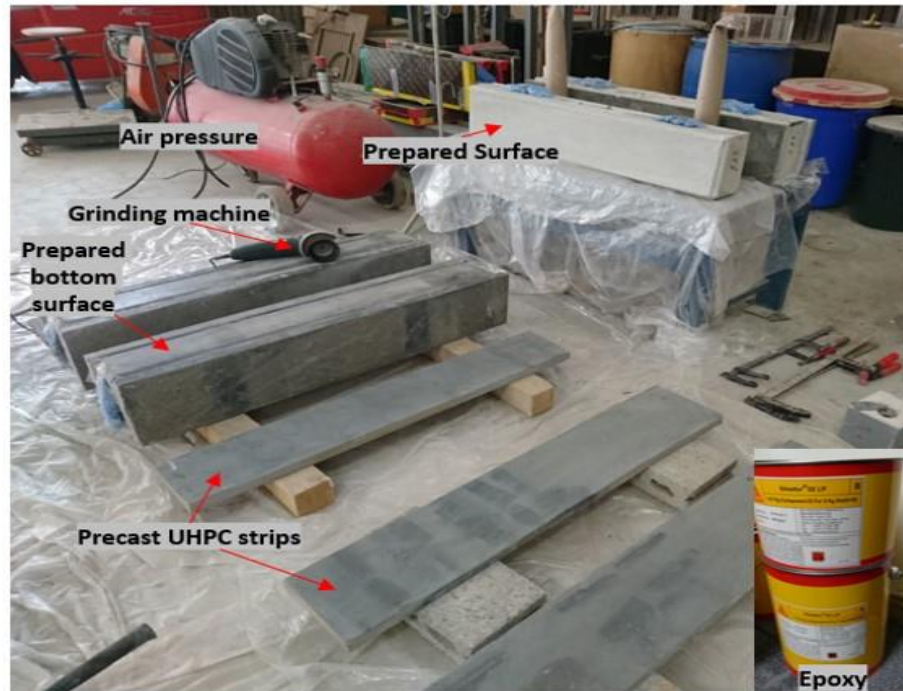


Figure 3.15 Procedure for epoxy technique



Figure 3.16 Epoxy technique: (a) Surface preparation of UHPC strips and substrate, (b) applying epoxy bonding

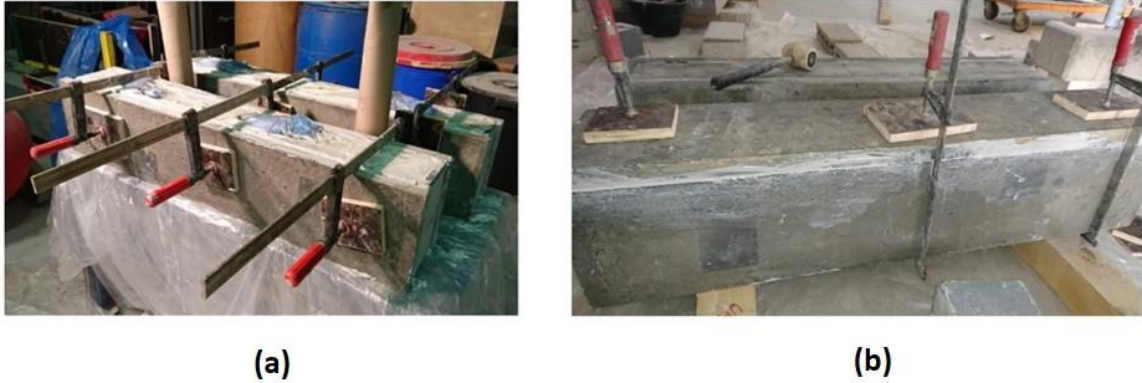


Figure 3.17 Applying the retrofitted strips to the beam substrate: (a) 2SJ, (b) 3SJ

### 3.5 Test of UHPC Material Properties

The UHPC is a new concrete and it is characterized as ultra-high strength concrete with superior properties. For evaluation of these properties and understanding the behaviour of such concrete, some experimental tests are needed to conduct. Accordingly, more than 100 specimens with different purposes were tested as presented in [Table 3.2](#). These specimens were prepared during the castings of UHPC and cured in the same conditions as beam specimens. In addition to evaluate the characteristics of UHPC, the results of these tests were also used for finite element modelling of UHPC. The following sub-sections elaborate procedure, approach, apparatus and results discussion of these tests.

#### 3.5.1 Uniaxial Compression Test

The compressive strength is an important property of UHPC [41], which is considered as brittle material. The compressive strength of concrete can be measured by the uniaxial compression test which is recognized by many material standards, including, ASTM C109 [42]. A total of 20 cubical specimens (50mm×50mm×50mm) were prepared from UHPC

mix and cured for 28-days. Then, they tested in the compression test machine and the load was applied continuously up to the crushing of concrete.

The average value of compressive strength was 151.4MPa with minimum and maximum value of 145.64MPa and 158.38MPa respectively and standard of deviation of 4.11 as shown in [Table 3.5](#).

**Table 3.5 Results of compression test on UHPC cube specimens**

UHPC mix	Compressive strength of cubes at 28-days			
	<i>Sample1</i>	<i>Sample2</i>	<i>Sample3</i>	<i>fc' (average)</i>
<b><i>UHPC#1</i></b>	142.6	147.4	146.92	145.64
<b><i>UHPC#2</i></b>	147	152.88	155.28	151.72
<b><i>UHPC#3</i></b>	154.6	144.36	155.3	151.42
<b><i>UHPC#4</i></b>	148.48	147.56	153.44	149.83
<b><i>UHPC#5</i></b>	165.92	152.5	156.72	158.38
<b>Minimum value</b>				<b>145.64</b>
<b>Maximum value</b>				<b>158.38</b>
<b>Average value</b>				<b>151.40</b>
<b>Standard of deviation</b>				<b>4.11</b>

### 3.5.2 Elasticity Test

The modulus of elasticity of UHPC was measured in accordance to ASTM C469 [36]. Since the UHPC has no coarse aggregate, the modulus of elasticity will depend on the cement matrix and its proportions. The modulus of elasticity can obtain from the linear part of stress-strain curve of concrete. For this purpose, the cylinder specimens (150×75mm) were prepared and cured for 28-days. The specimens are grinding to insure the end planeness of the top and bottom surfaces and the dimensions of specimens were re-taken.

The test setup consists of compression-testing machine, load cell, steel-rings, data logger and two LVDT's to measure the axial deflection, [Fig. 3.18](#). The cylinder specimen was fixed inside the steel-rings with gauge length of 95mm. The compression testing machine applied a static load up to 40% of failure load. The stresses versus strains was plotted and



from the linear part of the curve, the modulus of elasticity can be calculated using the ASTM C469 equation [36].

The average value of modulus of elasticity was 41.0GPa with minimum and maximum value of 34.5GPa and 50.1GPa respectively and standard of deviation of 4.42 as shown in [Table 3.6](#).

In addition to compute the elasticity of UHPC, the complete stress-strain response in compression can be obtained from this test by continuing the load up to the failure of the specimen. It was noticed that the specimen was broken in ductile behaviour without explosive failure as was observed when testing the normal concrete specimens. The following is the typical stress-strain curve of UHPC, [Fig. 3.19](#).

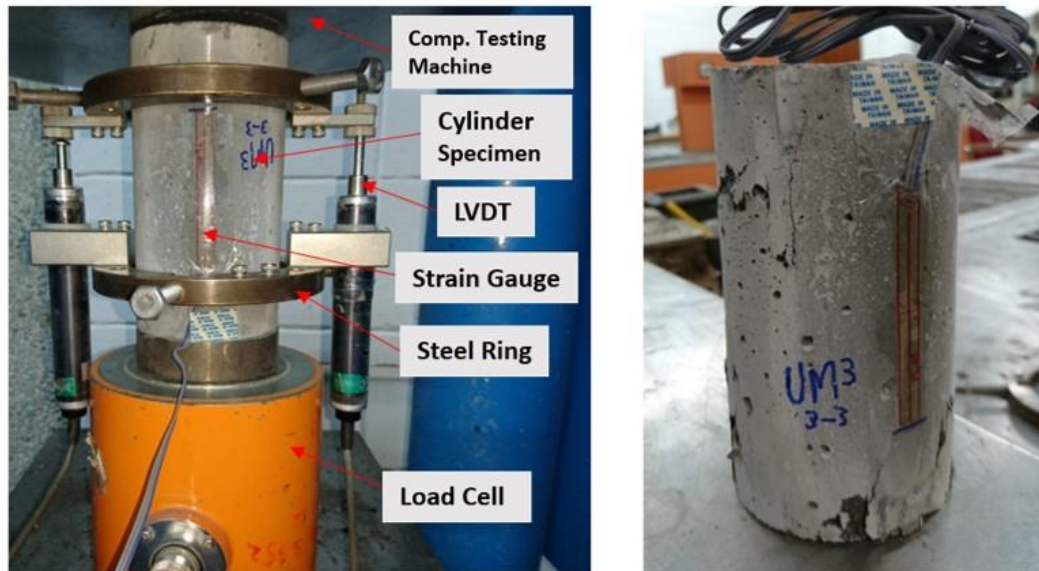


**Figure 3.18 Test Setup for determination the Modulus of Elasticity**

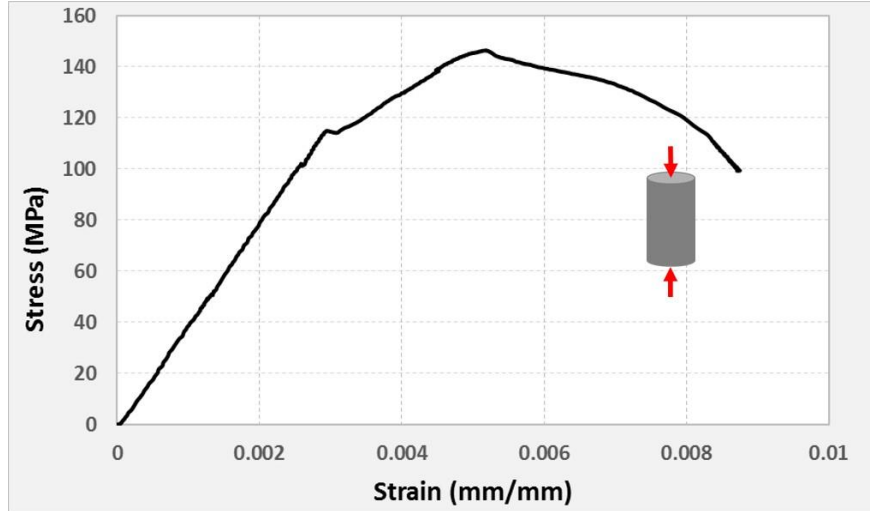


Figure 3.19 Compressive stress-strain behaviour of UHPC

### 3.5.3 Uniaxial Direct Tensile Test

The tensile strength of UHPC is a vital factor which significantly influences the shear behaviour. In this work, the dogbone-shape specimens (490mm length  $\times$  116mm width  $\times$  35mm thickness) were prepared, cast, cured and tested in the UTM. Prior to testing, the special treatments were made for purpose of obtaining the failure at the web of dogbone specimen between the extensometers. Therefore, some of specimens were treated by making a notch of 4mm around the midway of the web, whereas the rest strengthened with CFRP at the flanges and at the two-third of the web, *Figs. (3.20 & 3.21)*.

The test setup consists of UTM machine, load cell, prototype frame, data logger, LVDT, and two extensometers of strain gauges equals 50mm as shown in *Fig. 3.20*. The specimen was placed in the testing-frame and the extensometers were installed to web midway to measure the axial deformation. The LVDT was just used as displacement-controlled to record the axial deformations measured by the extensometers in the same rate as the UTM. The tensile load was applied in slow rate (0.5mm/minute) to monitor the first crack and



capture the strain resulting in the specimen. The load versus the longitudinal displacements were recorded using the computer system connected to the UTM and data logger. Finally, the actual stress-strain behaviour in tension was obtained from this test. [Fig. 3.22](#) shows the stress-strain curve of UHPC under tension, where UHPC exhibited an excellent behaviour in terms of strain hardening as compared with conventional concrete.

It was noted that the second method of treatment, i.e. using CFRP as strengthening of the specimen, had given the good results where it imposed the failure to be in the web exactly.

The average value of tensile strength was 8.9MPa with minimum and maximum value of 6.9MPa and 12.7MPa respectively and standard of deviation of 1.98 as shown in [Table 3.6](#).

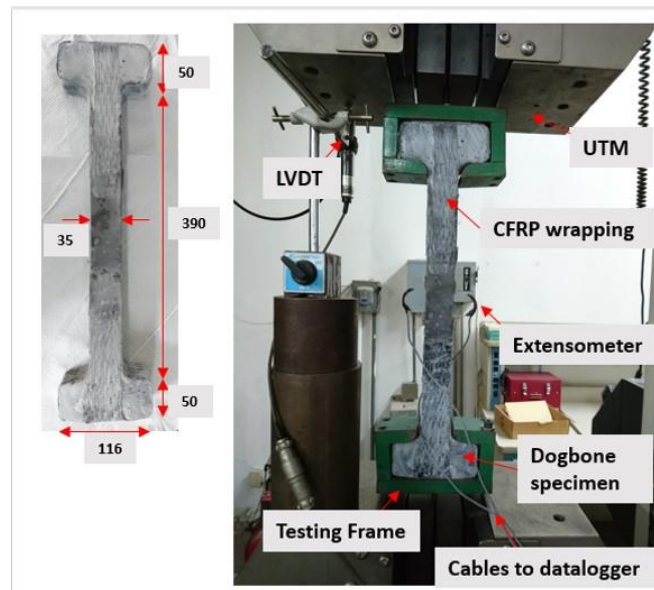


Figure 3.20 Setup for uniaxial direct tensile test on the UHPC dogbone specimen



Figure 3.21 failure of dogbone HUPC-specimen: (left) Dogbone with SFRP, (right) dogbone with notch

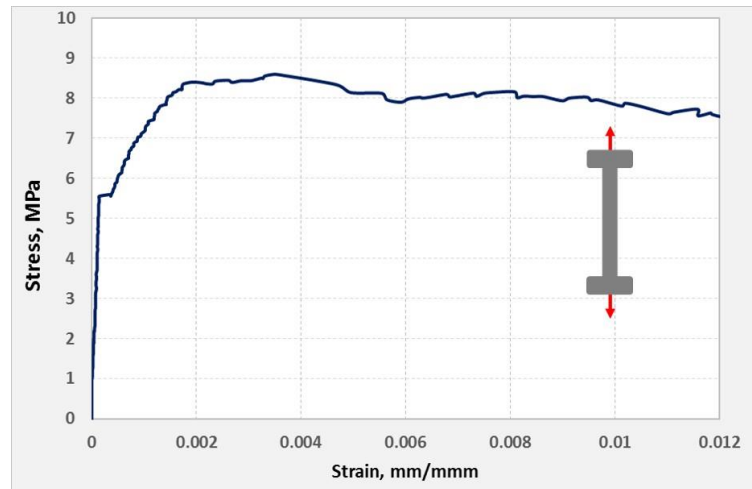


Figure 3.22 Tensile stress-strain behaviour of UHPC

### 3.5.4 Flexural Tensile Strength Test

Flexural strength of concrete can be obtained by testing the prism specimens (40mm×40mm×160mm) in flexural as reported in ASTM C78 – 02 [43] and ASTM C1018 [44] . The specimens were placed in test setup which consist of four-points loading frame, UTM, load cell, data logger and mid LVDT to measure the mid-deflection, [Fig. 3.23](#). The load was applied at the constant rate (displacement-controlled equals 0.01mm) and the deflections were recorded. During the test, the first crack was observed, but the load continues increasing, this because the steel fibers play an important role in bridging the faces of such cracks, thereafter the strain hardening behaviour takes place [13]. A typical

load- deflection curve of UHPC is given in [Fig. 3.24](#). To measure modulus of rupture can measured using the following equation [43]:

$$R = PL/bd^2$$

where:  $R$  is the modulus of rupture (in MPa),  $P$  is the maximum load,  $L$  is the span length of the specimen,  $b$  and  $d$  are the average width and depth of the cross-section, respectively.

The average value of modulus of rupture was 25.4MPa with minimum and maximum value of 21.8MPa and 29.3MPa respectively and standard of deviation of 2.55 as shown in [Table 3.6](#). This result is in compliance with that values of UHPC which available in the literature [41].

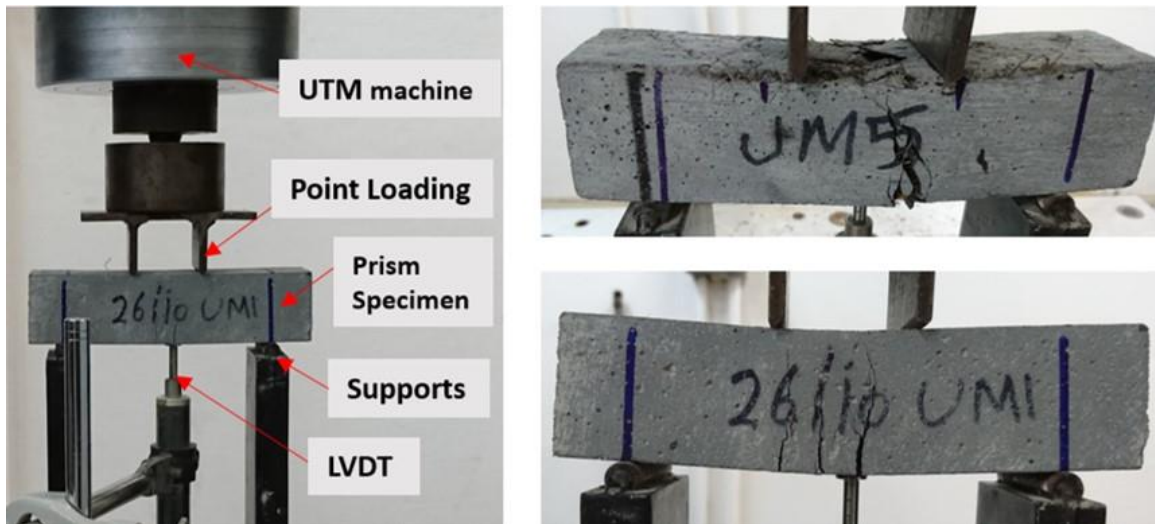


[Figure 3.23](#) Flxural test of UHPC prisms

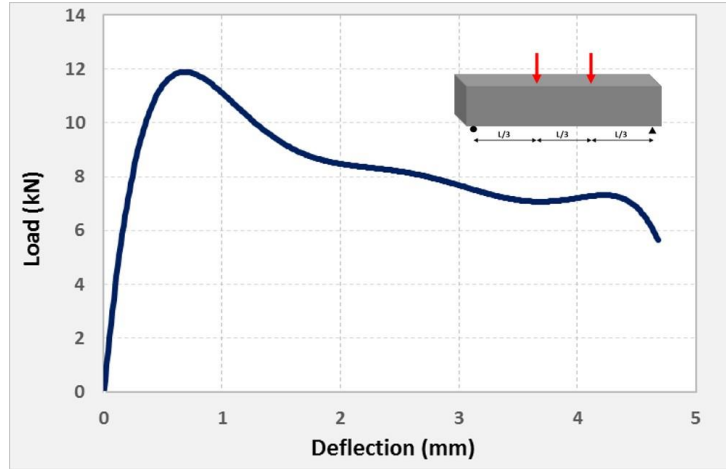


Figure 3.24 Load-deflection curve of UHPC prism under flexural test

Table 3.6 Mechanical properties of UHPC (at 28-days)

<i>Property</i>	<i>Min. Value</i>	<i>Max. Value</i>	<i>Average value</i>	<i>Standard od deviation</i>
Compressive strength, MPa	145.6	158.4	151.4	4.11
Tensile Strength, MPa	6.9	12.7	8.9	1.98
Modulus of Elasticity, GPa	34.5	50.1	41.0	4.42
Modulus of Rupture, MPa	21.8	29.3	25.4	2.55

### 3.6 Evaluation of Bond Strength

Through the last two decades, many researches have been conducted in the repair materials and strengthening techniques of existing concrete structures. Most of these repairing or retrofitting techniques were not cementitious materials. Therefore, the bond between the substrate concrete and repairing materials was a critical question due to loss of materials' compatibility. Therefore, the looking for a new material to be well-suited with the concrete is needed, and UHPC is a good option for that.

For assessment the bond quality of composite materials (NC and UHPC), some bond laboratory tests were carried out [45] in both strengthening techniques (sandblasting and

epoxy-adhesive). Namely, the splitting tensile strength test and slant shear strength test were conducted. A total of twelve composite cylinders were made of NC and UHPC in two different arrangement either in vertical plane (at 90°) or in the slant plane (at 30°).

In case of sandblasting method, the specimens of normal concrete were sandblasting-prepared with depth of 2mm and UHPC was cast directly to NC specimen inside the mold, whereas for epoxy method, the exposed surfaces were grinded and prepared before applying the epoxy adhesive.

### **3.6.1 Splitting Tensile Strength Test**

In this test, cylindrical normal concrete (NC) and UHPC specimens were prepared by cutting the cylinders in vertical plane at 90°. Each half NC-specimen was bonded to other semi-cylindrical UHPC-specimen using either sandblast preparation (surface roughness of 2mm) or epoxy adhesive (*Sikadur-32 Epoxy Bonding Agent*). The composite cylindrical specimen was placed horizontally in the testing machine and the load was applied along specimen's length where some bearing plates were provided on the top of the specimen, in accordance to ASTM C496 [46]. The load was applied until the failure occurs, where the failure in such loading case was in tension manner rather than in compression, [Fig. 3.25](#).

The splitting tensile strength of composite specimen can be calculated by dividing the applied load by the bonding area of bonding plane as the following equation which provided by ASTM C496 [46]:

$$T = 2P/\pi A$$

where:

$T$  = splitting tensile strength, Mpa,

$P$  = maximum applied load, N

$A$  = area of the bonding plane,  $\text{mm}^2$ ; where  $A = l \times d$  ( $l$  and  $d$  are the length and diameter of the specimen, respectively).



Figure 3.25 Splitting Tensile Test, (left) the tests setup, (b) the failure mode

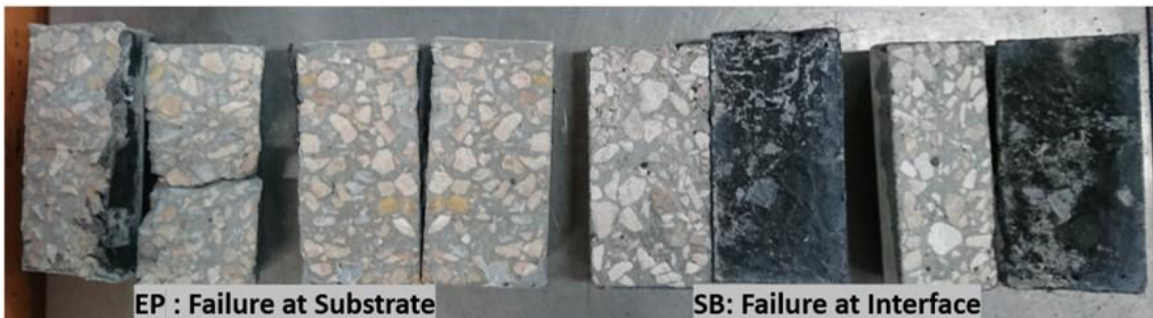


Figure 3.26 The failure modes of splitting tensile test

### 3.6.2 Slant Shear Strength Test

In this test method, the cylindrical specimens were cut in the slant plane at  $30^\circ$  measured from the vertical, and then bonded together using the two bonding methods, i.e. sandblasting or epoxy. The composite specimens were cured and sulfur capped, [Fig. 3.27](#).



The ASTM C882 [47] describes the procedure of this test. The composite cylinder, i.e. NC and UHPC test specimen, was placed in the compression-testing machine and the compressive strength was determined. The compressive strength was calculated by dividing the failure load by elliptical bonding area between the two concretes [47].

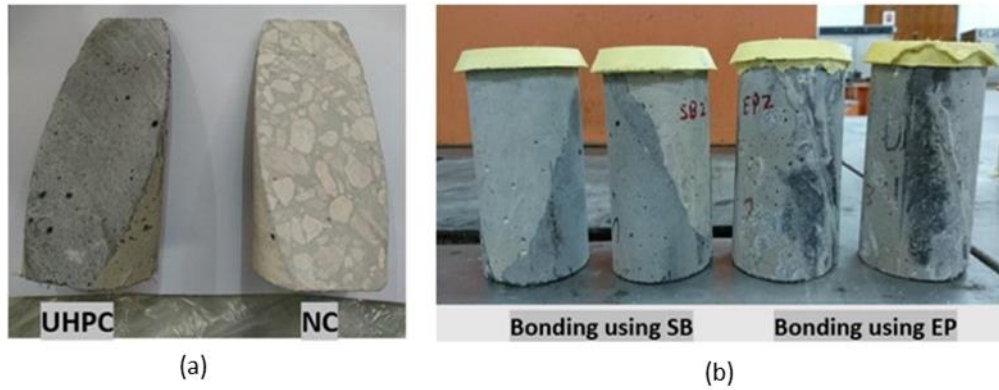


Figure 3.27 Slant shear test: (a) Cutting the specimens, (b) composite cylinder of NC/UHPC



Figure 3.28 Failure modes of specimens under slant shear test

### 3.6.3 Results and Discussion of Bonding Tests

The results of bond tests fall into two main categories: quality of the bond which depends upon the failure occurrence; and the quantity of the bond strength which depends upon the testing type.

The failure occurrence implies the bond quality and the behaviour of the composite materials. If the failure occurs at the substrate, this indicates that the bond strength is at least at the level of the substrate strength. On the other hand, if the failure forms at the interface between the two composite materials, this shows that the obtained strength is the bond strength [48].

The failure of tested composite cylinders showed that a substrate-failure for those specimens which bonded using epoxy adhesive. On top of that, the substrate failure was explosive and the epoxy bonding was not affected by either the high compression or shear stresses (in slant shear test) or tensile stresses (in splitting tensile test), *Figs. (3.26 & 3.28)*.

For composite specimens which treated by the sandblasting preparation, the failure was at the interface, however in some specimens it was partially at the substrate, *Figs. (3.26 & 3.28)*. In general, the epoxy specimens exhibited an excellent bonding behaviour under both tests.

As far as the numerical results of bond testing are concern, *Table 3.7* gives a summary of the obtained results. Moreover, these results were compared with the data from the literature. Particularly, *ACI-546 “Guide to Materials Selection for Concrete Repair”* [45] specifies the minimum accepted values of bond strength which depending on the bond



testing. As illustrated in the [Table 3.7](#), the results of both tests were in the accepted range and the overall bond assessment is in excellent performance.

**Table 3.7 Summary of bond testing results**

Related Work	Slant Shear Test (MPa)	Splitting Tensile Test (MPa)
<ul style="list-style-type: none"> <li><b><u>Testing Results (present study)</u></b></li> </ul>	<b>SB, average: 22.91</b>	<b>SB, average: 3.41</b>
	<b>EP, average: 26.54</b>	<b>EP, average: 8.32</b>
<ul style="list-style-type: none"> <li><b><i>Results from the Literature:</i></b></li> </ul>		
<b>1. ACI-546 (2006) [45]</b>	In range: 14 to 21	In range: 1.7 to 2.1
<b>2. Al-Osta et al (2017) [20]</b>	SB, average: 27.01	SB, average: 3.73
	EP, average: 23.15	EP, average: 5.89
<b>3. Sprinkel and Ozyildirim (2000) [49]</b>	N/A	Bond strength qualifies as: <ul style="list-style-type: none"> <li>• <math>\geq 2.1</math>, Excellent</li> <li>• 1.7 to 2.1, Very Good</li> <li>• 1.4 to 1.7, Good</li> </ul>
<b>4. Munoz et al (2014) [48]</b>	SB, average: 12.3	SB, average: 3.7

## 3.7 Experimental Tests of Beams

### 3.7.1 Outline

A total of thirteen RC beams were cast and cured. Ten of them were retrofitted with different strengthening techniques and different configurations. Experimental tests of these beams were carried out in the Heavy Structures Reaction-Floor Laboratory at KFUPM, where Civil Engineering Department provides a testing frame and all related equipment.

The experimental testing of beams covered the three considered variations: different strengthening techniques (*Sandblast Cast-in or Epoxy Adhesive*), different configuration schemes (*Two-sided or Three-sided jacketing*) and different shear-span to depth ratios ( $a/d$ )

= 1.0; 1.5; 2.0). Based on that, the beams are divided into five groups as illustrated in [Table 3.1](#).

The beams were tested in four-point loading arrangement where the test setup consists of the following, see ([Fig. 3.29](#)):

- *Support Plates*: to provide support reactions as hinge at one end and roller support at the other end.
- *Loading Plate*: the two-points loading was applied through a thick plate located on the top of tested beam.
- *Hydraulic Jack*: to apply the load at the constant rate over the loading plate.
- *Load Cell*: to monitor the load in kN.
- *Mid-LVDT*: a Linear Variable Differential Transformer located at the midspan and attached to the bottom face of tested beam to record the deflection.
- *Support-LVDT's*: two LVDT's located at the supports on the top face of tested beam to measure the rotations at the supports.
- *Data-Logger*: a digital device to record all related data of test through cables connecting to it. All instrumentation (load-cell, LVDT's and strain gauges) were cabled to the data-logger. The data logger recorded the data based on displacement-control.
- *Strain Gauge*: a small electrical device used to monitor the strains resulting from the stresses during the test. There are two types of strain gauges: Steel strain gauges (30mm long) and Concrete strain gauges (60mm long). The steel gauges were attached either to main reinforced bars or to the stirrups, whereas the concrete gauges were glued directly to the prepared concrete surface. The locations of

concrete gauges were on the top surface of beam to monitor the crushing of concrete and some gauges were placed at the beam side along the diagonal line joining support and point loading.

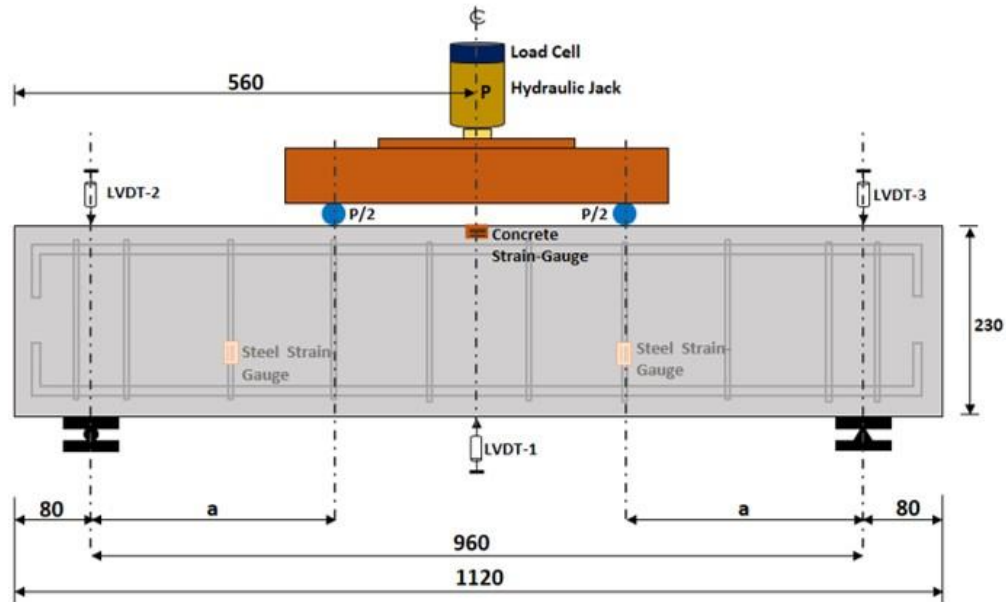


Figure 3.29 Schematic representation of beam testing setup

The beam was placed in the testing frame and all instruments were installed and connected to the data logger, [Fig. 3.30](#). The displacement-control load (at rate of 0.5mm/min) was applied monotonically until the failure was occurred. During the test, all useful data was reported, such as: first-crack load, crack patterns, bond between NC and UHPC, crushing of concrete, crack opening and failure modes. The load versus deflection data was plotted and such curves were analyzed and interpolated to understand the behaviour of the beam during the test.

The results, observations and interpretations of all tested beams, including the control and retrofitted specimens, are presented in the next subsections. Later, these outcomes are compared with the numerical and analytical models (see Chapters 4 & 5).



Figure 3.30 Beam test setup

### 3.7.2 Test Beams with $a/d=1.0$

In this category, five beams were tested. One is control beam, and the remaining are retrofitted beams with different strengthening techniques and different configurations as illustrated in [Table 3.1](#). The two-point loading were fixed at shear-span of ( $a = 200mm$ ) to maintain the ratio of shear span-to-depth of ( $a/d = 1.0$ ).

The control specimen (*CT-1.0*) was firstly tested, the load was gradually applied and the hair vertical cracks were initiated at the constant-moment region and the first crack load was 145kN. As load increased, the diagonal cracks were started to propagate at the constant-shear region (at the shear-span zone, 200mm). It was noted that the first inclined crack was initiated at the mid-height of the section where the state of pure shear stresses

exceeded the tensile strength of the concrete. The beam was broken suddenly in shear compression failure, *Fig. 3.31*, which occurred suddenly with single inclined crack ( $45^\circ$ ) at maximum load of 383kN. This failure is predictable because the beam was designed to be deficient in shear through insufficient transverse reinforcement, i.e. wide spacing between stirrups. Moreover, the load-deflection curve showed a sudden failure (i.e. softening part of the curve) after reached the ultimate load with corresponding displacement of 2.25mm, *Fig. 3.32*. The recording of strain gauges does not show any concrete crushing or steel yielding.

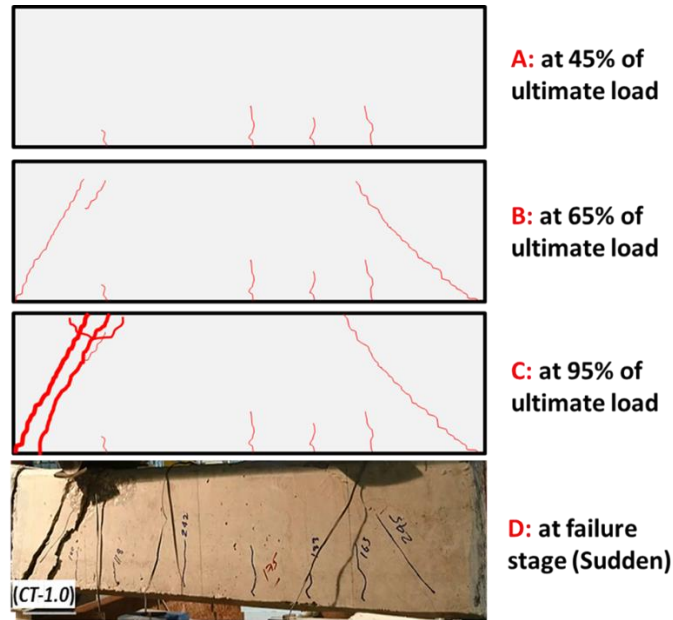


**Figure 3.31** Crack patterns of control beam (CT-1.0) with  $a/d=1.0$

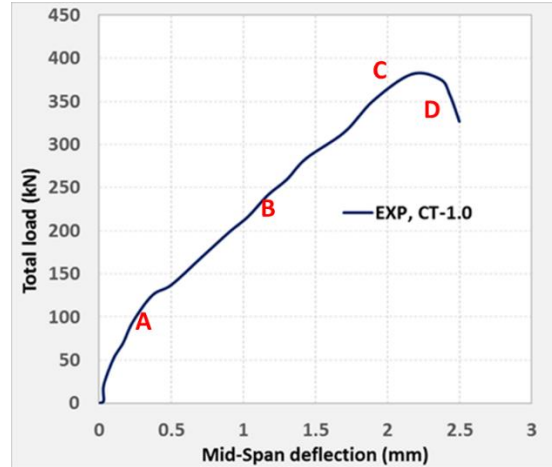


Figure 3.32 Load-deflection curve of control beam (CT-1.0)

The retrofitted beam (*SB-2SJ-1.0*) was strengthened in two-sides using sandblast cast-in technique. The flexural cracks (vertical cracks) were initiated at the mid span of beam followed by the secondary inclined cracks, [Fig. 3.33](#). The first crack load was reported as 168kN. The loading was increasing until the specimen failed in flexural-shear failure at ultimate load of 567kN. This is a good result of increasing the shear capacity of beam of around 48% more than the control beam. In addition, changing the failure mode from pure shear, which is considered a sudden and catastrophic, to flexural-shear failure is a respectable advantage of such strengthening technique. [Fig. 3.37](#) shows the typical load-deflection curve of the beam.



Figure 3.33 Failure mode of strengthened beam (*SB-2SJ-1.0*)

Beam (*EP-2SJ-1.0*) was retrofitted on both sides using the epoxy adhesive, behaves in similar way as that of sandblasted. The flexure-shear cracks were initiated and become wider as the load increasing until the failure occurs at ultimate load of 529kN (38% more than the control beam). At the failure stage, it was observed that the retrofitted strips were completely attached to the substrate beam without any debonding, accordingly, the quality of epoxy is in excellent quality. However, the post-peak response shows that the loss of ductility of the beam and this may attribute to the insufficient contact in some points between the original beam and the retrofitted strips. Therefore, the core beam failed in shear prior to develop full capacity of the UHPC jacketing.



Figure 3.34 Failure mode of strengthened beam (*EP-2SJ-1.0*)

The last two beams in this group (*SB-3SJ-1.0*) and (*EP-3SJ-1.0*) were strengthened in three sides (U-Jacketing) using the sandblasting cast-in and epoxy adhesive, respectively. The sandblasted beam (*SB-3SJ-1.0*) failed at ultimate load of 628kN (63% greater than the control beam) whereas epoxy-bonded beam (*EP-3SJ-1.0*) failed at max load of 625kN. The sandblasted beam (*SB-3SJ-1.0*) failed in flexure within the constant-moment region where fewer vertical cracks started and propagated. As such, strengthening was completely changed the failure from pure shear to flexure shear mode. Therefore, the bottom-side jacketing was greatly affected the behaviour of beam and made it more ductile than two-



sides jacketing. This behaviour was expected for the following reasons: firstly, the effective depth ( $d$ ) is increased, therefore the  $a/d$  ratio will be decreased resulting in enhanced the shear and flexural capacity of the section; secondly, the longitudinal steel starts to yield prior the shear failure takes place which causes a flexure failure; lastly, the effective of steel fibers in bottom face play an important role by their crack bridge capability.

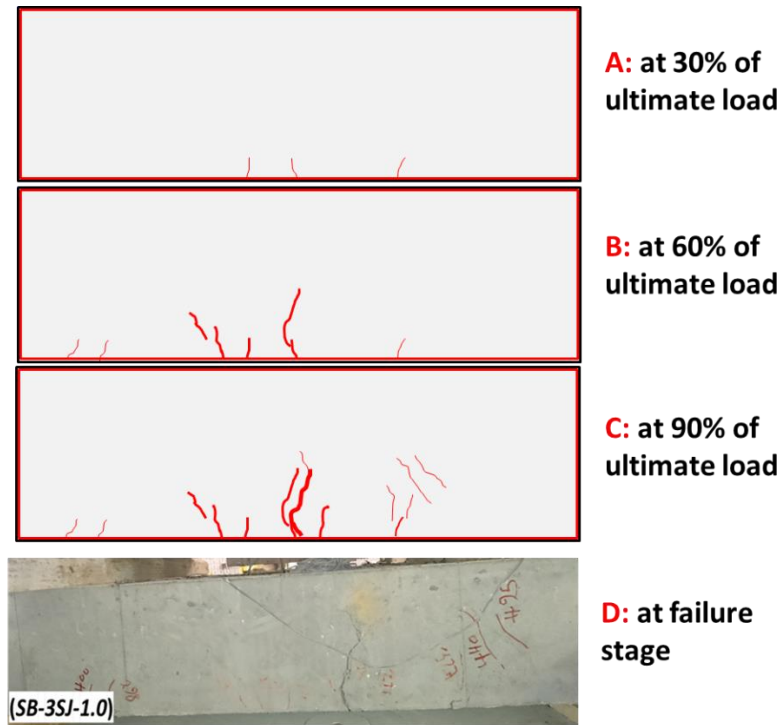


Figure 3.35 Crack pattern of retrofitted beam (SB-3SJ-1.0)



Figure 3.36 Failure mode of strengthened beam (EP-3SJ-1.0)



Although, the beams had broken in relatively high load, there is no debonding had occurred between the substrate and UHPC. However, it was observed that one problem with the retrofitted beam in three-sided jacketing by using epoxy adhesive, the problem was a mismatching between the bottom-retrofitted layer with the other two layers, *Fig. 3.36*. This made a disjointedness in the jacketing, therefore the deformation capacity after peak load was not effective and the composite beam was failed in the flexure-shear failure as it shown in *Fig. 3.37*.

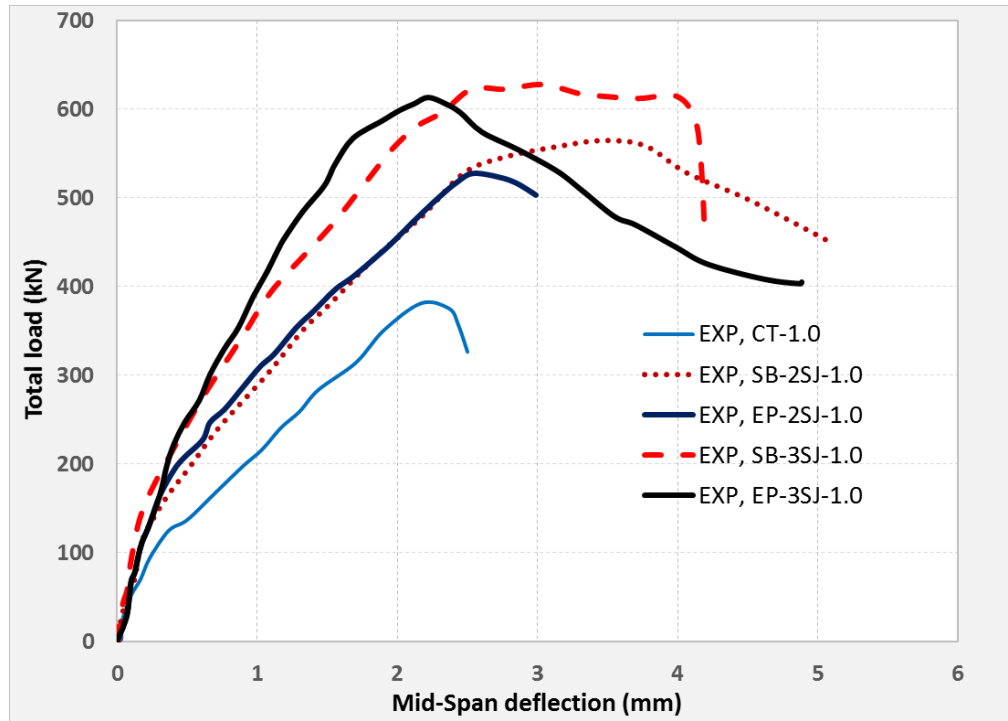


Figure 3.37 Load-deflection curves of all beams with  $a/d=1.0$

### 3.7.3 Test Beams with $a/d=1.5$

In this group of beams, the shear span was ( $a = 280\text{mm}$ ) with shear-span to depth ratio of ( $a/d = 1.5$ ). Five beam were tested including control beam, and four retrofitted beams.

The reference beam (*CT-1.5*) was tested and the first cracks were in diagonal direction along the line joining the load and the reaction. The beam was broken suddenly in pure shear failure as expected from the analysis of shear capacity of such shear-deficient beam. The ultimate load was 286kN which is less than (*CT-1.0*) with 33%. This occurred because the shear span in this case ( $a/d = 1.5$ ) was shifted from the support, therefore the wide-spacing stirrups were included within that shear span. Moreover, at more  $a/d$  ratio the effective of the arch action and dowel action is less which results in lower shear strength. The load-deflection response (*Fig. 3.41*) of the beam shows clearly a softening part after peak load which represents a shear failure.



**Figure 3.38 Failure mode of control beam (CT-1.5) with  $a/d=1.5$**

The retrofitted beams (*SB-2SJ-1.5*) and (*EP-2SJ-1.5*), with sandblasted and adhesively epoxy-bonding strengthening techniques respectively, were tested. The beam (*SB-2SJ-1.5*) was failed by forming vertical crack then it bent over to form an inclined shear crack as shown in *Fig. 3.39*. The beam eventually failed in flexure-shear failure as shown in *Fig. 3.41* which represents the whole behaviour of composite action of the beam.

The beam (*EP-2SJ-1.5*) was typically failed in flexure-shear failure as shown in *Fig. 3.39*. However, the load-deflection curve shows a shear failure, this inconsistency in the

behaviour between the beam itself and the load-deflection curve is attributed to the failure of the original beam prior to the retrofitted strip. Therefore the load-deflection curve is well represented the composite behaviour of such retrofitted beam. The failure loads of beams (*SB-2SJ-1.5*) and (*EP-2SJ-1.5*) were 402kN and 435kN, respectively, with average increasing in shear capacity of 46% as compared to the control beam (*CT-1.5*)



Figure 3.39 Failure modes of retrofitted beams (*SB-2SJ-1.5*) and (*EP-2SJ-1.5*)

The last two beams in this group (*SB-3SJ-1.5*) and (*EP-3SJ-1.5*) that were jacketed in three sides. The experimental tests were carried out and flexural cracks have initiated and propagated, [Fig. 3.39](#). Both beams failed in pure flexure at ultimate loads of 482kN and 487kN respectively, with average increasing of 69%. In addition, the load-deflection

curves of both beams showed an improved in ductility as well as stiffness as shown in [Fig. 3.41](#).

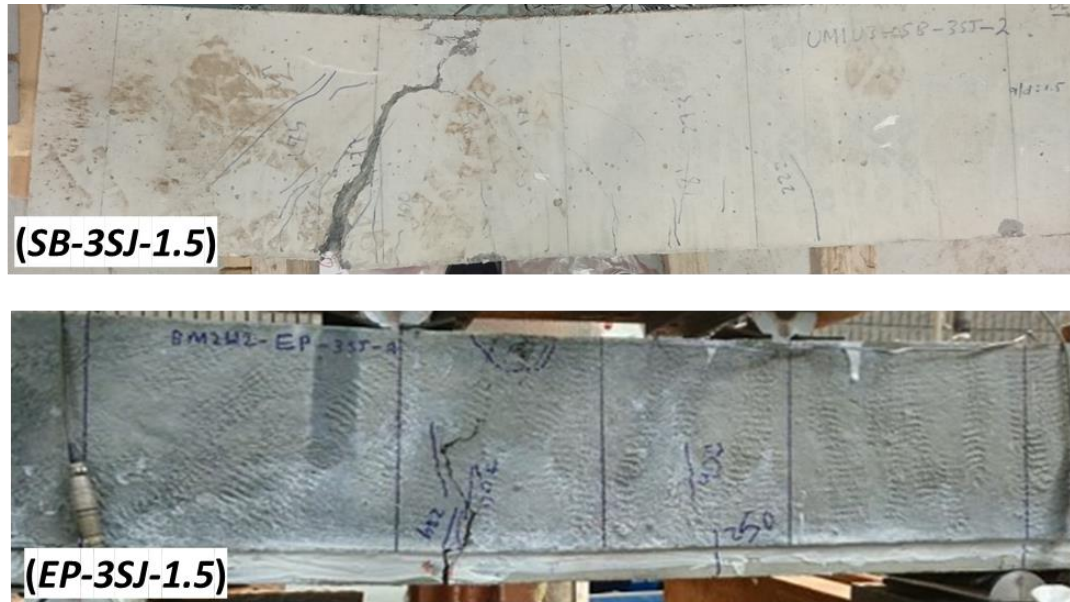


Figure 3.40 Failure modes of retrofitted beams (SB-3SJ-1.5) and (EP-3SJ-1.5)

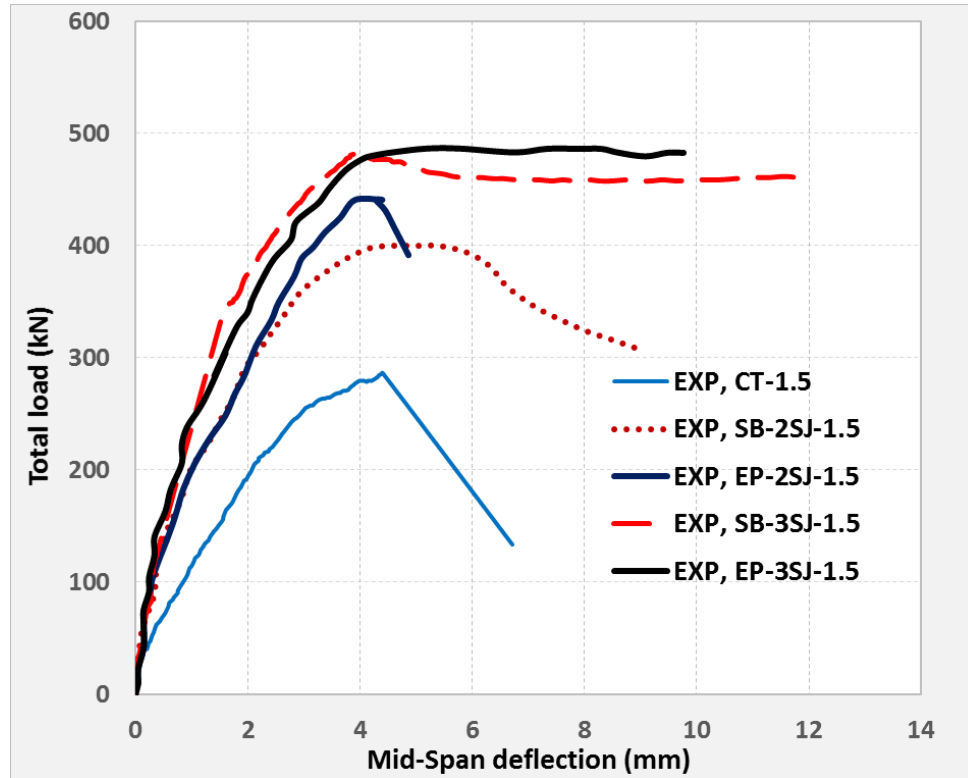


Figure 3.41 Load-deflection curves of all beams with  $a/d=1.5$

### 3.7.4 Test Beams with $a/d=2.0$

In this category, three beams were strengthened with sandblasted method only. The control beam (*CT-2.0*) was firstly tested and showed the shear compression failure at ultimate load of 276kN as shown in *Fig. 3.42*.

The retrofitted beam (*SB-2SJ-2.0*) was jacketed using sandblasting method in two opposite sides. It failed in flexure-shear mode at ultimate load of 346kN, *Fig. 3.43*. The last beam (*SB-3SJ-2.0*) was a U-jacketing with UHPC using sandblasting. The failure of this beam occurred in flexure near the section of maximum moment, *Fig. 3.43*. The load-deflection response of all beams tested with  $a/d = 2.0$  is shown in *Fig. 3.44*. Generally, the both beam behaved in similar way and failed in approximately the same load, this is attributed to the



high  $a/d$  ratio where the bottom layer will not be effective and the behaviour of the beams will be in flexure rather than shear.



Figure 3.42 Failure mode of control beam (CT-2.0) with  $a/d=2.0$

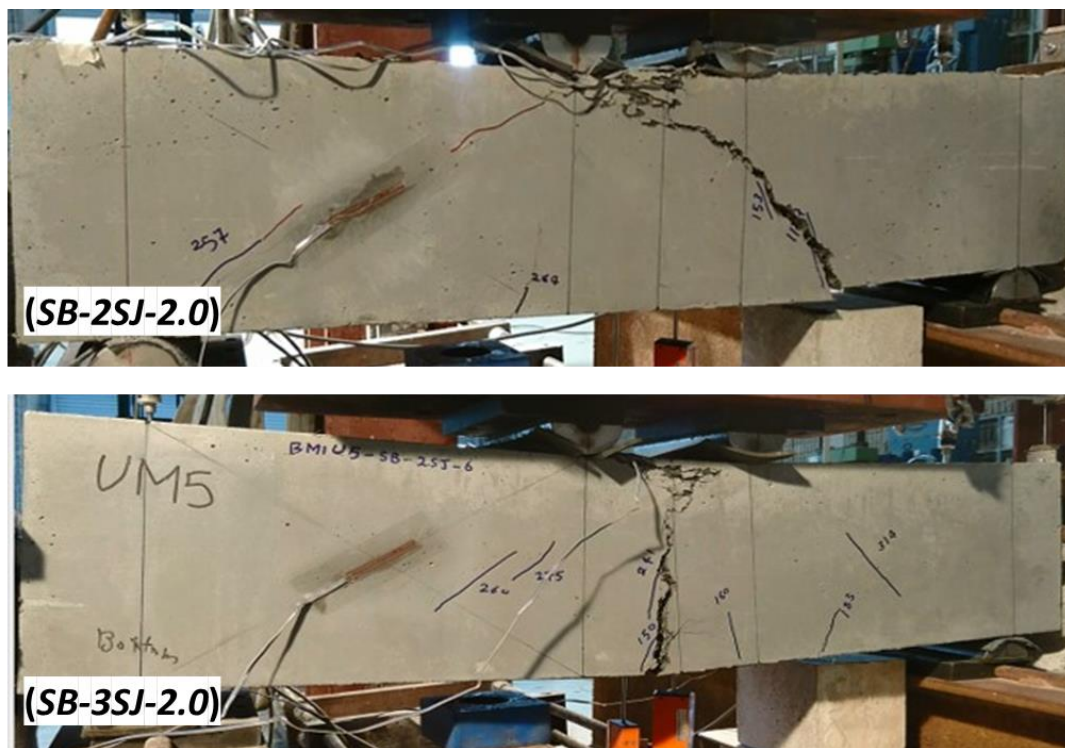


Figure 3.43 Failure modes of retrofitted beams (SB-2SJ-2.0) and (SB-3SJ-2.0)

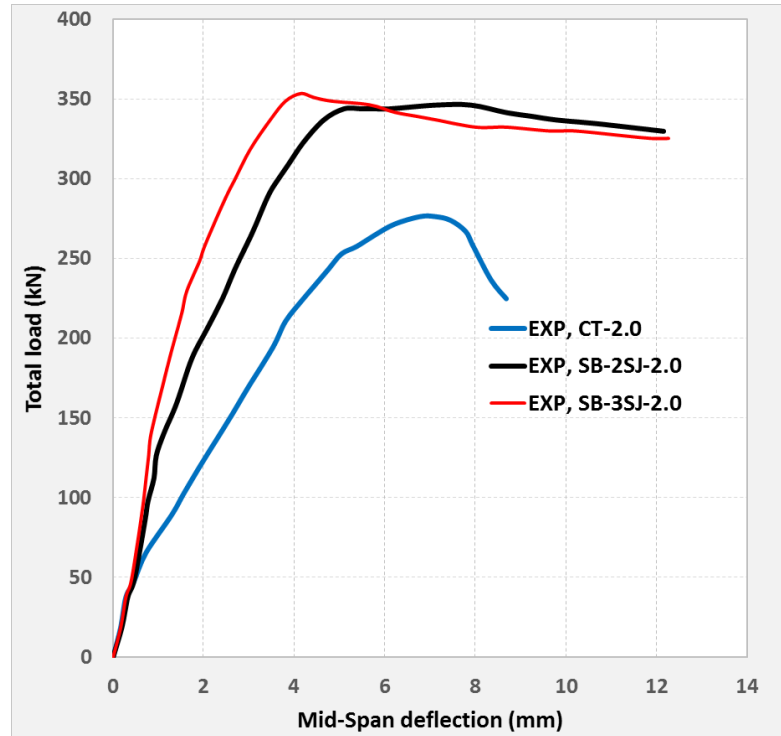


Figure 3.44 Load-deflection curves of all beams with  $a/d=2.0$

### 3.8 Summary of Experimental Test Program

*Table 3.8* and *Figs. 3.45 & 3.46* provide a summary of all results of experimental tested beams. The following conclusions are drawn:

- The experimental program was conducted to demonstrate the feasibility of utilizing the ultra-high performance concrete (UHPC) for strengthening of RC beams that present a shear weakness. A total of thirteen conventional RC beams were designed, prepared, cast and cured using the ready-mix concrete.
- The laboratory tests were carried out on evaluation the mechanical properties of the normal concrete and the steel rebars.
- The UHPC was batched, cast and cured in normal conditions. The mechanical properties were experimentally investigated. The results showed that outstanding

mechanical properties of UHPC: compressive (151 MPa) and tensile strength (8.9 MPa), flexural strength (25.4 MPa) and elasticity (40.9 GPa).

- In addition, the bond assessments using both sandblasted and epoxy bonding were carried out by conducting the splitting tensile test and slant shear test on the composite cylindrical specimens. Both tests highlighted the good bond between the normal concrete and the UHPC and this is generally attributed to the compatibility between the two concretes.
- A ten of the beams were retrofitted with the UHPC in different configurations, U-jacketing and two-sided jacketing. The UHPC was applied either by casting it directly on the substrate that prepared by sandblasting, or by bonding the precast UHPC strips to the parent beam by epoxy adhesive.
- The beams (control and strengthened) were experimentally tested in the four-point loading frame in the reaction floor laboratory at KFUPM. Three different shear span-to depth ratios with sandblasted technique were used, where two a/d ratios used with epoxy bonding technique.
- The results of experimental tested beams showed that a significant enhancement in the shear capacity, stiffness and deformational behaviour of strengthened beams. Moreover, the three-sided strengthening jacketing altered the failure from brittle to ductile behaviour. Specifically, the following conclusions are highlighted:
  - 1- All reference beams had suddenly broken in the pure shear compression failure, where the cracks initiated and propagated at the shear span region.
  - 2- The retrofitted beams in two-sided jacketing had generally failed in flexure shear behaviour.



- 3- The retrofitted beams in three-sided jacketing had failed in flexural mode at high levels of load. The beams exhibited a few cracks with considerable improvement in the ductility, especially for sandblasted type.
- 4- As the strengthening techniques are considered, the method of cast-in freshly UHPC with sandblasting is more efficient method for shear strengthening. Although, the epoxy bonding method gives an improvement in the shear strength and excellent bond property, the fabrication problem caused a loss of the continuity of the jacketing layers lowering the efficiency of the strengthening in the post-peak response.
- 5- The experimental evidence is affirmatively that the increasing in  $a/d$  ratio is resulting in reducing the shear capacity of the beam, as it is shown in [Fig. 3.46](#).

Table 3.8 Results of Experimental tested beams

Beam ID	a/d ratio	Exp. Failure Load (kN)	Shear Increasing (%)	Failure Mode
<i>CT-1.0</i>	1.0	383	0	Shear
<i>SB-2SJ-1.0</i>	1.0	567	48	Flexure-Shear
<i>SB-3SJ-1.0</i>	1.0	628	63	Flexural
<i>CT-1.5</i>	1.5	286	0	Shear
<i>SB-2SJ-1.5</i>	1.5	402	41	Flexure-Shear
<i>SB-3SJ-1.5</i>	1.5	482	69	Flexural
<i>CT-2.0</i>	2.0	276	0	Shear
<i>SB-2SJ-2.0</i>	2.0	346	25	Flexure-Shear
<i>SB-3SJ-2.0</i>	2.0	353	28	Flexural
<i>EP-2SJ-1.0</i>	1.0	529	38	Shear
<i>EP-3SJ-1.0</i>	1.0	625	63	Flexure-Shear
<i>EP-2SJ-1.5</i>	1.5	435	52	Shear
<i>EP-3SJ-1.5</i>	1.5	487	70	Flexural

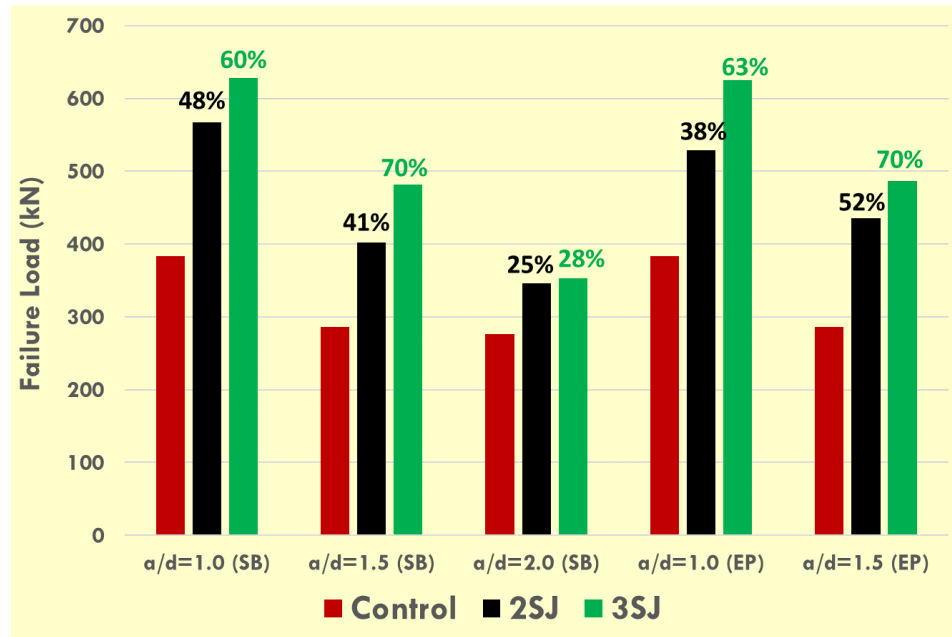


Figure 3.45 Comparative results of all tested beams

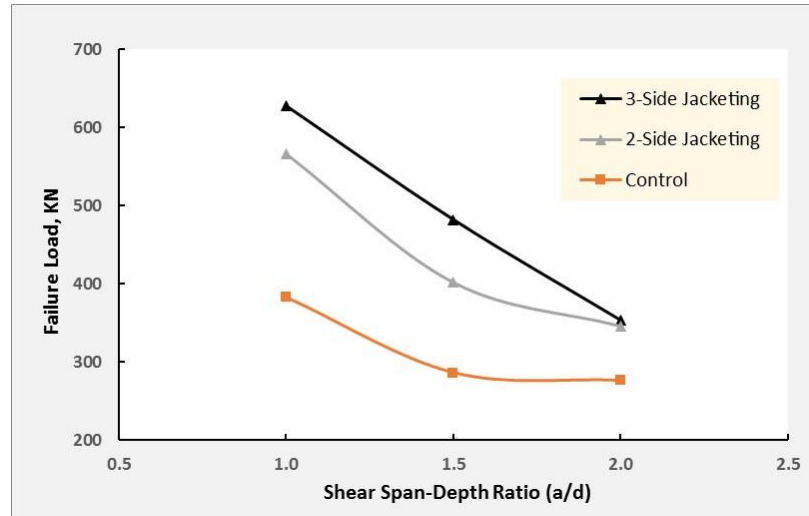


Figure 3.46 Effect of  $a/d$  ratio and strengthening jacketing in the failure load

\*\*\*\*\*

## **CHAPTER 4**

### **Finite Element Model**

#### **4.1 Introduction**

For long time, the experimental work has been playing a significant role in the researches. However, recently many studies are computer-based using the finite element method. Such modeling methods give dependable results and visual simulation of behaviour with effort-reducing and timesaving.

By means of that, this chapter presents the finite element model of all beams whether are control (NC-beams) or retrofitted beams (composite beams of NC and UHPC). The mechanical properties of all materials, including normal concrete, UHPC, and steel reinforcement, were taken from the experimental test program as explained in chapter (3).

The finite element model consists of modelling the geometry of elements with their materials and related constraints, such as boundary conditions, applying loads and the contacts between the different surfaces. The beams were modeled using three-dimensional elements in one of common commercial software named Abaqus. Moreover, the damage behaviour was also modeled using the concrete damage plasticity (CDP) approach.

The results of FE model were compared with the outcomes of experimental test program in order to validate the proposed model. Using the advantage of modelling the damage behaviour in Abaqus, the cracking patterns and failure modes were compared with experimental results.

## **4.2 Finite Element Model**

### **4.2.1 General**

FE method is a numerical approach to solve the problems of many engineering applications. These days, the use of FE method in structural engineering has been so common. For structural elements, which are complicated in loading, geometry and material, are not easy to solve by analytical methods. Therefore, the availability of commercial software programs makes the analysis of such problems effortless and timesaving. In this study, a non-linear finite element model was performed taking the advantage of these commercial programs.

The modelling of conventional reinforced concrete beams, which mainly made of quasi-brittle material - concrete, is a challenging task. In addition to that, the retrofitted RC-beams are more complicated in modeling due to composite elements and presence of steel fibers in UHPC. Because of that a limited researching had carried out in this area of modeling the composite beams.

However, some cracking concrete models were developed [50]. In this study, the concrete damage plasticity model was used which gives reliable results [51]. So, by using such model, the complete behaviour of full-scale strengthened beams can be achieved without any experimental beam testing.

### **4.2.2 Concrete Damage Plasticity Model (CDP)**

Many researches have been conducted on using the plasticity theory in model the quasi-brittle materials such as a concrete. The use of plasticity theory in compression may apply

with successful, but for tension zones, where the cracks play a significant role such as shear failure in concrete, cannot be applied [52].

Several models were developed in tension zones based on fracture mechanics, including: smeared crack model, fictitious crack model, and crack-band theory [53]. However, these models have faced some limitations. Therefore, the need for an approach which takes the non-linear behaviour of concrete in a single constitutive model. Lubliner and Oliver (1989) [52] formulated a plastic damage model for concrete based on plasticity theory.

Concrete Damage Plasticity (CDP) approach develops the constitutive behaviour of concrete by presenting the scalar damage variables for both compressive and tensile response as illustrated in *Fig. 4.1*. The damage variables in tension and compression are denoted by  $d_t$  and  $d_c$ , respectively, which are taken values in the range from zero to one. Abaqus user manual assumed zero for undamaged material and one for completely damaged (i.e. loss of stiffness) [54].

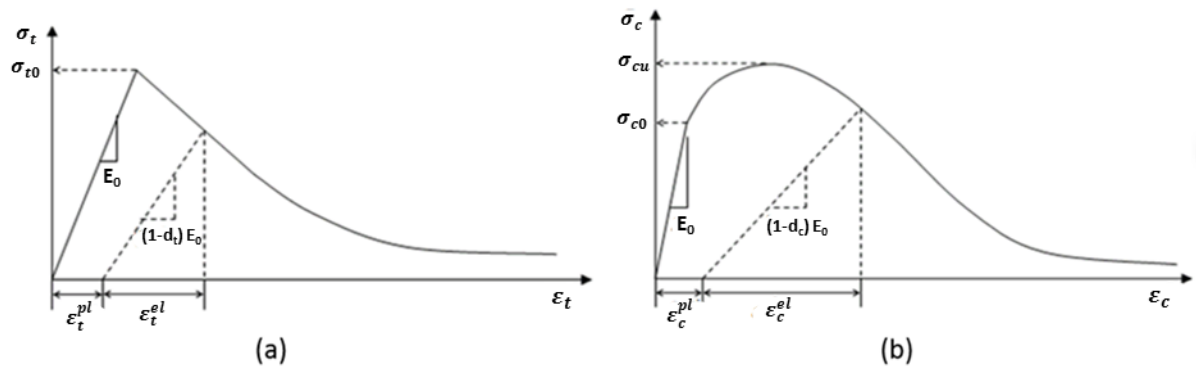


**Figure 4.1** Damage variables: (a) in tension, (b) in compression [54]

CDP introduces the main two failure mechanisms of tensile cracking and compressive crushing of concrete. The yield surface is governed by two hardening variables  $\varepsilon_t^{PL}$  and

$\varepsilon_c^{PL}$  which are associated to the failure mechanisms under tension and compression loading respectively.

In Abaqus, the yield surface is required to define the following parameters (*Abaqus User's Guide, 2016*) [54]:

- Angle of dilation ( $\varphi$ ) which is an angle measured in p-q plane at high confining pressure.
- Eccentricity ( $\varepsilon$ ) of plastic potential surface. It was taken as default value of 0.1.
- Ratio of initial biaxial compressive yield stress to initial uniaxial compressive yield stress ( $\sigma_{b0}/\sigma_{c0}$ ) which taken as default value equals to 1.16. To find this parameter, complex tests are needed which beyond the scope of this research.
- Ratio of second stress invariant on tensile meridian to compressive meridian at initial yield ( $k_c$ ). It is defined as default value of 2/3.

*Table 4.1* shows all input parameters that required for finite element model in Abaqus. As aforementioned, most of these parameters were taken as default values because their effects were insignificant in the modeling as reported in the literature [7].

Table 4.1 Input parameters for Abaqus modeling

Input value	Concrete Material	UHPC Material	Steel Reinf. Material
<ul style="list-style-type: none"> <li><b><u>Material Parameters:</u></b></li> </ul>			
Strength, MPa	65 (Comp)	151.4 (Comp)	610 (Tension)
Modulus of Elasticity, GPa	31.1	41.0	204.6
Poisson's Ratio	0.15	0.18	0.3
<ul style="list-style-type: none"> <li><b><u>Concrete Damage Plasticity Parameters:</u></b> [54]</li> </ul>			
Dilation Angle ( $\varphi$ )	30	25	--
Eccentricity ( $\epsilon$ )	0.1	0.1	--
$\sigma_{b0}/\sigma_{c0}$	1.16	1.16	--
$k_c$	0.667	0.667	--

### 4.3 Parameters of Materials for FEM

Modelling the RC and UHPC in Abaqus required defining the mechanical properties of these materials. Furthermore, the nonlinear behaviour in tension as well as in compression of both the normal concrete and UHPC are required. [Fig.4.2](#) shows the nonlinear behaviour of materials being tested in the experimental program.

In addition, for cracking pattern simulations, the compressive and tensile damage parameters are calculated based on the equations provided by Birtel and Mark (2006) [55]:

- *Compressive Damage Parameter ( $d_c$ ):*

$$d_c = 1 - \frac{\sigma_c E_c^{-1}}{\epsilon_c^{pl}(1/b_c - 1) + \sigma_c E_c^{-1}}$$

- *Tensile Damage Parameter ( $d_t$ ):*



$$d_t = 1 - \frac{\sigma_t E_c^{-1}}{\varepsilon_t^{pl}(1/b_t - 1) + \sigma_t E_c^{-1}}$$

where:

$d_c$  and  $d_t$  = Compressive and Tensile damage parameters

$\sigma_c$  and  $\sigma_t$  = Compressive and Tensile stresses of concrete

$E_c$  = Modulus of elasticity of concrete

$\varepsilon_c^{pl}$  and  $\varepsilon_t^{pl}$  = Plastic strains corresponding to compressive and tensile strengths of concrete.

$b_c$  and  $b_t$  = Constant parameters,  $0 < b_{c,t} \leq 1$ .

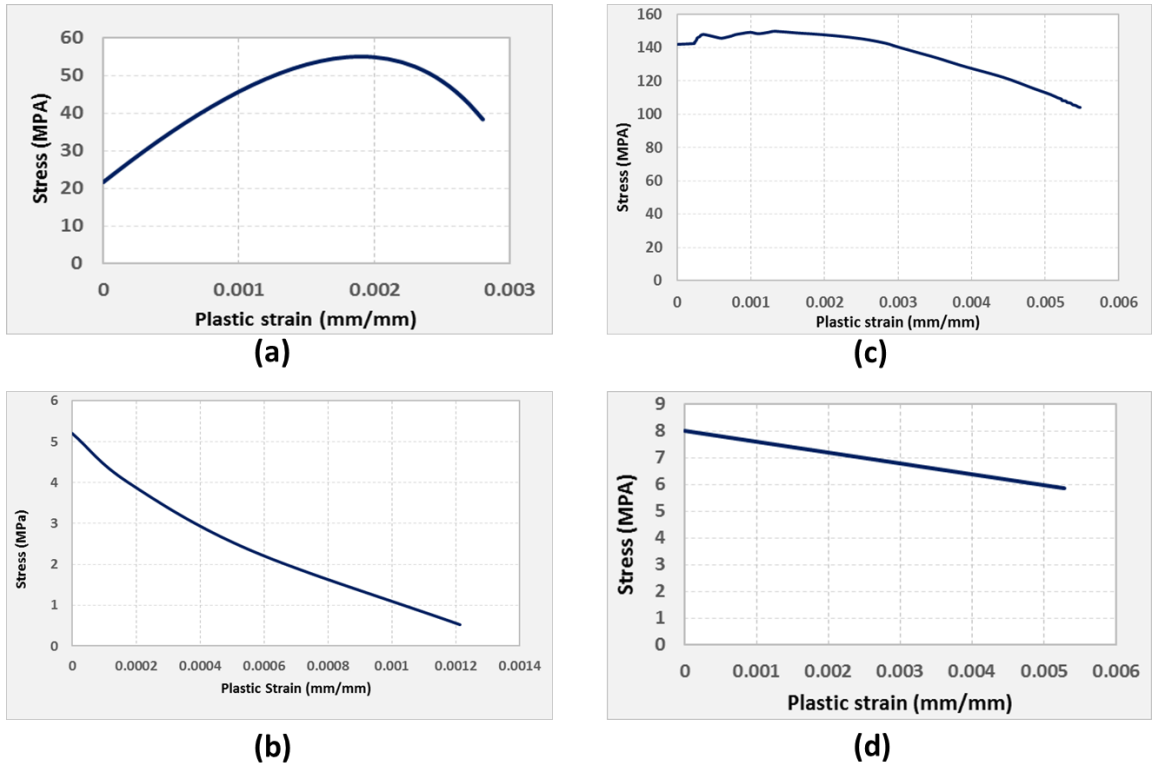


Figure 4.2 Nonlinear behaviour of materials: (a) concrete in compression (b) concrete in tension (d) UHPC in compression (d) UHPC in tension

## 4.4 Finite Element Model of Beams

### 4.4.1 Outline

Finite element model was developed using non-linear commercial program (Abaqus). The RC beams were modeled with cross-section of (140×230×1120mm) and the specified reinforcement details of longitudinal bars (Bottom: 2 $\phi$ 20; Top: 2 $\phi$ 12), stirrups ( $\phi$ 8@120mm) and optimum cover of 20mm, *Fig. 4.3*. In addition, the UHPC strips were modeled with desired dimensions (thickness of 30mm) and different proposed configurations.

The materials (concrete, UHPC and steel reinforcement) were modeled using the data of experimental program as summarized in *Table 4.1*. The steel was modeled with elastic-perfectly plastic behaviour with properties of  $F_y = 610$  MPa and elasticity of 204 GPa. The steel-plates with size of (50×140×25 mm) were used at the supports and loading points. Moreover, the nonlinear behaviour of NC and UHPC in tension and compression, which obtained from experimental tests, were entered. For stress-strain behaviour of NC was obtained from the model code [56].

For simulation the cracking patterns, the damage parameters in both compression and tension were calculated and inputted in the CDP model in Abaqus library.

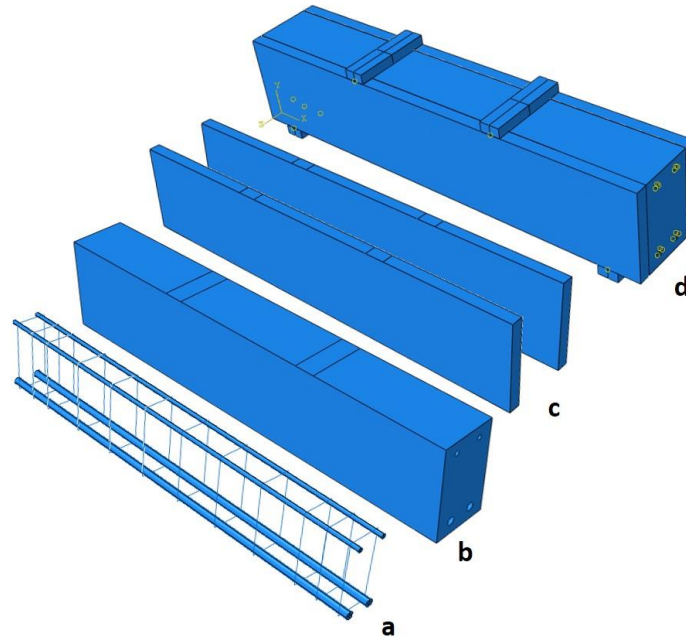


Figure 4.3 Modeling the retrofitted beams: (a) steel cage, (b) NC, (c) UHPC strips, (d) retrofitted beam

#### 4.4.2 Modeling Considerations

The numerical solution of the beams using Abaqus package necessitates some assumptions and considerations. The reliability of such considerations was validated successfully through many research studies [20][32].

The concrete, UHPC and steel-plates were modeled using the three-dimensional 8-noded brick elements. Whereas, the reinforcement steel (longitudinal and transverse) were modeled with two-noded 3D truss elements. Since the UHPC was made from steel fibers which were randomly distributed and orientated, therefore they could not be exactly simulated in the matrix. As such, in FE model, the UHPC was modeled as homogenous material.

The bonding between different surfaces was modelled using the available options in Abaqus library. The bond between concrete and reinforcement steel was taken as embedded region, where the concrete is the host element. The adhesive between normal concrete and UHPC was considered as perfect-bond because during all experimental tests there was no debonding observed. The steel palates were bonded to the concrete surfaces with tie-bond.

The boundary conditions were utilized at the supports. Simulated to the experimental tests, one support was assumed a hinge and the other was roller.

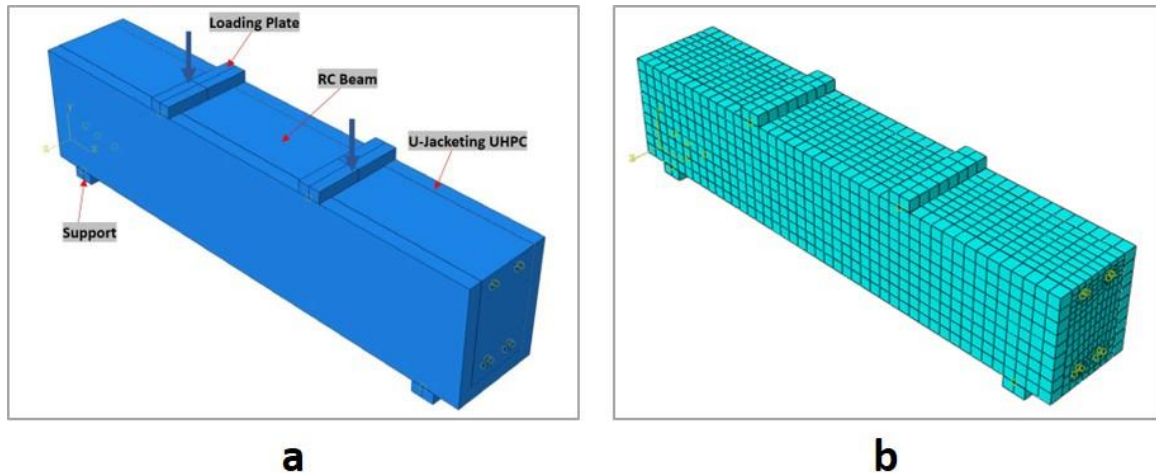


Figure 4.4 (a) beam constraints, (b) meshing of beam

In Abaqus, the most dependable approach of applying the load is the explicit dynamic method. Among many researches in the literature, this method was performed successfully for two main reasons: first, it gives reliable results with less problems of convergence, second, it is the most suitable for materials like concrete to capture the concrete cracks and overall failure behaviour [57]. Furthermore, in explicit dynamic analysis, the inertial effects can be minimized either by reducing the loading rate or increasing the mass density

of concrete in order to approach the static solution. Thus, in Abaqus, the time increments are automatically calculating and the loading rate is setting as one second.

The meshes were generating on model parts using the explicit 3D elements. The parts were partitioned into sub-regions to allow the loads being transferred through the different constraints, such as interactions, and boundary conditions. The size of meshing was adopted as 25mm after several iterations as shown [Fig.4.4](#). This discretization attributes had given usable results with good visualization of failure patterns.

#### **4.4.3 FE Results of Beams with $a/d=1.0$**

Three beams were modeled with shear span to depth ratio of 1.0 (shear span = 200mm). The RC control beam (*CT-1.0*) was failed as expected in diagonal tension crack (shear failure), [Fig.4.5](#). The failure load was 373 kN. The retrofitted beam (*SB-2SJ-1.0*), which strengthened by UHPC strips on two-sides, was broken in flexure-shear crack at failure load of 546 kN, [Fig.4.6](#). For beam strengthened on three sides (*SB-3SJ-1.0*) was failed in pure flexure failure at ultimate load of 611kN.

#### **4.4.4 FE Results of Beams with $a/d=1.5$**

On the FE modeling, the two points loading were closed to each other by 160mm to satisfy the experimental  $a/d$  ratio of 1.5. The three beams were modeled, the control beam (*CT-1.5*) failed at load of 294kN by forming the tension crack (shear-failure) as shown in [Fig.4.8](#). The reaming two beams (*SB-2SJ-1.5*) and (*SB-3SJ-1.5*) were failed on flexure-shear mode and pure flexural failure, respectively. The failure loads were 407kN and 486kN, respectively ([Figs.4.9 & 10](#)).

#### **4.4.5 FE Results of Beams with $a/d=2.0$**

The last three beams with  $a/d$  of 2.0 were modeled in this stage. Shear failure was a dominant in the control beam (*CT-2.0*) which failed at load of 270kN (*Fig.4.11*). Similar to the former cases, the strengthened beams (*SB-2SJ-2.0*) and (*SB-3SJ-2.0*) were failed in flexure-shear and pure flexural failures as shown in (*Figs.4.12 & 13*), respectively. The ultimate loads were reported as 352kN and 344kN, respectively.

#### **4.5 Outcome of Experimental Test Program**

As discussed in chapter 3, the experimentally tested-beam program involves the testing of five groups of beams. Since, in Abaqus the used of bonding assumptions for UHPC strips to RC-beams can be used only for sandblasting technique, therefore, only the results of sandblasted retrofitted beams were considered to validate the FE model. The outline of these test results is summarized in *Table 4.2*. Based on those outcomes, the comparison with FE model was studied in detail in the next section.

#### **4.6 Comparative Study of Experimental and FE Results**

A comparative study between the finite element model outcomes obtained using the proposed constitutive model and the experimental tests is discussed. All experimental results, including failure load, crack pattern, failure mode and load-deflection curves, were validated with FE model. This comparison had showed that the FE model was able to capture most of the failure modes with good accuracy.

##### **4.6.1 Beams with $a/d=1.0$**

FE results of this group of beams were in good accuracy with experimental test. Control (*CT-1.0*) beam was failed experimentally in shear at load of 383kN, closed value was

obtained in FE with failure load of 373kN (difference of 3%). Moreover, crack patterns in FE showed a clear shear compression failure at constant shear region, [Fig. 4.5](#).

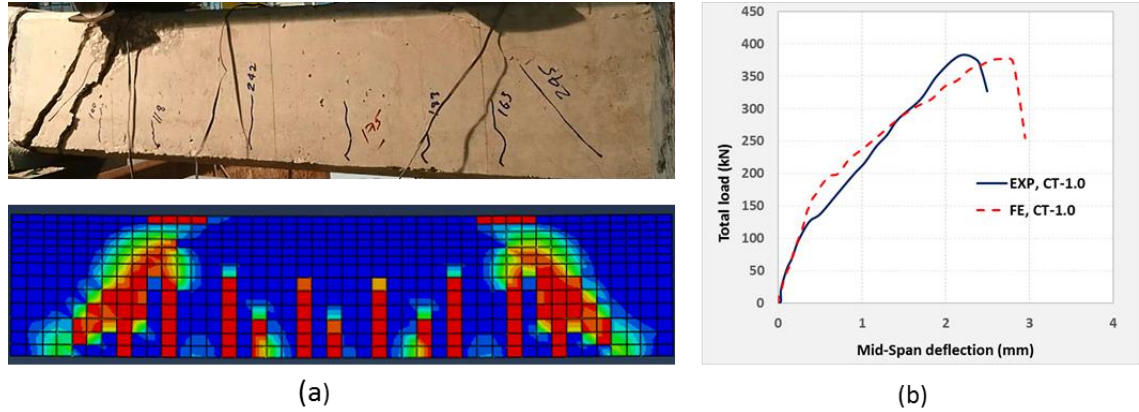


**Figure 4.5 Control beam (CT-1.0): (a) failure mode of experimental and FE, (b) Load-deflection response**

Similarly, FE was captured the failure of retrofitted beam (*B-2SJ-1.0*). The crack pattern showed a flexure shear failure at max load of 546kN, whereas the test load was 567kN. [Fig. 4.6](#) shows the load-deflection curve where a slight reduction in the stiffness of experimental curve after elastic region, this is probably because the effect of orientation of steel fibers which affects the experimental result. Moreover, in Abaqus, the damage of interfacial side of normal concrete beam (original beam) can be observed. [Fig. 4.7](#) shows clearly that the failure mode was shifted from diagonal shear crack to a combination of flexure and shear cracks. Therefore, the UHPC strips take the load once the inclined crack was initiated and the internal forces are redistributed, this action is in similar way to the role of steel stirrups.

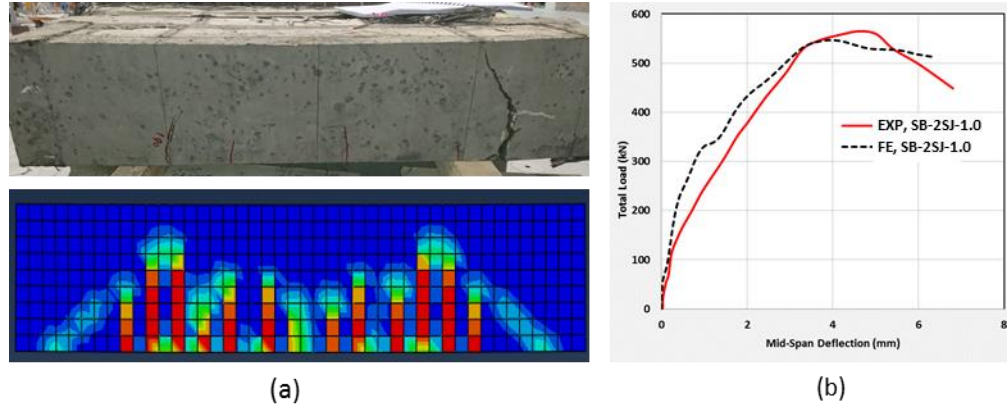


Figure 4.6 Retrofitted I beam (SB-2SJ-1.0): (a) failure mode, (b) Load-deflection response

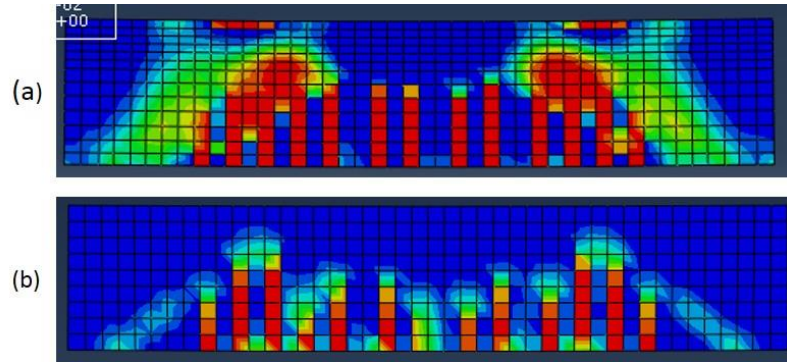


Figure 4.7 Retrofitted beam (SB-2SJ-1.0): (a) interfacial surface of NC – shear failure, (b) flexural failure at retrofitted beam

#### 4.6.2 Beams with $a/d=1.5$

For beams with  $a/d = 1.5$ , the load-deflection behaviour of FE were in good accuracy with the experiment outcome. The shear failure was dominant in control beam (*CT-1.5*) with diagonal crack. The FE was overestimated the peak load by 3% as compared to corresponding experimental value of 286kN. In addition, a crushing in concrete was observed in experimental test at loading location, which well predicted in FE damage behaviour as shown in Fig. 4.8.



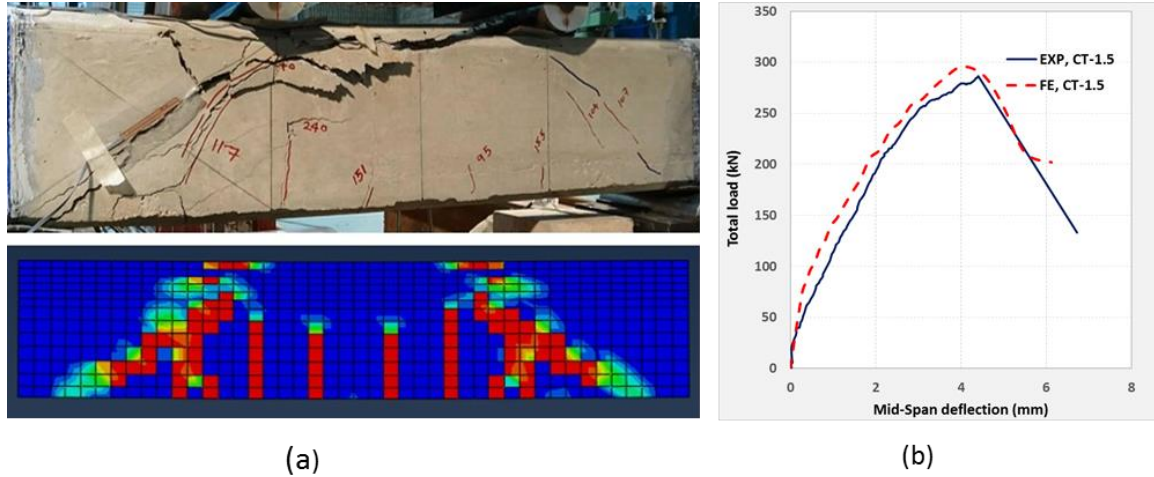


Figure 4.8 Control beam (CT-1.5): (a) failure mode, (b) Load-deflection response

The retrofitted beams (*SB-2SJ-1.5*) and (*SB-3SJ-1.5*) failures loads were in agreement with experimental results with difference of 1%, Figs. (4.9 & 4.10). However, the crack patterns for beam (*SB-2SJ-1.5*) was slightly different from the experimental test, which reported as shear failure at one end, whereas in FE it was a flexure-shear failure. This inconsistency in failure mode of experimentally tested beam may occurs due to one or more of the following reasons: (i) the steel fibers accumulation and orientation during the pouring of concrete, where the UHPC becoming weak on one side having no enough steel fibers to shift the failure; (ii) the applying load was not equally distributed over the normal concrete and the retrofitted sides due to some error in leveling of UHPC during the casting which lowered the UHPC strips; (iii) insufficient contact at critical section between the substrate concrete and UHPC resulting in the lack of load transferring and therefore ineffective strengthening practice.

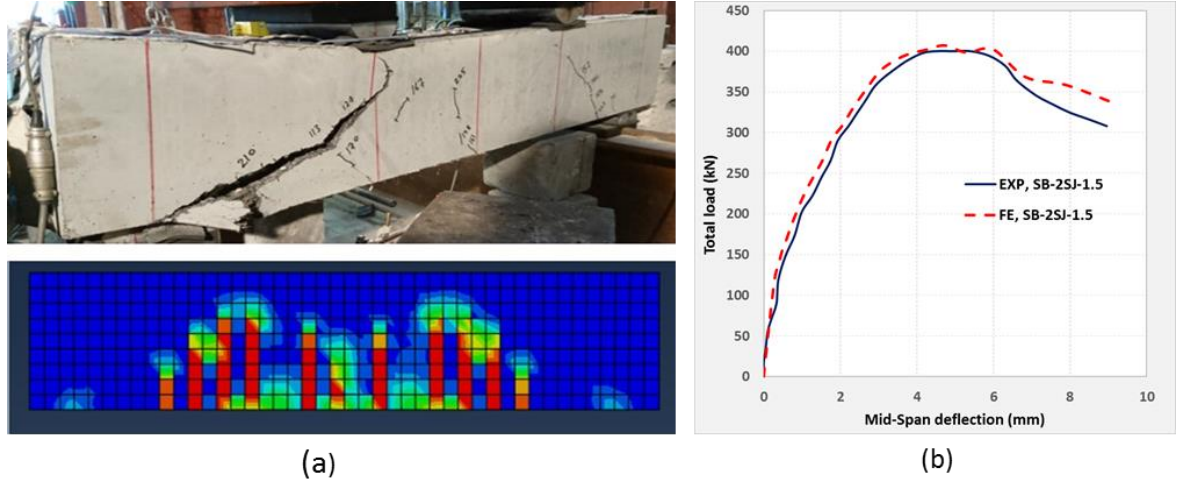


Figure 4.9 Retrofitted beam (SB-2SJ-1.5): (a) failure mode, (b) Load-deflection response

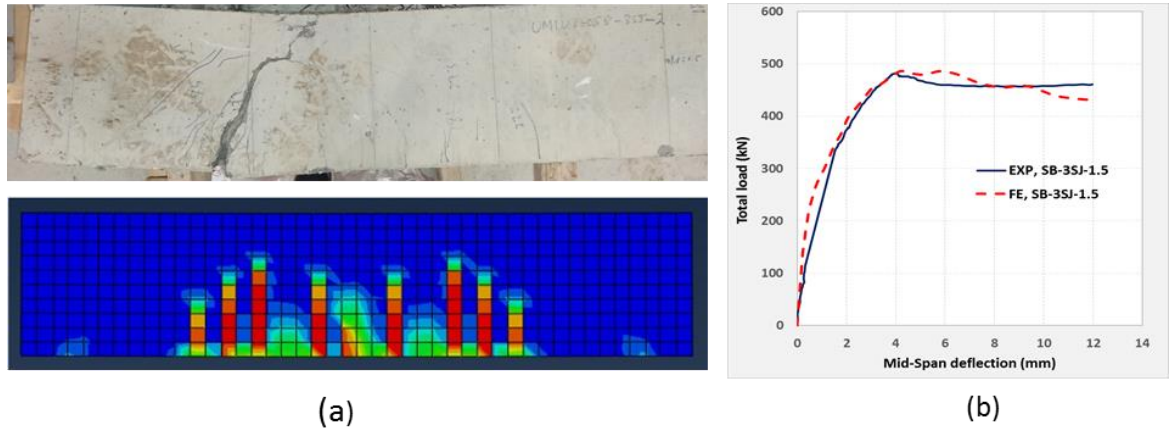


Figure 4.10 Retrofitted beam (SB-3SJ-1.5): (a) failure mode, (b) Load-deflection response

#### 4.6.3 Beams with $a/d=2.0$

In similar manner, the experimental results of beams belong to this case of  $a/d=2.0$ , were highly resembled in FE model. The failure modes of all beams (*CT-2.0*), (*SB-2SJ-2.0*) and (*SB-3SJ-2.0*) were shear, flexure-shear, and flexural failures, Figs. (4.11, 4.12 & 4.13), respectively, which are the same as the experimental tests. Moreover, a high agreement was observed in the load-deflection curves with average difference in failure load of around 2%.

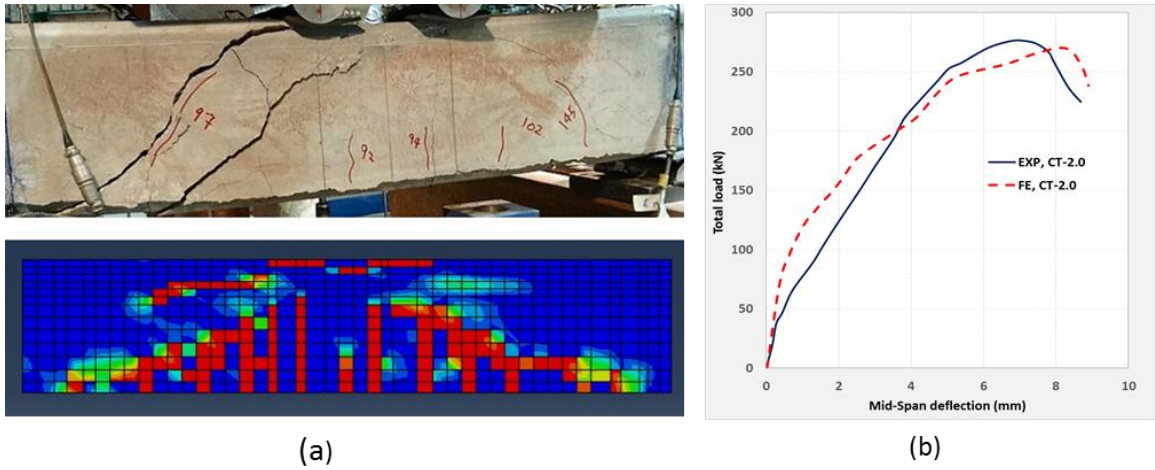


Figure 4.11 Control beam (CT-2.0): (a) failure mode, (b) Load-deflection response

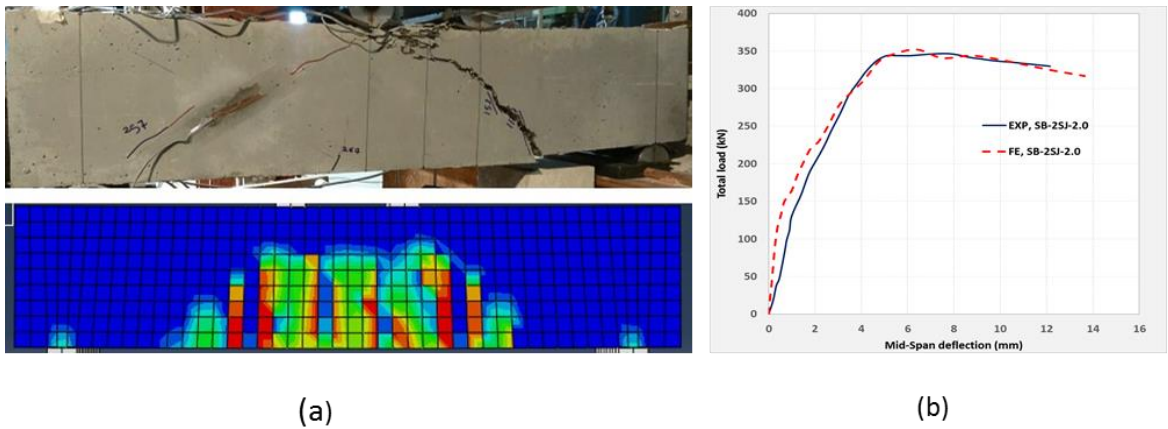


Figure 4.12 Retrofitted beam (SB-2SJ-2.0): (a) failure mode, (b) Load-deflection response

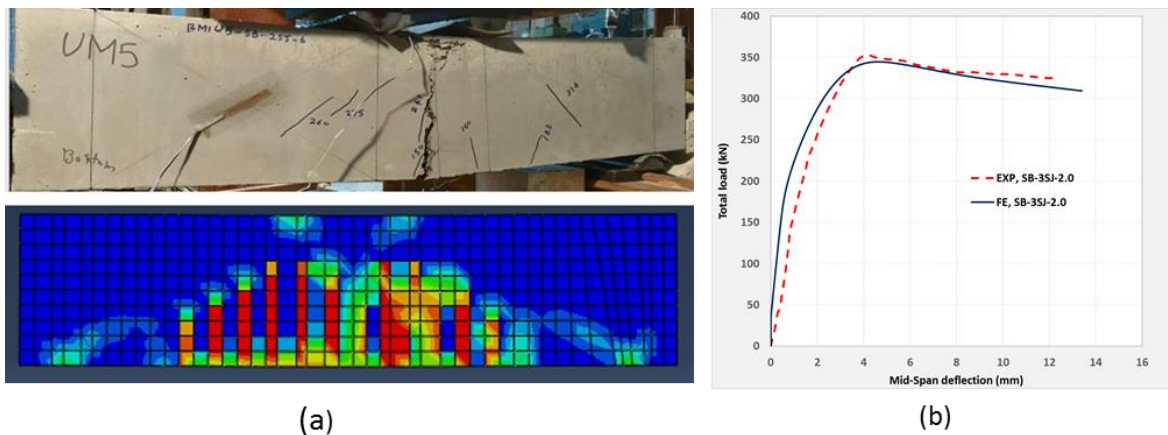


Figure 4.13 Retrofitted beam (SB-3SJ-2.0): (a) failure mode, (b) Load-deflection response

## 4.7 Summary of FE Results

The evaluation of dependability of FE model was investigated successfully through the accuracy of obtained results being compared with experimental tests. Specifically, peak loads, displacement values, and failure behaviour were appropriately closed to the experimental outcomes. The load-deflection response, deformational behaviour and ductility improvement of retrofitted beams were in good agreements with those obtained from experimental tests. [Table 4.2](#) summarizes all FE results and as compared with the experimental outcomes.

**Table 4.2 Comparison of Failure Loads between Experimental Tests and FE Results**

Beam ID	a/d ratio	Exp. Failure Load (kN)	FE Failure Load (kN)	Difference ( $P_{Exp}/P_{FE}$ ), (%)
<i>CT-1.0</i>	1.0	383	373	2.7
<i>SB-2SJ-1.0</i>	1.0	567	546	3.8
<i>SB-3SJ-1.0</i>	1.0	628	611	2.8
<i>CT-1.5</i>	1.5	286	294	2.7
<i>SB-2SJ-1.5</i>	1.5	402	407	1.2
<i>SB-3SJ-1.5</i>	1.5	482	486	0.8
<i>CT-2.0</i>	2.0	276	270	2.2
<i>SB-2SJ-2.0</i>	2.0	346	352	1.7
<i>SB-3SJ-2.0</i>	2.0	353	344	2.6

Moreover, the proposed constitutive model (Concrete Damage Plasticity Model - CDP) well predicted the crack patterns and overall failure behaviour. Although, the shear behaviour is difficult to exactly predict because of its sensitivity to tensile strength of materials, CDP well simulated all damages through the cracking in tension and crushing in compression.

The FE model can be used to generate many useful outputs which cannot be easily obtained through the classical experimental test of beams. For example, the shear strains in the stirrups required to install several strain gauges in order to evaluate the stirrup contributions to overall shear strength, and this is costly and unpractical in real situations. Specifically, the strengthening issue needs to assess the contributions of all components in load capacity enhancing. Therefore, for all practical purposes, numerical simulation is a great tool to reduce the effort and cost of many structural engineering problems.

In summary, the proposed numerical FE model can be extended to evaluate UHPC strengthening technique of full-scaled beams having a deficient in shear. What is more, a parametric study is needed to carry out the influence of using different thickness of retrofitted UHPC strips and strengthened at certain regions instead of entire span.

\*\*\*\*\*

## **CHAPTER 5**

### **MECHANISTIC MODEL**

#### **5.1 General**

This chapter presents an empirical equation for shear strength gained from using the UHPC as strengthening of RC beams. The previous analytical models in the literature was first reviewed. Then an attempt to develop an empirical equation based on the available experimental results was undertaken.

A successful model for shear strength prediction should take in the account the following factors: geometry of member, shear span-to-depth ratio ( $a/d$ ), concrete strength in compression and tension, curing regime, transverse and longitudinal reinforcements, loading conditions, shear transfer mechanics and individual contributions of concrete and reinforcement.

Specifically, the shear resistance contributed by UHPC should be evaluated based on the variations on the  $a/d$  ratio and different jacketing configurations. In this thesis, three  $a/d$  ratios and two jacket patterns were used. Therefore, the contribution of UHPC will be added to shear carried by normal concrete and stirrups.

#### **5.2 Analytical Models: A State-of-the-Art Review**

Extensive studies have been conducted in the shear behaviour of conventional RC beams. However, no exact model was created because of complex nature of shear. For that reason, there is no robust design equation has been obtained. Most of design provisions available

in the literature were collected from a scatter experimental data and they based on simplification assumptions.

Moreover, the mechanics of shear transfer in reinforced concrete is not easy to predict. The available design expression of shear strength is based on the additive rule of individual contributions of concrete and steel:  $V_n = V_c + V_s$ ; [34] [58].

The shear strength prediction of strengthened beams using UHPC is more complicated than those of conventional RC beams. The presence of steel fibers and interact mechanics between the normal concrete and UHPC made the shear prediction of retrofitted beams a challenging task. To date, a few researches have been conducted on shear strength of fiber reinforced concrete. Most of these studies were attempted to develop an analytical model for shear prediction instead of design model.

Sharma (1986) [59] developed an empirical equation for shear prediction of steel fiber reinforced concrete (SFRC) beam. The equation looks simple, but it was not taken in to account for the steel fiber effects. It was reported that the shear strength of steel fiber reinforced concrete is affected mainly by the tensile strength, fiber fraction and dimensions and the a/d ratio [60].

Another analytical model was developed by Narayanan and Darwish (1987) [61]. They proposed an expression for shear prediction which was to somewhat a more reliable than that for Sharma.

Recently, the ACI issued a new document for design the FRP strengthening systems (ACI 440) [3]. This code gives a formula for shear prediction of FRP which based on area and

arrangement of FRP laminates. This formula was investigated by many researchers including El-Ghandour [62] who reported that the ACI 440 for shear is more conservative.

In summary, the need for a rigorous estimation of UHPC in shear contribution is important in strengthening process, despite the difficulties associated with the shear behaviour itself. However, an attempt was undertaken to develop a perceptible analytical model of failure shear load based on the experimental data. It should be noted that the prediction of cracking shear load is far from being settled and it is beyond the scope of this thesis.

### 5.3 Proposed Analytical Model

The shear contribution of UHPC should be added to the shear strength resulting from the normal concrete and shear reinforcement (i.e. stirrups). The analysis and design process should be also in compliance with ACI 318 code requirements for shear design [34] and ACI-ASCE Committee 445 [58]. In general, the nominal shear strength of beam member should exceed the required shear strength: (ACI 318-14, section 22.5.5)

$$\phi V_n \geq V_u \quad (1)$$

where,

$$V_n = V_c + V_s + V_{uc} \quad (2)$$

$$V_c = \left( 0.16\lambda \sqrt{f'_c} + 17\rho_w \frac{V_u d}{M_u} \right) b_w d \quad (3)$$

$$V_s = \frac{A_v F_y d}{S} \quad (4)$$

$$V_{uc} = A (f'_{uc})^B \left( \frac{d}{a} \right)^C \left( \frac{h}{t} \right)^D h_e t \quad (5)$$



$$V_n = V_c + V_s + V_{uc}$$

$V_n$  is the total shear strength of the beam,  $V_c$  is the shear carried by concrete (including the shear stress in the compression zone, aggregate interlock, and dowel action of longitudinal reinforcement),  $V_s$  is the shear carried by the stirrups, and the last new term ( $V_{uc}$ ) is the proposed UHPC contribution in shear capacity.  $f'_c$  is the compressive strength after 28-days of curing (in MPa),  $\rho_w$  is the percentage of longitudinal reinforcement,  $V_u$  and  $M_u$  are the shear and moment at the intended section,  $d$  and  $b_w$  is the effective depth and width of cross-section. The parameters for UHPC contributions are:  $f'_{uc}$  is the compressive strength of UHPC (in MPa),  $a$  is the shear span,  $h$  and  $t$  are the overall depth and the thickness of the retrofitting strip,  $h_e$  is the effective depth of the UHPC jacketing ([Fig. 5.1](#)),  $A$ ,  $B$ ,  $C$  and  $D$  are constants that need to be evaluated using the regression of experimental data.

The reduction factor that proposed by ACI 318 [34] for nominal shear strength is applied for normal concrete. However, it may require to apply additional reduction factor for the last term ( $V_{uc}$ ) [3], because such strengthening technique depends mainly on the configuration scheme, in other words, the bonding issue plays an important role in this regarding. Unfortunately, the limited experimental data of using UHPC as strengthening material leads to assume the full contribution of UHPC in the total shear capacity, i.e. the reduction factor for UHPC was assumed a unity.

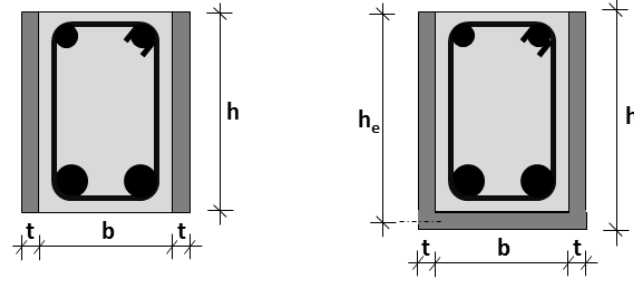


Figure 5.1 Symbols used in the proposed analytical model

The proposed expression for UHPC contribution in shear is a function of tensile strength of UHPC, the  $a/d$  ratio, and the area of strengthening jacketing. From hereafter, these factors that influence the shear contribution of UHPC are discussed.

### 1- Tensile Strength of UHPC:

The tensile strength of UHPC depends mainly on the fiber content, geometry, and properties. It is found that the steel fibers increase the post-cracking tensile behaviour of concrete and therefore the shear capacity will be enhanced [63]. In this thesis, the steel fiber content was constant, therefore it can be related directly to the compressive strength by inserting the A-constant in the proposed equation.

### 2- Shear Span-to-Depth Ratio ( $a/d$ )

The shear span ( $a$ ), the distance from the support to the application load, to the depth ( $d$ ) of the section is the key factor which governs the shear failure mode of strengthened beams as it was evidenced in the experimental test program. The  $a/d$  or  $(M/Vd)$  affects the diagonal shear cracks and the failure shear load as it illustrates in [Fig. 5.2](#).

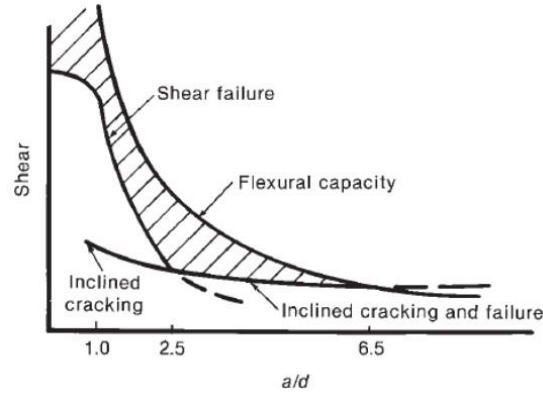


Figure 5.2 Effect of  $a/d$  ration on the shear failure of beams [63]

### 3- Jacketing Configuration:

The retrofitting arrangements is considered by adding the area of this configuration in the last term of proposed model. In this thesis, either the two-sided or three-sided jacketing was used. Therefore, for two-sided jacketing, the area will be the thickness of retrofitted strip multiplied by the depth, whereas for three-sided jacketing it will be the thickness multiplied by adding of depth and the thickness of bottom side, i.e. the central area of bottom side will be assumed as ineffective in strengthening. In fact, the last assumption of neglecting the central are of bottom side is to somewhat true, since it is confirmed by the experimentally results.

#### 5.3.1 Regression of Experimental Data

All data that obtained from experimental test program was presented in [Tables \(5.1 & 5.2\)](#). The shear carried by concrete and stirrups were calculated in compliance with ACI-318 code.

Using the above tables, the regression of data results in developing the best fitting solution for proposed model. The constants were found to be: A=0.026; B=1/3.5; C=1.1, D=2.4.

Thus, by substituting these constants, the following model is obtained:

$$V_{uc} = 0.026 (f'_{uc})^{1/3.5} \left(\frac{d}{a}\right)^{1.1} \left(\frac{h}{t}\right)^{2.4} h_e t$$

**Table 5.1 Input Data and Output Result of Proposed Analytical Model (for Sandblasted Cast-in Beams)**

Beam ID	$f'_{uc}$	$a/d$	$h$	$h_e$	$t$	$V_{uc}$ , Exp. (kN)	$V_{uc}$ , Model (kN)	Error (%)
<b>SB-2SJ-1.0</b>	150	1.0	230.0	230.0	30	<b>103.1</b>	<b>99.7</b>	3
<b>SB-3SJ-1.0</b>	150	1.0	260.0	245.0	30	<b>133.6</b>	<b>142.5</b>	7
<b>SB-2SJ-1.5</b>	150	1.5	230.0	230.0	30	<b>71.7</b>	<b>63.8</b>	11
<b>SB-3SJ-1.5</b>	150	1.5	260.0	245.0	30	<b>111.7</b>	<b>91.2</b>	18
<b>SB-2SJ-2.0</b>	150	2.0	230.0	230.0	30	<b>45.7</b>	<b>46.5</b>	2
<b>SB-3SJ-2.0</b>	150	2.0	260.0	245.0	30	<b>49.2</b>	<b>66.5</b>	35
<i>Average Error</i>								13

**Table 5.2 Input Data and Output Result of Proposed Analytical Model (for Epoxy-Bonding Beams)**

Beam ID	$f'_{uc}$	$a/d$	$h$	$h_e$	$t$	$V_{uc}$ , Exp. (kN)	$V_{uc}$ , Model (kN)	Error (%)
<b>EP-2SJ-1.0</b>	150	1.0	230.0	230.0	30	<b>84.1</b>	<b>99.7</b>	18
<b>EP-3SJ-1.0</b>	150	1.0	260.0	245.0	30	<b>132.2</b>	<b>142.5</b>	8
<b>EP-2SJ-1.5</b>	150	1.5	230.0	230.0	30	<b>88.2</b>	<b>63.8</b>	28
<b>EP-3SJ-1.5</b>	150	1.5	260.0	245.0	30	<b>114.2</b>	<b>91.2</b>	20
<i>Average Error</i>								19

**Table 5.3 Comparison of Failure Loads between Experimental, FE and Analytical Model**

Beam ID	a/d ratio	Exp. Failure Load (kN)	FE Failure Load (kN)	Model Failure Load (kN)
<b>SB-2SJ-1.0</b>	1	567	546	561
<b>SB-3SJ-1.0</b>	1	628	611	646
<b>SB-2SJ-1.5</b>	1.5	402	407	386
<b>SB-3SJ-1.5</b>	1.5	482	486	441
<b>SB-2SJ-2.0</b>	2	346	352	348
<b>SB-3SJ-2.0</b>	2	353	344	388

## 5.4 Validation of the Proposed Analytical Model

The researches in shear strengthening using the high or ultra-high strength concretes are very limited. The proposed analytical model is validated using one of the studies that conducted in that area of strengthening.

Runao et al (2014) [26] conducted an experimental study on the strengthening and repairing of shear deficient RC beams using steel fiber reinforced concrete SFRC. RC beams having length of 1600mm, and cross-section of 250mm height and 150mm width, *Fig. 5.2*. The steel reinforcements were as follows: longitudinal reinforcement of 3 $\phi$ 16 in the bottom and 2 $\phi$ 8 in the top; and  $\phi$ 6 stirrups at spacing of 125mm were provided as shear reinforcement.

The SFRC concrete with thickness of 30mm was cast directly on the all three beams surfaces. Two different dosages of steel fibers were used 30 kg/m<sup>3</sup> and 60 kg/m<sup>3</sup>. The strengths of normal concrete, steel reinforcement, and SFRC as the follows: 26.3MPa, 484.6MPa, and 86.5MPa (with 30 kg/m<sup>3</sup> steel fibers) and 95.5MPa (with 60 kg/m<sup>3</sup> steel fibers), respectively. *Table 5.4* shows the input data of strengthened beam. The experimental results of the beam tests are validated using the proposed model, it is found that the model predicts in good accuracy the contribution of SFRC jacketing, as illustrated in *Table 5.4*, with an average error of 9%.

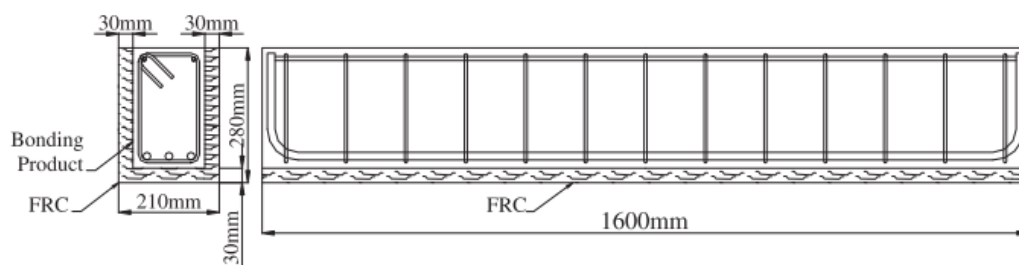


Figure 5.3 Beam details and strengthening configurations of work done by Runao et al (2014) [26]

Table 5.4 Validation of Model using Experimental Results of Ruano et al (2014) [26]

Beam ID	$f'_{uc}$	$a/d$	$h$	$h_e$	$t$	$V_{uc, Exp. (kN)}$	$V_{uc, Model (kN)}$	Error (%)
<b>B7</b>	86.5	1.7	280	265	30	81.2	86.1	6
<b>B8</b>	86.5	1.7	280	265	30	80.1	86.1	8
<b>B13</b>	95.5	1.7	280	265	30	73.2	88.6	21
<b>B14</b>	95.5	1.7	280	265	30	91.0	88.6	3
<i>Average Error</i>								9

\*\*\*\*\*

## **CHAPTER 6**

### **CONCLUSIONS AND RECOMMENDATIONS**

#### **6.1 General**

The feasibility of using Ultra-High Performance Concrete (UHPC) for strengthening of conventional reinforced beams which deficient in shear is investigated in this thesis. An extensive experimental work was conducted in the laboratories of Civil Engineering Department at KFUPM. In addition, the numerical and mechanistic models were developed to validate the experimental tests.

The first phase of experimental program was the casting of RC beams which presented a shear failure. The strengthening using UHPC was carried out by proposed two different techniques and two jacketing configurations. The UHPC was cast either inside a beam mold by sandblasting preparation, or by bonding the precast UHPC strips using the adhesive epoxy. Two retrofitting configurations were used: firstly, by jacketing the beam in three full-length sides (like U-wrapped), secondly: by jacketing only the two opposite sides.

The mechanical properties of normal concrete, steel reinforcement, and UHPC were studied by conducting many laboratory tests. The retrofitted beams were experimentally tested by varying the  $a/d$  ratios. The results of experimental investigation confirmed that the UHPC strengthening technique is one of the best way for retrofitting the shear-deficient beams.

Moreover, a non-linear finite element model was developed using the advantage of computer software (Abaqus). The shear failure load and crack patterns were predicted and simulated. The results of proposed numerical model were in good match with the experimental outcomes.

In the last stage of this study, an analytical model was developed. An empirical equation was set to predict the shear failure load and the contribution of UHPC to the shear capacity of RC beams.

## 6.2 Application of the Research Study

The current study of using UHPC as strengthening technique of concrete structures can be applied to the either deteriorated or newly produced beams as shown in Fig.

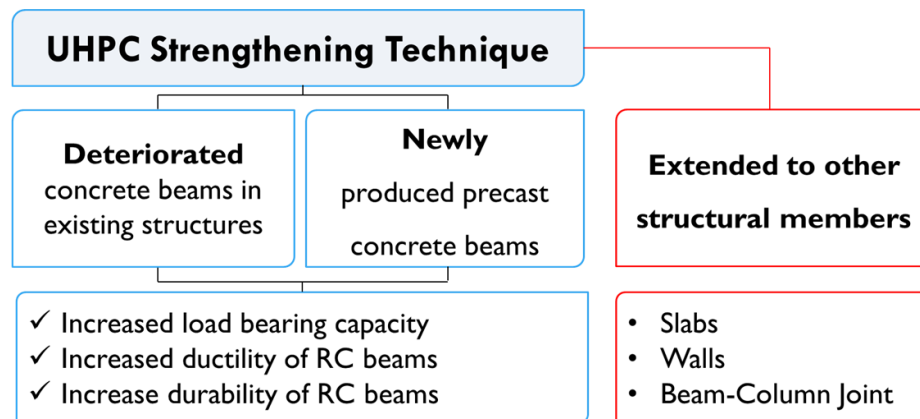


Figure 6.1 Application of UHPC strengthening technique

## 6.3 Conclusions

The experimental, numerical and analytical studies that had conducted in this thesis confirmed the possibility of utilizing UHPC as an effective strengthening technique in shear. Based on that result, the following conclusions are drawn:



- 4- ***UHPC as Strengthening Material***: through the experimental investigation, it is worth to conclude that using UHPC concrete for strengthening of conventional RC beams is an effective, durable and easy to apply. As such, the UHPC can be cast in thin thickness, cured in ambient temperature and easily bonded to prepared surface. Beside the superior structural properties of UHPC, it has an excellent compatibility with the concrete substrate which make it a good option for repairing and strengthening tasks. As durability viewpoint, UHPC exhibited an excellent durable surface through low permeability and dense microstructure, therefore it protects the core beam from being deteriorated.
- 5- ***Control Beams***: all control beams were behaved in shear mode and the inclined cracks were propagated during the test caused the shear-compression failure. The beams were failed suddenly and there was a variation in failure loads due to the different a/d ratios and the complicity nature of shear behaviour. No anchorage failures had reported since all longitudinal bars were bent upwards.
- 6- ***Retrofitted Beams in Two-Sides***: the strengthening in two sides with both different techniques of strengthening shifted the failure from shear to flexure-shear failure. In two-sided jacketing beams, the flexural cracks first initiated and followed by propagation of secondary inclined cracks.
- 7- ***Retrofitted Beams in Three-Sides***: in these beams, the efficiency of UHPC strengthening is more dominant. The failures in most beams were in flexure with a good ductility and fewer cracks. Most of beams have failed in high loads compared to the control beams, therefore this configuration gives a high load

capacity enhancement. In addition, no debonding is reported either for sandblasting or epoxy techniques. Moreover, an enhancement in serviceability, i.e. displacement and crack width, was observed in all retrofitted beams, especially in those of three-sided jacketing.

8- ***a/d Variation:*** from the investigation results, it was shown that as the shear span-depth ratios increasing as the shear strength of beams decreasing. The beams with  $a/d = 1.0$  and  $1.5$  are more effective in shear resistant than those with  $a/d = 2.0$ . Therefore, it is recommended to set the range of  $a/d$  between  $1.0$  and  $1.5$  for shear strengthening using UHPC.

9- ***Different Strengthening Techniques:*** both strengthening techniques (Sandblasting Cast-in and Epoxy Adhesive) are effective in retrofitting of shear- deficient beams. All retrofitted beams were behaved in monolithic way without any debonding or prior failure of such retrofitted strips. Thus, both techniques can be used where the sandblasting cast-in technique requires a formwork which is not applicable in some cases. On the other hand, the epoxy adhesive technique does not require any formworks and the retrofitted strips can be cast outside the filed. However, in case of using the epoxy adhesive method, the discontinuity of fabricated strips, i.e. the bottom layer with other two-side layers, caused a significant drop in the contribution of UHPC for shear strength. So, the retrofitted in three-sided jacketing with epoxy bonding is ineffective.

10- ***Bonding Evaluation:*** in all experimentally tests of beams, no debonding was observed either for using sandblasting or epoxy adhesive techniques. In

addition, the bond evaluation tests (Slant shear test and Splitting tensile test) showed a good bond between the normal concrete and the UHPC. The remarkable thing of this good bond is resulting in the integrity of the composite structure and overall durability.

11- **Numerical Model:** the developed finite element model predicted the failure load and crack pattern in high accuracy. In addition, the proposed damage model, i.e. concrete damage plasticity approach, captured all damage behaviour either for control beams or the retrofitted beams. Thus, this model can be used successfully in modeling the ultra-high strength concretes.

12- **Analytical Model:** to date, there is no mechanistic model for calculating the contribution of UHPC in the shear capacity of strengthened beams. Therefore, the developed analytical model in this study is of great importance. The proposed equation predicts the shear carried by the UHPC in good accuracy (average thirteen per cent). However, extensive tests have to conduct by varying the all paraments that influence the shear capacity.

## 6.4 Recommendations for Future Research

The strengthening or repairing of existing concrete structures is a challenging task. Many structures around the world necessitate the strengthening intervention to extend their service life. Therefore, a progress research needs to continue to set a guideline for the reliable strengthening techniques. Based on this research work, some of recommendations are suggested as follows:

- The most care must be paid during the casting of UHPC by using the correct casting practices that elaborated in chapter three.

- The need for investigate the shear strengthening using UHPC of RC beams that have no stirrups.
- Examine the partially retrofitting of beams by using the strengthening strips over the critical shear zones instead of full-length jacketing.
- Study the effect of different steel-fiber contents, geometry and size on the behaviour of retrofitted beams.
- A parametric study on the UHPC strengthening should be conducted by varying the thickness of retrofitted strips, different arrangements and patterns, and use a wide range of  $a/d$  ratios.
- Develop a numerical model to simulate the UHPC as heterogenous material instead of homogenous materials in order to capture the steel fibers distribution and orientation.
- Conducting more research to generate extensive tests data to develop more accurate mechanistic model to predict the cracking shear strength of retrofitted beam.
- Study the efficiency of UHPC for strengthening the other structural elements: columns, slabs and walls
- Finally, investigate the feasibility of UHPC strengthening under the cyclic loading.

\*\*\*\*\*

## References

- [1] A. A. Shah and Y. Ribakov, "Recent trends in steel fibered high-strength concrete," *Mater. Des.*, vol. 32, no. 8–9, pp. 4122–4151, 2011.
- [2] S. Altin, Ö. Anil, and M. E. Kara, "Improving shear capacity of existing RC beams using external bonding of steel plates," *Eng. Struct.*, vol. 27, no. 5, pp. 781–791, 2005.
- [3] American-Concrete-Institute, *ACI 440.2R-08 Guide for the design and construction of externally bonded FRP systems*. 2008.
- [4] J. F. Chen and J. G. Teng, "Shear capacity of FRP-strengthened RC beams : FRP debonding," *Constr. Build. Mater.*, vol. 17, pp. 27–41, 2003.
- [5] V. C. Li, "High performance fiber reinforced cementitious composites as durable material for concrete structure repair," *Restor. Build. Monum. an Int. J. = Bauinstandsetz. und Baudenkmalpfl. eine Int. Zeitschrift*, vol. 10, no. 2, pp. 163–180, 2004.
- [6] S. Iqbal, A. Ali, K. Holschemacher, T. A. Bier, and A. A. Shah, "Strengthening of RC beams using steel fiber reinforced high strength lightweight self-compacting concrete (SHLSCC) and their strength predictions," *Mater. Des.*, vol. 100, pp. 37–46, 2016.
- [7] G. H. Mahmud, Z. Yang, and A. M. T. Hassan, "Experimental and numerical studies of size effects of ultra-high performance steel fibre reinforced concrete (UHPRFC) beams," *Constr. Build. Mater.*, vol. 48, pp. 1027–1034, 2013.

- [8] B. A. Graybeal, *Material property characterization of ultra-high performance concrete*, no. August. 2006.
- [9] S. Ahmad, I. Hakeem, and M. Maslehuddin, "Development of an optimum mixture of ultra-high performance concrete," *Eur. J. Environ. Civ. Eng.*, vol. 20, no. 9, pp. 1106–1126, 2015.
- [10] K. Habel, M. Viviani, E. Denarié, and E. Brühwiler, "Development of the mechanical properties of an ultra-high performance fiber reinforced concrete ( UHPFRC )," *Cem. Concr. Res.*, vol. 36, pp. 1362–1370, 2006.
- [11] S. Rahman, T. Molyneaux, and I. Patnaikuni, "Ultra High Performance Concrete (UHPC): applications and research," *Aust. J. Civ. Eng.*, vol. 8353, no. August, pp. 12–20, 2004.
- [12] A. R. Lubbers, "Bond performance between ultra-high performance concrete and prestressing strands," Ohio University, 2003.
- [13] S. Kang, Y. Lee, Y. Park, and J. Kim, "Tensile fracture properties of an ultra-high performance fiber reinforced concrete ( UHPFRC ) with steel fiber," *Compos. Struct.*, vol. 92, no. 1, pp. 61–71, 2010.
- [14] K. Telleen, T. Noshiravani, R. Galrito, and E. Bruhwiler, "Experimental investigation into the shear resistance of a reinforced UHPFRC web element," in *8th fib PhD Symposium in Kgs. Lyngby, Denmark*, 2014, no. January 2010.
- [15] B. A. Graybeal and F. Baby, "Development of direct tension test method for Ultra-High- Performance Fiber-Reinforced Concrete," *ACI Mater. J.*, no. 110, pp. 177–

186, 2014.

- [16] M. Bastien-Masse and E. Brühwiler, “Ultra-high performance fiber reinforced concrete for strengthening and protecting bridge deck slabs,” *Bridg. Maintenance, Safety, Manag. Life Ext.*, pp. 2176–2182, 2014.
- [17] J. Son, B. Beak, C. Choi, S. Korea, and S. Korea, “Eperimental study on shear strength for ultra-high performance concrete beam,” in *18th Internal confernce on composite materials*, 1992, pp. 3–6.
- [18] P. Marchand *et al.*, “Shear resistance of ultra-high performance fibre-reinforced concrete I-beams,” *Fract. Mech. Concr. Concr. Struct.*, 2010.
- [19] A. P. Lampropoulos, S. A. Paschalis, O. T. Tsioulou, and S. E. Dritsos, “Strengthening of reinforced concrete beams using-ultra high performance fibre reinforced concrete (UHPFRC),” *Eng. Struct.*, vol. 106, pp. 370–384, 2016.
- [20] M. A. Al-Osta, M. N. Isa, M. H. Baluch, and M. K. Rahman, “Flexural behavior of reinforced concrete beams strengthened with ultra-high performance fiber reinforced concrete,” *Constr. Build. Mater.*, vol. 134, pp. 279–296, 2017.
- [21] G. Martinola, A. Meda, G. A. Plizzari, and Z. Rinaldi, “Strengthening and repair of RC beams with fiber reinforced concrete,” *Cem. Concr. Compos.*, vol. 32, no. 9, pp. 731–739, 2010.
- [22] S. Mostosi, A. Meda, P. Riva, and S. Maringoni, “Shear strengthening of RC beams with high performance jacket,” *Symp. A Q. J. Mod. Foreign Lit.*, pp. 1–9, 2011.

- [23] F. J. Alaei, B. L. Karihaloo, and F. Asce, "Retrofitting of reinforced concrete beams with CARDIFRC," *J. Compos. Constr. ASCE*, vol. 7, no. August, pp. 174–186, 2003.
- [24] T. Noshiravani and E. Brühwiler, "Experimental investigation on reinforced ultra-high performance fiber reinforced concrete composite beams subjected to combined bending and shear," *ACI Struct. J.*, vol. 110, no. 2, 2013.
- [25] L. Hussein and L. Amleh, "Structural behavior of ultra-high performance fiber reinforced concrete-normal strength concrete or high strength concrete composite members," *Constr. Build. Mater.*, vol. 93, pp. 1105–1116, 2015.
- [26] G. Ruano, F. Isla, R. I. Pedraza, D. Sfer, and B. Luccioni, "Shear retrofitting of reinforced concrete beams with steel fiber reinforced concrete," *Constr. Build. Mater.*, vol. 54, pp. 646–658, 2014.
- [27] C. E. Chalioris, G. E. Thermou, and S. J. Pantazopoulou, "Behaviour of rehabilitated RC beams with self-compacting concrete jacketing - Analytical model and test results," *Constr. Build. Mater.*, vol. 55, pp. 257–273, 2014.
- [28] F. A. Farhat, D. Nicolaides, A. Kanellopoulos, and B. L. Karihaloo, "High performance fibre-reinforced cementitious composite (CARDIFRC) - Performance and application to retrofitting," *Eng. Fract. Mech.*, vol. 74, no. 1–2, pp. 151–167, 2007.
- [29] K. Habel, E. Denarié, and E. Brühwiler, "Experimental investigation of composite concrete and conventional concrete members," *ACI Struct. J.*, no. 104, pp. 93–101,



2007.

- [30] G. Ruano, F. Isla, D. Sfer, and B. Luccioni, “Numerical modeling of reinforced concrete beams repaired and strengthened with SFRC,” *Eng. Struct.*, vol. 86, pp. 168–181, 2015.
- [31] L. Ombres, “Structural performances of reinforced concrete beams strengthened in shear with a cement based fiber composite material,” *Compos. Struct.*, vol. 122, pp. 316–329, 2015.
- [32] U. Khan, M. A. Al-Osta, and A. Ibrahim, “Modeling shear behavior of reinforced concrete beams strengthened with externally bonded CFRP sheets,” *Struct. Eng. Mech. An Int. J.*, vol. 61, no. 1, pp. 127–144, 2017.
- [33] J. A. Abdalla, A. S. Abu-Obeidah, R. A. Hawileh, and H. A. Rasheed, “Shear strengthening of reinforced concrete beams using externally-bonded aluminum alloy plates : An experimental study,” *Constr. Build. Mater.*, vol. 128, no. October, pp. 24–37, 2016.
- [34] American-Concrete-Institute, *ACI 318M-14 Building Code Requirements for Structural Concrete*. 2014.
- [35] ASTM International, *ASTM C39 Standard test method for compressive strength of cylindrical concrete specimens*. 2017.
- [36] ASTM International, *ASTM C469 Standard test method for static modulus of elasticity and Poisson ’ s ratio of concrete*, vol. 4. 2002.
- [37] ASTM International, “ASTM A370 Standard test methods and definitions for

mechanical testing of steel products,” pp. 1–48, 2013.

- [38] S. T. Kang and J. K. Kim, “The relation between fiber orientation and tensile behavior in an ultra high performance fiber reinforced cementitious composites (UHPFRCC),” *Cem. Concr. Res.*, vol. 41, no. 10, pp. 1001–1014, 2011.
- [39] ASTM International, *ASTM C1437 - 15 Standard test method for flow of hydraulic cement mortar*. 2015.
- [40] Sika-Company, “Sikadur ® -32 LP, Product data sheet,” 2014.
- [41] G. H. Russel and B. A. Graybeal, *Ultra-high performance concrete : A State-of-the-Art report for the bridge community*, no. June. 2013.
- [42] ASTM International, *ASTM C109: Standard test method for compressive strength of hydraulic cement mortars*, vol. 4, no. May. 1999.
- [43] ASTM International, *ASTM C78 Standard test method for flexural strength of concrete (using simple beam with third-point loading)*. .
- [44] ASTM International, *ASTM C1018-97 Standard test method for flexural toughness and first-crack strength of fiber-reinforced concrete (using beam with third-point loading)*, vol. 4, no. October. 1997.
- [45] ACI-Committee, *ACI 546 Guide to materials selection for concrete repair*. .
- [46] ASTM International, *ASTM C496/C 496M Standard test method for splitting tensile strength of cylindrical concrete*. .
- [47] ASTM International, *ASTM C882 – 99 Standard test method for bond strength of*

*epoxy-resin systems used with concrete. .*

- [48] M. A. C. Munoz, D. K. Harris, T. M. Ahlborn, and D. C. Froster, “Bond performance between ultra-high performance concrete and normal strength concrete,” *J. Mater. Civ. Eng.*, vol. 26, no. 2004, pp. 1–6, 2014.
- [49] M. M. Sprinkel and C. Ozyildirim, “PhD Thesis: Evaluation of high performance concrete overlays placed on route 60 over lynnhaven inlet in virginia,” University of Virginia), 2000.
- [50] B. L. Wahalathantri, D. P. Thambiratnam, T. H. T. Chan, and S. Fawzia, “A material model for flexural crack simulation in reinforced concrete elements using ABAQUS,” *First Int. Conf. Eng. Des. Dev. Built Environ. Sustain. Wellbeing*, pp. 260–264, 2011.
- [51] Y. Sümer and M. Aktaş, “Defining parameters for concrete damage plasticity model,” *Chall. J. Struct. Mech.*, vol. 1, no. 3, pp. 149–155, 2015.
- [52] J. Lubliner, J. Oliver, S. Oller, and E. Oñate, “A plastic-damage model for concrete,” *Int. J. Solids Struct.*, vol. 25, no. 3, pp. 299–326, 1989.
- [53] J. Lee and G. Fenves, “Plastic-damage model for cyclic loading of concrete structures,” *Eng. Mech.*, vol. 124, no. 8, pp. 892–900, 1998.
- [54] Online Documentation Simulia, “Abaqus user’s manual, 2016.” .
- [55] P. M. V. Birtel, “Parameterised finite element modelling of RC beam shear failure,” in *ABAQUS Users’ Conference*, 2007, pp. 95–108.

- [56] I. F. for S. C. (fib), *Fib: model code for concrete structures 2010*. 2013.
- [57] B. Mercan, “PhD Thesis: Modeling and behaviour of prestressed concrete spandrel beams,” 2011.
- [58] ACI-ASCE-Committee, *ACI 445R-99 Recent approaches to shear design of structural concrete*. 2000.
- [59] A. K. Sharma, “Shear strength of steel fiber reinforced concrete beams,” *ACI J. Proc.*, vol. 83, no. 4, pp. 624–628, 1986.
- [60] Y. Kwak, M. O. Eberhard, W. Kim, and J. Kim, “Shear strength of steel fiber-reinforced concrete beams without stirrups,” *ACI Struct. J.*, no. 99, pp. 1–9, 2003.
- [61] R. Narayanan and I. Y. S. Darwish, “Use of steel fibers as shear reinforcement,” *ACI Struct. J.*, vol. 84, no. 3, pp. 216–227, 1987.
- [62] A. A. El-Ghandour, “Experimental and analytical investigation of CFRP flexural and shear strengthening efficiencies of RC beams,” *Constr. Build. Mater.*, vol. 25, no. 3, pp. 1419–1429, 2011.
- [63] J. K. WIGHT and J. G. MacGregor, *Reinforced concrete: mechanics and design*, 6th edition. 2012.

## Vitae

Name :Ashraf Awadh Abdullah Bahraq

Nationality :Yemeni

Date of Birth :8/20/1988

Email :ashrafawadh101@gmail.com

Phone :+966 509773734 / +967 711887861

Address :Seiyun - Hadramout - Yemen

### Academic Background:

- Master of Science (MSc) in Civil Engineering (2017), King Fahd University of Petroleum and Minerals – Kingdom of Saudi Arabia (Excellent degree of 3.906/4.00)
- Bachelor of Science (BSc) in Civil Engineering (2013) Aden University – Republic of Yemen (Excellent degree of 4.6/5.0)

### Experience:

- Work at Research Institute - KFUPM in Building Materials Research Group

### Research Interests:

- Finite Element Modelling of Reinforced Concrete Behaviour
- Strengthening Techniques of Reinforced Concrete Structures